U.S. DEPARTMENT OF
ENERGY

Office of
ENERGY EFFICIENCY &
RENEWABLE ENERGY

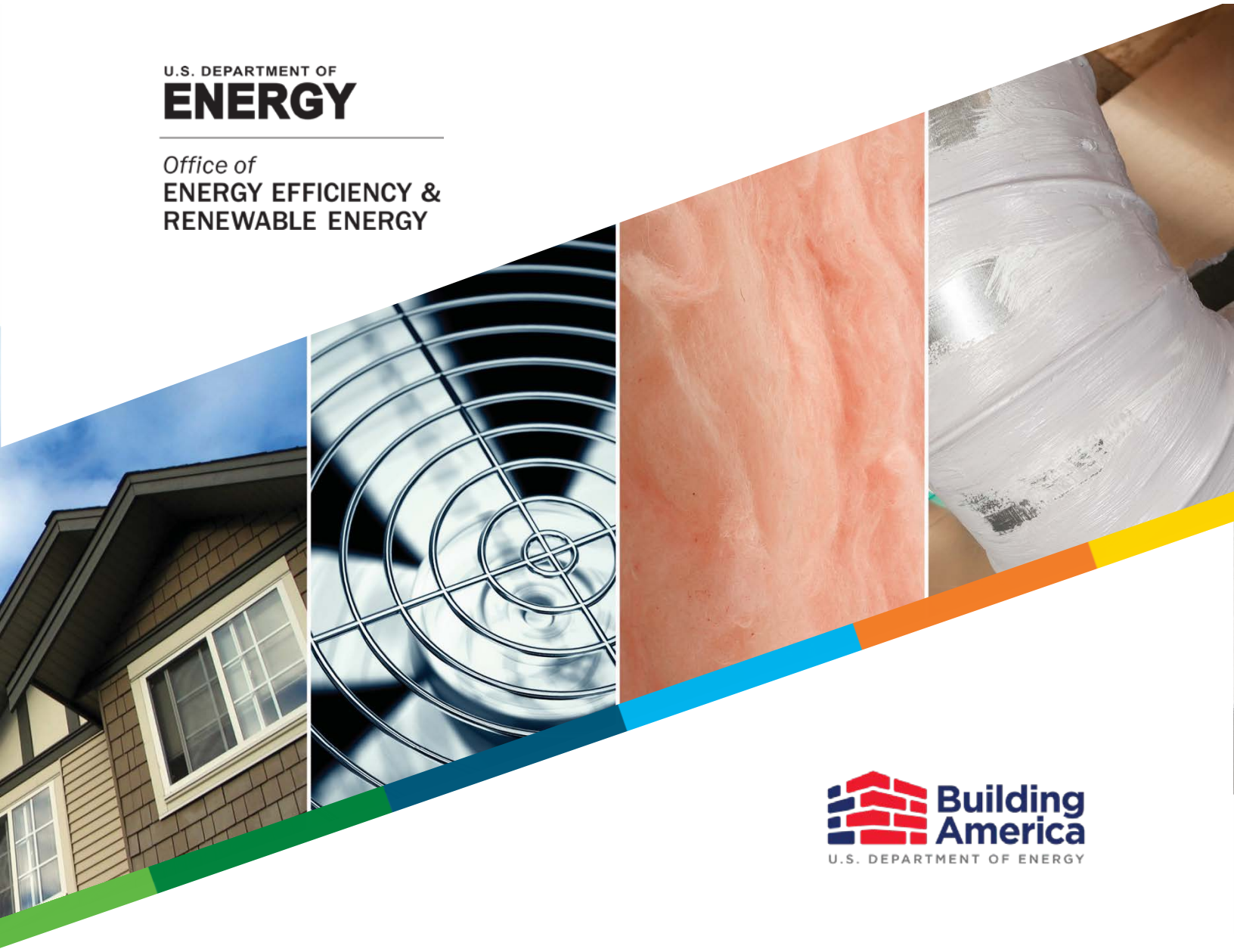

Building America
U.S. DEPARTMENT OF ENERGY

Moisture Performance of Unvented Attics With Vapor Diffusion Ports and Buried Ducts in Hot, Humid Climates

September 2024

Disclaimer

Authors

The authors of this report are:

Zoe Kaufman, National Renewable Energy Laboratory (NREL)

Anthony Fontanini, NREL

Charles Withers, FSEC Energy Research Center

Craig Marden, Owens Corning

Kohta Ueno, Building Science Corporation

Ross Philip, Mountain Energy Partnership

Greg Barker, Mountain Energy Partnership

Ed Hancock, Mountain Energy Partnership

Lieko Earle, NREL

Robbin Garber-Slaght, NREL

Sam Meleika, NREL

Acknowledgments

The authors would like to acknowledge the valuable contributions from the following groups and organizations. We would like to thank the:

- K. Hovnanian neighborhood developers and supporting staff for coordinating the necessary construction techniques to be evaluated in the field experiments and for helping us monitor these homes
- Residents and homeowners for allowing us access to the attics
- Project's technical monitor, Eric Werling at DOE, for guiding the project team and ensuring success of the project.

List of Acronyms

AHU	air handling unit
CV-RMSE	coefficients of variation of the root mean square error
FSEC	FSEC Energy Research Center (originally Florida Solar Energy Center)
HVAC	heating, ventilating, and air conditioning
IECC	International Energy Conservation Code
MBE	mean bias error
OSB	oriented strand board
RH	relative humidity
RMSE	root mean square error

Executive Summary

Energy efficiency measures, such as cool roofs, radiant barriers, interior radiative control coatings, and buried ducts are increasing in popularity and are promoted by energy codes because of their energy-saving potential. However, these strategies can also pose moisture risks in attics by lowering surface temperatures and increasing condensation potential and moisture accumulation. Of particular concern in hot-humid climates is dripping condensation on cold air-conditioning ductwork in the summer—commonly referred to as duct “sweating”—which threatens the attic floor with conditions conducive to mold growth and rot. One strategy to mitigate these moisture issues is to wrap ductwork in thicker duct-wrap insulation with an integrated exterior vapor barrier, but thick duct wrap can be difficult to come by, expensive, and unwieldy to work with.

This study explores an alternative strategy of reducing moisture issues while embracing energy efficiency by using unvented attics with vapor diffusion ports and buried ductwork in hot-humid climates. Vapor diffusion ports have been studied so far in a wide range of U.S. climates, mostly in the context of conditioned attics. In this study, the strategy is implemented in the novel context of hot-humid climates with ductwork sitting atop blown-in attic floor insulation in unconditioned attics. Using a combination of field experiments and hygrothermal modeling, the findings of this project indicate that an unvented attic with vapor diffusion ports and buried ducts may be a key part of a successful low-cost method for reducing the attic moisture load by venting excess moisture out of the attic, keeping duct-jacket surfaces above dew point temperature, and keeping the roof deck safe from winter moisture accumulation.

The study monitored occupied experimental homes in DeBary, Florida (International Energy Conservation Code [IECC] Climate Zone 2A), to evaluate in-situ hygrothermal performance at the roof deck and attic floor over the course of nine months (including summer, fall, and winter). The homes were all new construction production homes in the same residential development. The five construction variations in the monitored homes were:

1. **Baseline construction**: Unconditioned, vented attic; ducts hung and wrapped in typical R-8 duct insulation
2. **Buried ducts**: Unconditioned, vented attic; R-8 ducting buried in minimum R-11 attic insulation
3. **Diffusion port**: Unconditioned, unvented attic with vapor diffusion ports replacing off-ridge vents; ducts hung and wrapped in typical R-8 duct insulation
4. **Diffusion port + radiant barrier**: Unconditioned, unvented attic with vapor diffusion ports replacing off-ridge vents and a radiant barrier draped at the roof deck; ducts hung and wrapped in typical R-8 insulation
5. **Diffusion port + radiant barrier + buried ducts**: Unconditioned, unvented attic with vapor diffusion ports replacing off-ridge vents and a radiant barrier draped at the roof deck; R-8 ducting buried in minimum R-11 attic insulation.

Although all five attics were monitored for ductwork condensation and surrounding conditions, the baseline (#1) and diffusion port + radiant barrier + buried duct (#5) cases were instrumented in greater detail. The configurations were monitored for moisture performance of the attic floor and roof deck in order to assess the potential for diffusion ports to address the hygrothermally stressful conditions posed by the combined energy efficiency measures. A one-dimensional hygrothermal model was developed to represent the diffusion port + radiant barrier + buried duct case and was later implemented to explore what-if scenarios involving more hygrothermally stressful conditions, including cool roofs, site shading, cooler climate, lower occupant set points, and higher occupant moisture generation.

Both measured and modeled cases were assessed using industry-standard criteria for mold, rot, and corrosion risk. Field observations showed no signs of sustained mold, rot, or corrosion risk in any of the experimental homes, although the weather was generally warm during the measurement period compared to historical averages. Visual observations during decommissioning confirmed the absence of moisture issues, including no indication of mold, rot, corrosion, or stains from puddling below ductwork. No evidence of condensation dripping from ductwork was present, but the authors note that future field experiments should instrument both the top and bottom of the exterior duct jacket at various locations along the duct runs to better detect presence of condensation, because relative humidity (RH) can be higher above the ducts than it is below them.

The hygrothermal models were then created to “stress test” the diffusion port + radiant barrier + buried duct home for potential moisture risk under more hygrothermally stressful conditions. The modeled results demonstrated high sensitivity to occupancy conditions, indicating that low temperature set points can be highly impactful to mold index and corrosion at both the roof deck and attic floor. The stress test case indicated that, although observed conditions did not prompt moisture concerns, the diffusion-port strategy should not be widely recommended as the sole method to mitigate attic moisture issues in hot-humid climates without further study.

Additional findings of this study include that unvented attics may boast improved extreme-weather resistance, as demonstrated by their reduced humidity levels during and directly after Hurricane Ian and Tropical Storm Nicole. Additionally, unlike in unvented-attic studies in conditioned attics where the highest mold risk is found toward the roof ridge, the roof deck in these unconditioned attics had higher mold risk lower down the roof slope. Several factors may influence this finding, but of particular note is the presence of a suspended radiant barrier, whose implementation may influence stratification trends and cause convective looping. Additional study is required to investigate the specific influence of radiant barriers on the effectiveness of vapor diffusion ports, as well as sensitivity to other construction strategies (such as the introduction of small amounts of conditioned air to the attic, different configurations of diffusion ports, and variations in attic airtightness). After further tuning the hygrothermal models, additional sensitivity studies beyond this preliminary modeling effort could also be performed to assess the impacts of climate, construction materials, roof reflectivity, and occupancy variation.

Table of Contents

List of Figures

List of Tables

1 Introduction

1.1 Background and Motivation

Placing space-conditioning ducts in the attic is appealing to architects and home builders for a few reasons: (1) space is limited in many homes, ductwork is bulky, and there may not be a route using interior walls and floors; (2) the design of homes focuses on the living space, and space to run the ductwork is usually an afterthought; and (3) construction is a competitive market and it is cheaper to run the ductwork through the attic than through the interior walls and floors. However, millions of homes in hot and humid climates are at risk of forming condensation on ductwork in unconditioned attics, potentially leading to mold growth and structural deterioration (see Figure 1). Energy efficiency measures such as cool roofs, radiant barriers, and interior radiative control coatings have the potential to save energy but can create potentially risky hygrothermal conditions in attics. These durability concerns can undermine the market acceptability of these energy efficiency solutions.

Figure 1. Condensation on ductwork (left). Mold growing on attic floor and ceiling joists as a result of dripping condensation from ductwork (right) [1]

Source: Bailes 2012

Moisture problems in vented attics in hot and humid climates are caused by multiple interacting factors:

1. **Radiation control:** Radiant control energy efficiency measures in hot climates work to make the attic significantly cooler by reducing radiative heat transfer to attic surfaces and ducts. Examples of radiant control measures include high mass roofing materials such as exterior tile, reflective exterior metal, and low-emissivity materials used at or near the interior roof deck known as radiant barriers. More reflective roof coverings result in cooler roof surfaces, thus

[1] https://energycodeace.com/site/custom/public/reference-ace-2016/index.html#!Documents/appendixdeligibilitycriteriaforradiantbarrierssectionra421.htm

transmitting less heat through the roof deck and into the attic, and can save up to 15% of the annual cooling load for single-story buildings (DOE 2011). Similarly, radiant barriers and interior radiative control coatings work by reducing the amount of radiative energy from the attic roof deck to the attic floor and the ductwork. Radiant barriers and interior radiative control coatings can reduce the radiation heat transfer by 90% (ASTM 2015a) and 75% (ASTM 2015b), respectively and attic-generated cooling loads by 34% and 24%, respectively (Fallahi et al. 2013). Home Energy Rating System scores are encouraging use of these radiant energy efficiency measures, as does the 2016 California Energy Commission's Residential Compliance Manual (California Energy Commission 2015). These technologies reduce energy gains to the conditioned spaces, but can place the surface temperature of the suspended ductwork below the dew point, increasing the possibility of condensation forming.

2. **Longer heating, ventilation, and air-conditioning runtime:** Heating, ventilating, and air-conditioning (HVAC) systems that run more continuously can fully cool the exterior surface of the ducts where they interface with attic air, increasing condensation concerns. The ducts also do not have time to warm between cycles, so moisture accumulation is more continuous. Higher efficiency variable-speed HVAC systems run longer than two-stage or single-speed systems. Low interior cooling set points also result in longer run times and can contribute to these HVAC runtime condensation problems. Over time, the "sweating" ductwork leads to wet spots on building material that can eventually lead to rot or mold (Figure 1).

3. **Insufficient duct insulation:** For the exterior duct-jacket surface to "sweat," it must be in contact with humid air that condenses upon meeting the cold surface. The exterior duct-jacket surface must become cold enough such that moisture in the air can condense on it. Condensation on exposed ducts usually occurs where the duct insulation is compressed, thereby diminishing the R-value. Wrapping ductwork with sufficient R-value increases the exterior surface temperature, and an airtight insulation jacket with Class I vapor retarder prevents the bypass of humid attic air to the colder inner duct surface. When these measures are properly implemented, condensation can be controlled. Less insulation also allows for more heat transfer from the duct air to the attic air. The reduced surface temperature of poorly insulated ducts increases the risk of condensation and mold growth, which can lead to negative health impacts and deterioration of the ductwork and HVAC system.

4. **Attic Ventilation:** During summer weather, vented attics in hot, humid climates introduce high dew point air to the attic, which can condense upon meeting the ductwork carrying cold air. During warm, humid weather, outdoor air entering attic vents contains approximately 80% more moisture than indoor conditioned air. This added moisture increases the dew point within the attic, making it easier for condensation to occur. Winter air is typically drier than conditioned indoor air. The airtightness of the ceiling/attic plane may also impact the humidity in the attic as moisture from activities like cooking and showering can migrate into the attic.

> Attic venting during dry winter conditions may help decrease condensation of interior generated moisture upon colder building surfaces.

The combination of these factors creates a situation in which ductwork surface temperature continually drops below the dew point, condensation occurs, and there is not enough time between HVAC cycles for the condensation to evaporate. Over time, the moisture level increases and eventually causes permanent damage to the roof framing and attic floor (Figure 1).

To deal with potential moisture issues in attics (in summer and winter), several moisture control strategies can be implemented:

1. Properly designed attic ventilation
2. Added/improved ductwork insulation
3. Sealing of air leaks
4. Dehumidifiers or interior air change/ventilation
5. Vapor diffusion ports.

The most common control strategy is to allow for adequate attic ventilation, which can vent moisture buildup in the attic out of the space to the outdoors if temperature and humidity levels are lower outside than at the attic vent. However, in hot and humid climates specifically, ventilation might also be a source of moisture problems (Rudd and Lstiburek 1998). The problems are more likely to occur when the humid air encounters the cold duct surfaces, which is why adding an insulation jacket around the ductwork, and thus preventing humid air from reaching the cold duct surface, can prevent duct sweating. Sealing air leaks from the conditioned space stops moisture migration from showers, cooking, etc. into the attic. Mechanical dehumidification can remove moisture in the attic, but comes at a substantial energy cost. More recently, vapor diffusion ports (an airtight but vapor-open membrane) have been posed as a potential solution for moisture control in attics (Lstiburek 2020).

Figure 2. Example application of vapor diffusion membrane over a ridge vent opening before the installation of final roofing materials (left), and attic view of vapor diffusion port with membrane over an off-peak vent opening (right).

Source: Charles Withers grants full permission to use and publish these photos.

This project focuses on the use of vapor diffusion ports (Figure 2) and buried attic ducts in hot-humid climates. The builder partner for this research effort, K. Hovnanian Homes, is a prominent production builder attempting to assess whether it could continue using attic space to house ductwork while anticipating new code requirements and minimizing additional material usage and changes to construction methods.

1.1.1 Existing Research on Vapor Diffusion Ports

Vapor diffusion ports are a recently developed concept for moisture mitigation in attics (Lstiburek and Cole 2017). A vapor diffusion port is a vapor-permeable membrane stretched over an opening in the roof ridge that allows water vapor to passively diffuse from the attic, but does not allow air or liquid water to enter or leave the attic (Figure 3). Water vapor is transported from the attic through the port to the outside.

This process is aided by thermal stratification and buoyancy in the attic space. Solar radiation absorbed by the roof deck drives thermal stratification of the air in the attic. As the air near the roof deck increases in temperature, buoyancy drives the air upward to the attic ridge, carrying along water vapor through advective transport. Both buoyancy and advective transport help create a higher concentration of water vapor at the ridge of the roof during the day. The vapor pressure gradient (higher inside the attic and lower in the outdoor environment) causes water vapor to diffuse through the vapor permeable membrane to the outdoor environment when the outdoor vapor pressure is lower (i.e., when temperature and RH are lower outside than inside the attic).

In an unvented attic, it becomes imperative to avoid conditions in which the roof deck becomes the vulnerable condensing surface, which can happen especially in cooler seasons when the surface temperature of the roof deck may be low, but the humidity in

the unvented attic (from the living space or outdoors) remains high. The performance of these diffusion ports has been promising in ASHRAE 169-2013 (ANSI/ASHRAE 2017) climate zones 1, 2, and 3, but the system design was pushed to the limit in ASHRAE 169-2013 climate zone 5 (Chicago, Illinois) (Ueno 2016). More data are needed around the design parameters (vapor permeance, vapor vent area, and roof slope requirements) of vapor diffusion ports to fully understand the mechanisms that drive the performance of these systems.

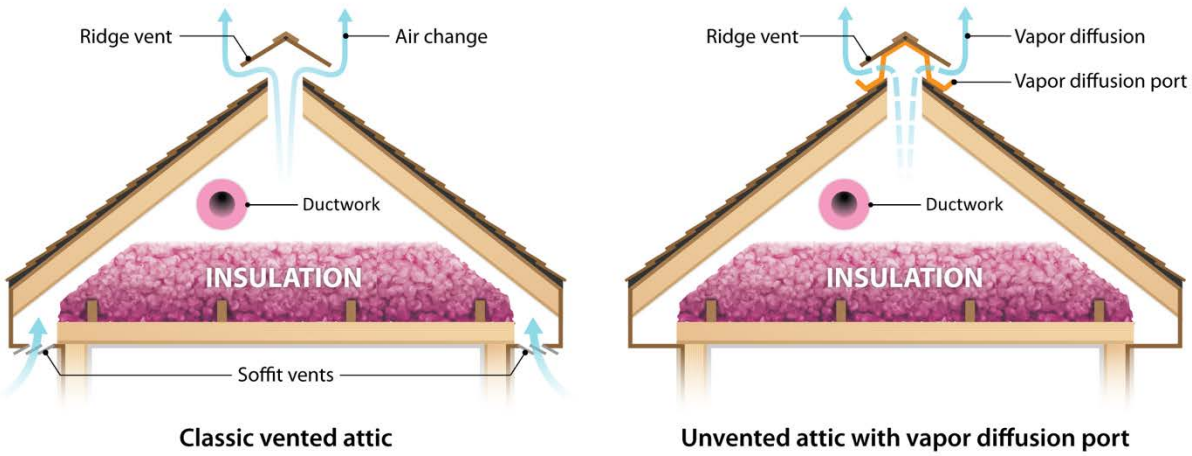

Figure 3. Standard vented attic (left) compared with an unvented attic with a vapor diffusion port (right)

Source: Lstiburek and Cole 2017

1.1.2 Buried Ducts in the Attic

Burying ductwork in insulation is not a new concept (Mallay 2016; Shapiro, Magee, and Zoeller 2013). The main purpose in burying the ductwork is to apply additional insulation to the insulated ductwork, thus reducing duct thermal losses. This energy saving strategy is a compliance path for California Energy Commission Title 24 codes (Wei et al. 2014), and 2018 International Energy Conservation Code (IECC 2018; ICC 2017).

However, although adding air-permeable insulation around ductwork insulates cold ducts from a hot attic, it still allows moist attic air to reach the duct-jacket surface that is now colder. This increases risk of condensation on buried ducts, which is why the model 201 requires increased duct-wrap insulation levels on buried ducts in hot-humid climates (R-13 compared to R-8 for the rest of the United States.). However, R-13 duct wrap is less prevalent, more expensive, and requires more space than typical R-8 duct insulation. The process of applying extra duct wrap around ductwork within confined workspace is very labor intensive, further amplifying installed costs. Although both IECC and Title 24 allow ducts to be buried in attic insulation to reduce thermal losses, there has not been rigorous hygrothermal research to determine if burying the R-8 insulated ducts in a sealed unvented attic without extra duct insulation is a viable solution—at least under specific conditions. If viable, the question becomes: what construction methods and materials are required to achieve expected energy savings with minimal moisture risks?

1.1.3 Project Motivation

With the moisture and durability challenges in hot and humid climate zones, the purpose of this research is to field validate solution strategies containing vapor diffusion ports and buried ductwork in unvented attics in hot and humid climates (Figure 4). A set of field experiments were set up and monitored through 9 months beginning in July 2022 and ending in May 2023, which offered a window into performance of each configuration during summer, winter, and a swing season. Because a longer observation period is ideal for durability assessments, these measurements were used as a basis to compare against hygrothermal models, which were run for multiple years (for more details, see Section 2.3).

The goal of the experiments was to identify and validate methods of enhancing energy efficiency and extreme-weather durability in hot-humid climates using simple construction methods.

The construction strategies evaluated included:

- Bury R-8 ducts in blown-in attic fiberglass insulation without using additional duct insulation or moving ducts to conditioned space.
- Seal attic and vent moisture via vapor diffusion ports to mitigate moisture issues.

Evaluation included:

- Measuring moisture performance in occupied experimental homes
- Observing resilience of homes in extreme weather (e.g., hurricanes)
- Modeling moisture and envelope durability performance to generalize and expand experimental observations.

Figure 4

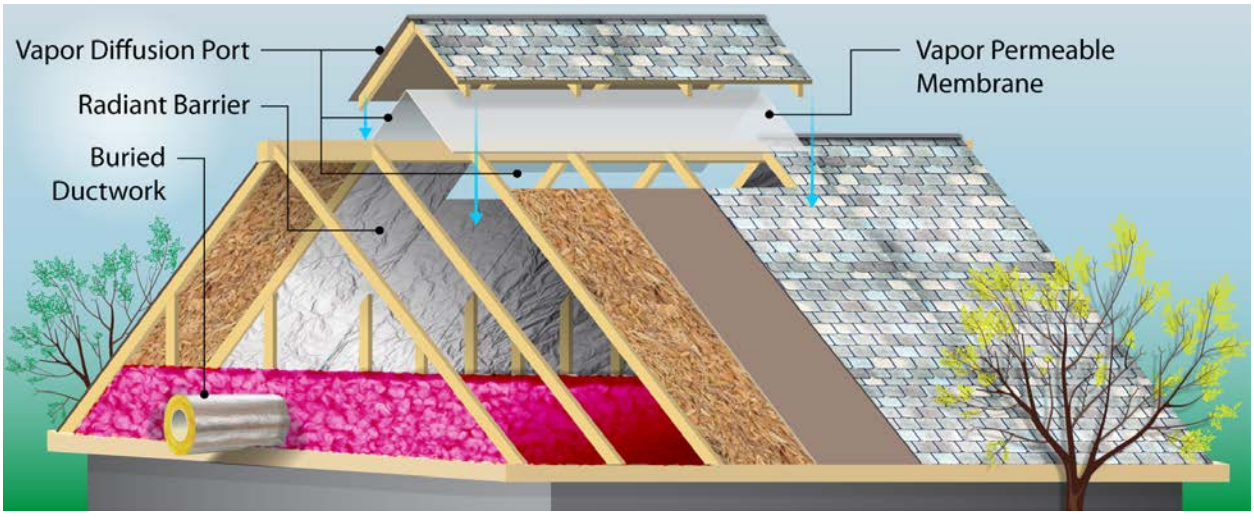

Figure 4. Diagram of an attic employing vapor diffusion ports, buried ductwork, and a radiant barrier

Source: NREL

1.2 Research Questions

The research questions for this project are as follows.

Can R-8 buried ducts work in hot-humid climates?

Although Florida's Energy Conservation Code does not list a minimum duct-wrap R-value for buried ducts in particular (ICC 2020), using R-8 buried ducts instead of the R-13 IECC model-code specified values effectively moves the air-vapor barrier closer to the air inside the duct. The temperatures on the exterior duct-jacket surface will be colder compared to those in the case of R-13 duct-wrap. Will condensation occur on the duct-jacket surface during the hot summer months?

Can unvented attics with diffusion ports mitigate moisture concerns from burying ducts?

Sealing the attics and adding diffusion ports provides a moisture control mechanism, because less hot and humid air can get close to the ductwork. Does this moisture control mechanism mitigate condensation concerns for the ductwork during times of active cooling?

Does the roof deck experience any moisture issues during cooler months in a hot-humid climate?

Humidity that enters the attic from the outside or from a home's occupancy can build up at the roof deck, especially without traditional air venting. This can be due to excessive latent loads within the home, insufficient ceiling airtightness, insufficient incidental dehumidification by duct leakage, or simply because of roof deck airtightness with insufficient diffusion-port area at the ridge. The "ping-pong effect," as described in Lstiburek (2016) based on observations of conditioned attics, notes that diurnal temperature cycling can push moisture into and out of wood products. The result is concentration of moisture toward the ridge because of the moisture gradient created by rising warmer air holding more moisture, coupled with adsorption-desorption cycling. Moisture can accumulate at the attic roof sheathing, especially when the roof deck is cold compared to the surrounding air.

What challenges and benefits does this altered construction pose to production builders?

Can the attics be sufficiently sealed with simple construction methods? Do the potential benefits from a durability and design standpoint outweigh the increased effort and fastidiousness required to implement these approaches at scale? Other potential benefits of sealing an attic could be better resilience to hurricane force winds, rain penetration, and floating embers.

1.3 Applicable Building Technology

The building typology that is applicable for the suggested construction methods are single-family detached and single-family attached homes with ducts in the attic in hot

and humid climate zones (IECC 1A and 2A). This project obtained access to single-family attached units and a single-family detached newly constructed home.

2 Experimental Approach

2.1 Durability Metrics

The durability metrics used to quantify the overall performance of the experimental configurations are as follows:

Surface Wetting

Wetting of the material surface may be a condition that will put moisture-sensitive materials at risk. Condensation occurs on any building material when the surface temperature drops below the dew point of the surrounding air. Extended periods of surface wetness can lead to material failure and mold growth. Moisture accumulation in and on wood surfaces can lead to mold growth and/or rot. Moisture accumulation on duct surfaces can drip and cause wetting and pooling on nearby drywall or wood surfaces. For the field experiments and modeling, the team identifies when condensation may be a concern and on which surfaces.

Mold Growth

Under humid conditions mold may grow on wood and even older dirty duct-wrap surfaces. When the wood surface moisture content rises above a threshold, it creates an environment that is conducive for mold to grow. The concern in unvented attics in hot and humid climates is near the attic ridge where moist conditions may be conducive for mold growth. Without allowing for moisture to escape, the moisture is concentrated near the ridge in winter as a result of the stack effect and moisture stratification. The north roof deck is at higher risk because the surface receives little direct sunlight and, as a result, is cooler than other roof decks during the day.

The amount of mold growth on a surface can be predicted by the VTT mold index model (Viitanen and Ojanen 2007). The calculations were adopted by ASHRAE 160 (ANSI/ASHRAE 2021). The premise of the model is that mold growth depends on temperature and RH experienced at the material surface. Mold is able to grow between 0°C and 50°C. Outside of these temperature bounds, the model assumes the temperature is either too cold or too hot for mold to grow. In this temperature range, if the RH of the surface is above a critical RH (a function of surface temperature and material sensitivity class), then the mold index will increase. The mold index declines slowly during long periods where the environment is not conducive for mold to grow (such as when the surface RH is less than the critical RH and the surface temperature is within the temperature bounds).

The model classifies materials with various mold sensitivity classes. Wood products are either classified as “very sensitive” or “sensitive.” The material’s rate of decline for mold index, unless specifically studied, is also dictated by ASHRAE 160 and depends on the sensitivity of the material. Highly sensitive materials also tend to experience faster mold decline.

The failure point according to ASHRAE Standard 160 is a mold index greater than 3.0. The VTT model classifies a mold index of 3 or greater as visual evidence of mold on the surface, while a mold index of less than 3 may still involve microscopic mold growth on the surface. A value of 0 indicates no mold growth.

Wood Rot

Beyond indoor environmental quality and health risks associated with mold growth, wood rot causes material decay and structural damage. Wood rot is an immediate threat to safety and the structural integrity of a building. Rot is considered likely when wood moisture content rises beyond 30% for extended periods of time without drying and can be initiated between 20% and 30% moisture content (Griffin 1977; Zabel and Morrell 1992). For unvented attics in hot and humid climates, the location of highest concern is the roof deck and trusses at the attic ridge.

Corrosion

In the context of a wood-framed attic, corrosion can have a significant impact on the structural integrity of metal fasteners. Corrosion risk is defined by ASHRAE 160 as the 30-day running average of the metal's hourly surface RH values reaching 80%. One consequence of corrosion on the metal fasteners is reduced load-bearing capacity, which leads to overall weakening of the attic structure. Additionally, compromised nails may not properly hold waterproofing membranes or shingles.

2.2 Field Experimentation

2.2.1 Methodology

We identified experimental sites in DeBary, Florida (Figure 5), which is located in Climate Zone 2A. This hot-humid climate is a common location for the partner production builder to build in. The site included four attached townhomes and one single-family dwelling directly east of the townhomes (Figure 6). All homes were two stories. The townhomes' conditioned floor areas ranged from 1,276 to 1,532 square feet and had attic floor areas of 889 to 940 square feet. The single-family home had a conditioned floor area of 2,987 square feet and attic floor area of 1,378 square feet. The townhome block was oriented east-west, and all homes had both northern and southern wall and roof deck exposure. No environmental shading was present in the new development. The dwellings were constructed according to the 2017 Florida Residential Building Code, 6th Edition. Roof slope was primarily 5:12. Additional photos of construction and instrumentation can be found in Appendix B.

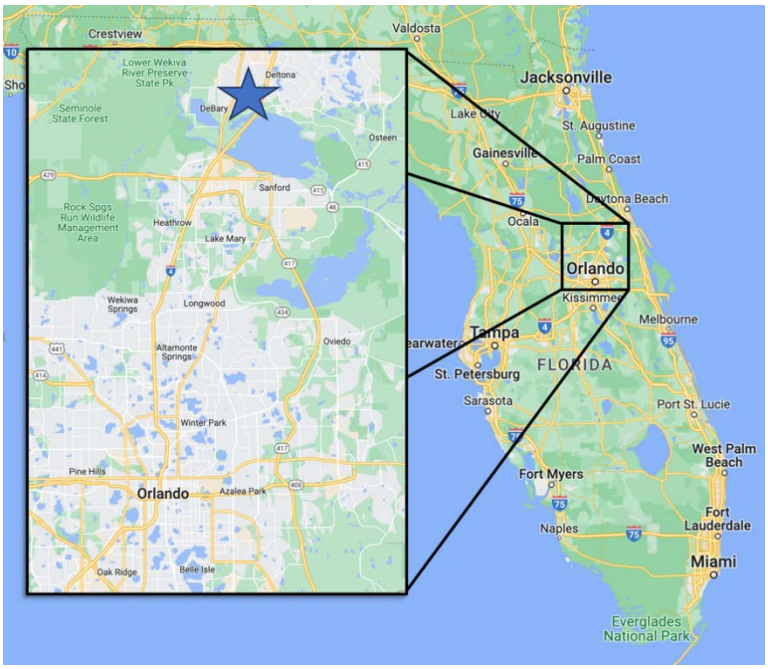

Figure 5. Location of the experimental sites in DeBary, Florida

Source: Google Maps

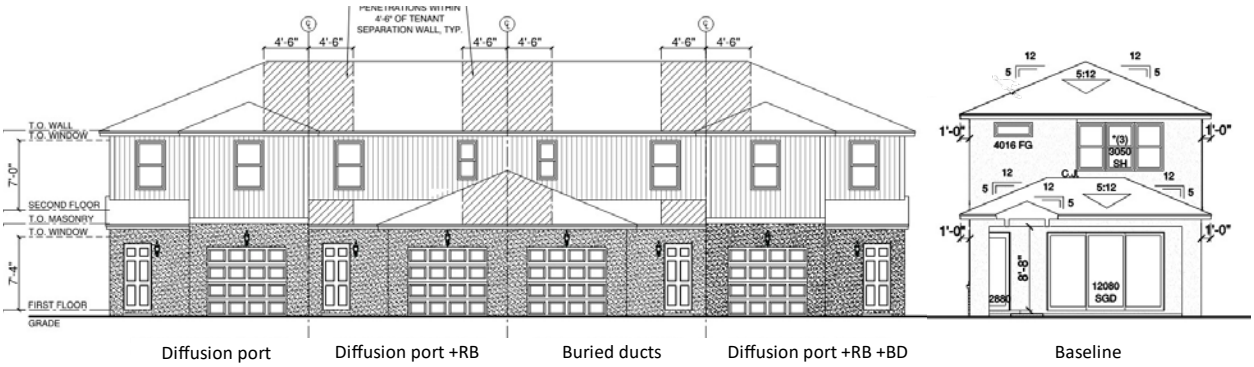

Figure 6. Rear (south) elevation of experimental townhomes and single-family home

Source: K. Hovnanian Homes

Roof decks in the development had off-ridge vents about a foot below the peak and continuous soffit vents along the eaves (Figure 55). Off-ridge vent areas were designed in accordance with building-code minimum requirements (1/300 of attic floor area). As described below, the experimental homes with diffusion ports did not have air vents. The experimental homes with diffusion ports had the same vent area dedicated to venting except that the vent cutouts were covered with Dörken Delta Foxx vapor-open (550 perms), airtight membranes. The townhomes' shared walls, including in the attic, were designed as firewalls with two layers of drywall and were firestopped at seams, which minimized communication between attic spaces (Figure 7). Ducts were all wrapped in R-8 duct wrap. Ducts that were buried had at least 3.5 inches (R-11) of

insulation blown on top of the ducts, per IECC-2018 R403.3.6. IECC-2018 R403.3.6.3 also indicates that buried ducts in climate zones 1A, 2A, and 3A shall have R-13 insulation and comply with Section 604.11 of the *International Mechanical Code* or Section M1601.4.6 of the *International Residential Code*. In Section 604.11 of the *International Mechanical Code*, the insulation shall be covered with a vapor retarder. This project intended to explore whether the unvented attic with diffusion ports could adequately mitigate moisture concerns so as not to require R-13 duct wrap.

Figure 7. Fire-rated party-wall assembly between townhome attics prior to final insulation blowing. The drywall strips over “Shaftliner” were used to cover panel seams. All panel edges were caulked (red).

Source: Withers and Martin 2022. Charles Withers grants full permission to use and publish these photos.

Table 1 presents the configurations used to assess each variable and the combination of variables and construction methods.

Table 1. Experimental Home Configurations

Short Name	Building Type	Unvented Attic and Vapor Diffusion Port	Radiant Control Measure	Buried Ductwork	Reason for Configuration
Baseline	Single-family detached	✗	✗	✗	Baseline attic
Buried Ducts	Townhome unit	✗	✗	✓	Buried duct effect
Diffusion Port Attic	Townhome unit	✓	✗	✗	Diffusion port performance
Diffusion Port + Radiant Barrier	Townhome unit	✓	✓	✗	Radiant barrier effect
Diffusion Port + Radiant Barrier + Buried Duct	Townhome unit	✓	✓	✓	Effectiveness of combined methods

2.2.2 Data Collection

2.2.2.1 Data Acquisition System

The data acquisition system comprises 5 stations (one for each dwelling unit). Each station had a basic topology as illustrated in Figure 8, which included a Campbell Scientific Inc. CR1000 data logger, AM25T thermocouple multiplexer, AM16/32 analog input multiplexer, cellular modem (Campbell Scientific Inc. Cell210 or Sierra Wireless RV50), and 12-V power supply with 7 ampere hours backup battery. Appendix A contains additional description of the data acquisition protocol.

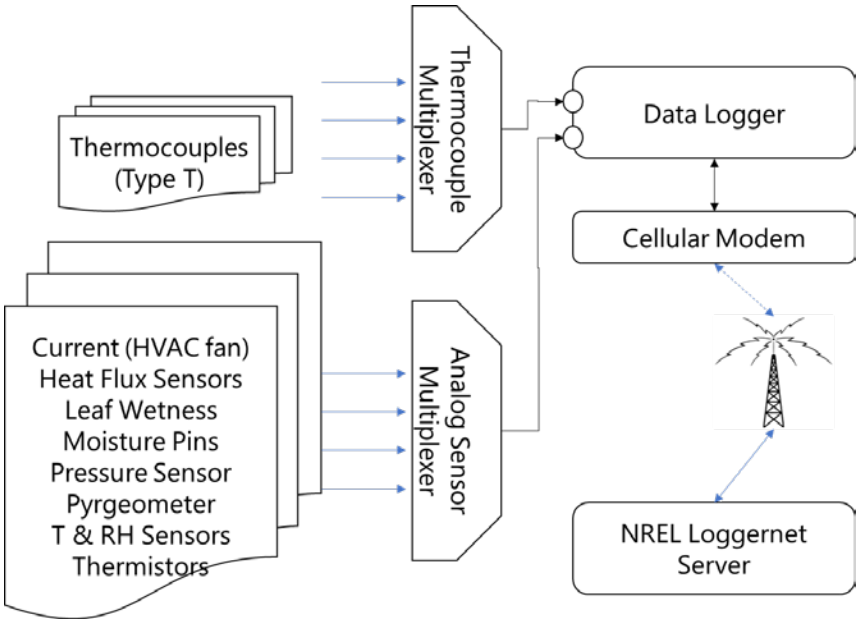

Figure 8. Typical data acquisition system station

Source: Ross Philip, Mountain Energy Partnership

2.2.3 Instrumentation

Homes were instrumented according to Appendix B. Typical details are shown in Figure 9, Figure 10, and Figure 11.

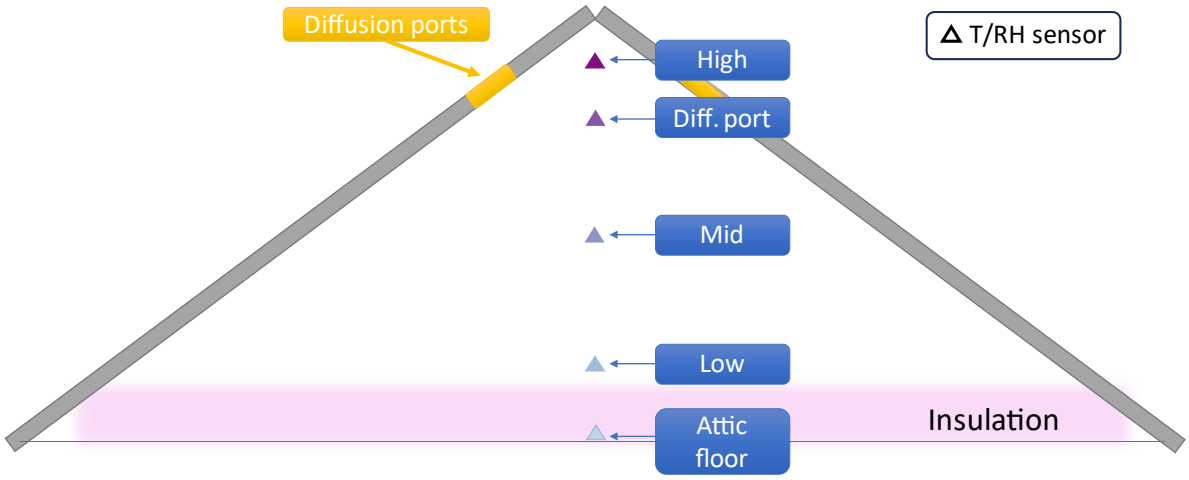

Figure 9. Temperature and RH sensor locations spaced vertically to measure attic air conditions

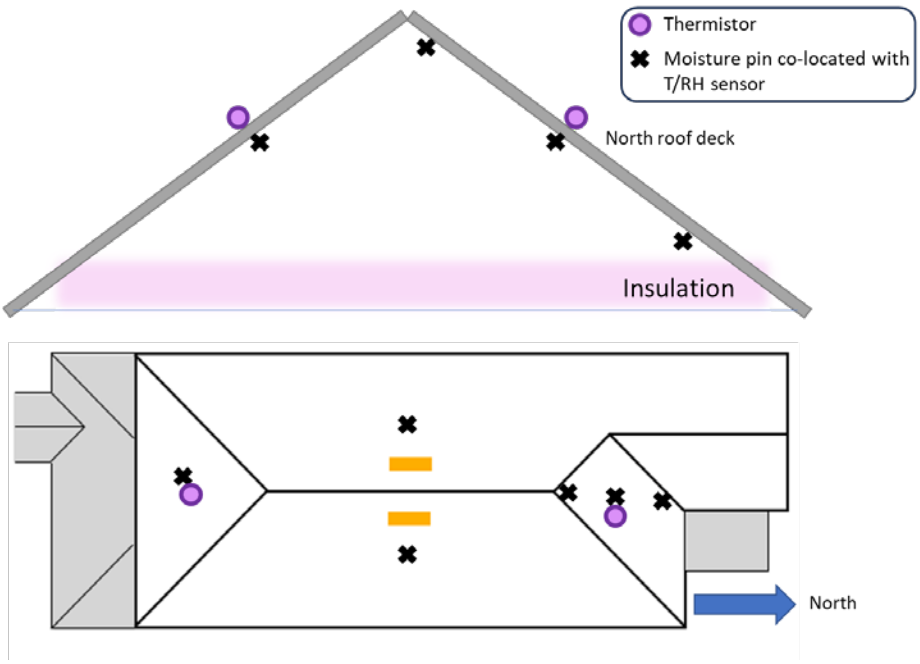

Figure 10. Representative temperature/RH and moisture-pin locations along baseline roof deck

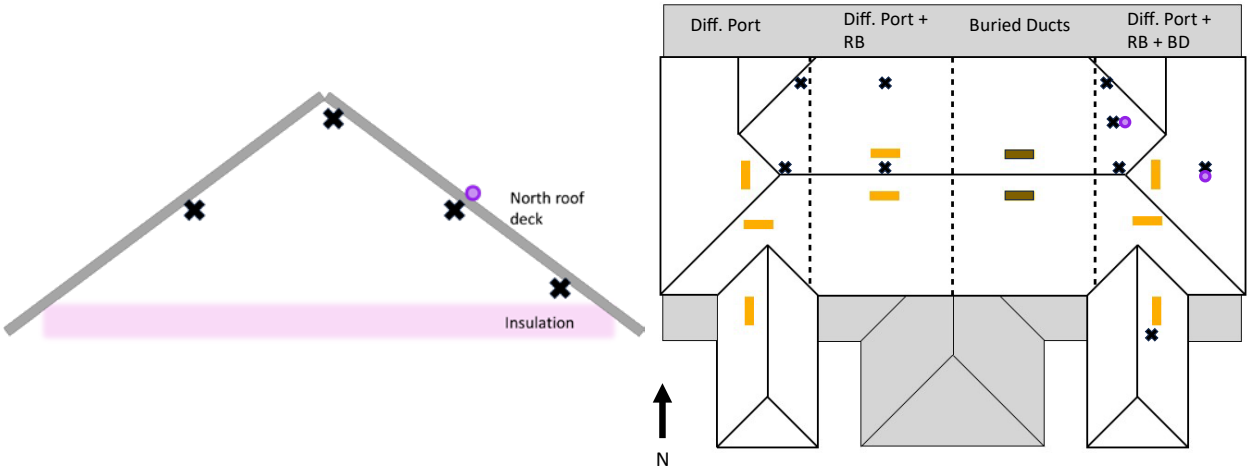

Figure 11. Representative temperature/RH and moisture-pin locations along townhome roof decks

Appendix A.2 lists the sensor types used in the study. Voltage output sensors were read directly by the data logger. Current output sensors were converted to voltages using 1% accuracy, 100-Ohm low thermal coefficient completion resistors. Thermistors were read with a 2.5-V excitation voltage divider circuit; temperature was calculated by the Hart-Steinhart equation. Thermocouples were read directly by the data logger, which includes an onboard platinum resistance thermometer to provide a reference temperature junction at the thermocouple multiplexer.

The wood moisture pin sensors were fabricated by Phillip Childs of Oak Ridge National Laboratory based on the lab's industry standard specifications, and resistance was measured with a 2.5-V excitation voltage divider circuit. As illustrated in Appendix A

Figure 46, the very large resistance encountered by the pins at low moisture content (>50 megaohms at 10% moisture content) necessitated a post-installation redesign of the voltage divider circuit to desensitize the measurement to data logger input impedance. The configuration was adjusted as shown in Appendix A Figure 45 to correspond with the circuitry demonstrated by Miller et al. (2016). See Appendix A for details.

Moisture pin measurements are often adjusted to fit the specific wood species, but no adjustments were applied to the moisture content readings in this case because raw moisture content readings were not high enough to merit detailed attention and adjustments to convert to plywood or oriented strand board (OSB) are not uniformly agreed upon and can be product-specific.

2.2.3.1 Occupancy and Occupancy Simulation

The experimental homes served as model homes at first but later became occupied one by one. In an attempt to ensure that attic and living space conditions were representative of an occupied home, space conditioning was kept on in the unoccupied homes, and an occupancy simulation plan was developed to introduce latent gains. Details about occupancy simulation and occupancy dates can be found in Appendix A.4.

2.3 Modeling

Although the field experiments provided tangible examples of the solutions and some potential outcomes, hygrothermal modeling was required to simulate more stressful conditions not observed for long durations during the field experiments. Variations in occupancy set points, occupant moisture generation, levels of attic floor and roof deck air sealing, outdoor weather conditions, and construction assembly alternatives can potentially lead to different outcomes in terms of moisture durability of the roof deck and attic floor. These factors were adjusted in order to hygrothermally “stress test” the assemblies without having to physically evaluate each variation.

Because both the roof deck and attic floor were monitored in field experiments, both were modeled hygrothermally and assessed for performance in terms of mold index and, in the case of the roof deck, moisture content and corrosion.

We chose to use WUFI Pro 6.7, the industry-standard hygrothermal simulation tool, which employs a physics-based approach to modeling the intertwined moisture and energy transport through assemblies. Table 2 details the modeled assemblies.

Table 2. Basic Attributes of Modeled Construction Assembly Components for Attic With Diffusion Ports, Buried Ducts, and a Radiant Barrier

Construction Assembly	Component (listed outside to inside)	Thickness (inches)	Thermal resistance (°F-ft^2-hr/Btu)	Permeance (perms)
Attic Floor/Ceiling	Low density fiberglass insulation	9.0	30.0	11.82
	Gypsum board	0.5	0.442	42.94
	Interior surface: latex paint	N/A	N/A	9.00
North Roof Deck	Asphalt shingles	0.2	0.109	0.70
	Felt	0.03	0.001	6.67
	Plywood/oriented strand board[a]	0.5	0.859/0.783	0.24/0.32
	Radiant barrier air gap; metallic coating	0.39[b]	1.420	451.28

[a] The home with diffusion ports, buried ducts, and radiant barrier used plywood for its roof decking. The hypothetical stress case described in Section 2.3.1 employed oriented strand board given that it is more susceptible to mold and rot. Properties of both materials are therefore provided in Table 2.

[b] Note that although the thickness of the air gap between the radiant barrier and the roof deck was greater than 0.39 inches, using thicker metallic air layers yielded results that aligned less with the temperatures and relative humidities experienced at the roof deck surface. A discussion of challenges modeling the radiant barrier and the impact on the results is included in the Discussion and Conclusions section.

Monitoring positions of interest included the top of the attic floor gypsum board and both the interior and exterior surfaces of the roof deck OSB. These assemblies are made of organic materials and have the highest risk of failure.

The modeling approach was to first model the observed case, align the model as closely as possible with measured results, and then introduce stress test scenarios.

The data points used for comparing the model to the field measurements included surface temperature and RH at the interior surface of the roof deck and the top surface of the attic floor drywall because these data points are used for failure analysis. Moisture content could have been used as a point of comparison, but moisture-pin measurements were considered rough estimates used primarily to observe trends, not direct measurement of gravimetric moisture content. Post-processing adjustments (discussed in Appendix E) were made to the modeled surface temperature and RH based on monthly biases for each modeled feature.

2.3.1 Stress Testing

Because weather and attic and living space boundary conditions are interdependent, regression models were used to predict attic and living space conditions based on hypothetical stress test alterations. Given that the field experiments collected data for

summer, winter, and a swing season (fall), the data upon which the regression models were based covered virtually all anticipated weather conditions. The primary differences in the stress test weather were long-term trends and the duration of more hygrothermally stressful conditions. The chosen stress test weather data were ASHRAE RP 1325's most hygrothermally stressful year for the nearby location of Daytona Beach, Florida (Salonvaara 2011). This data set is referred to as "ASHRAE Year 1" below.

The living space conditions were estimated using a regression model that predicts hourly living space conditions as a function of climate conditions, and the attic conditions were estimated using a regression model that predicts hourly attic conditions as a function of climate conditions and living space conditions. Where predicted temperature or RH values demonstrated seasonal bias using a linear regression model, we used a decision tree regression model, allowing for differing resulting conditions depending on, for instance, time of year or any other independent variable. For interior conditions (attic and living space), a linear regression model or decision tree regression model (per the procedure mentioned above) was employed, where the observed conditions served as the training dataset. Five-fold cross validation was used to quantify root mean square error (RMSE), mean absolute error, and mean bias error (MBE)—metrics that were used to ensure correlation between attic conditions, living space conditions, and exterior conditions. Results of the regression model fitting can be found in Appendix E.

Cooler temperatures, provided they are above freezing, lead to higher moisture risk. To simulate more hygrothermally stressful occupancy conditions, we artificially lowered living space temperature set points beyond the regressed values based on the following rules:

- If the regressed indoor temperature fell between the observed set point (20°C) and 16.7°C, it was reduced by 1°C to account for a new set point of 19°C with similar dead band to that in the observed case.
- All regressed indoor temperatures below 16.7°C were brought up to 16.7°C.
- If the regressed indoor temperature was above the existing cooling set point (22°C), it was reduced to the new cooling set point of 20°C.
- If the regressed indoor temperature was between 20° and 22°C, the temperature was reduced by 2°C.

We did additional post-processing on living space conditions to further increase stress test humidity levels by 10%, as listed in Table 3. This increase in RH was meant to represent higher occupancy conditions. We performed attic temperature and RH regressions after this manipulation of living space conditions. We also did post-processing to increase attic RH by 5% beyond the regression model conditions to represent a likely end range of stress test humidity conditions in the attic, accounting for possible limitations in the regression models that were not trained on high-occupancy conditions.

Once the models for the existing home with buried ducts, radiant barrier, and diffusion-port attic construction were established and adjusted to simulate the observed case, the roof deck and attic floor/ceiling assemblies were stress tested using the following scenarios:

Table 3. Hygrothermal Stress Test Conditions Modeled

Parameter	Observed—Measured in Diffusion Port + Radiant Barrier + Buried Duct Case	Stress Test Case
Weather File	Observed	ASHRAE Year 1 (ASHRAE RP 1325 most hygrothermally stressful year)
Roof Orientation	North	
Shading on Roof Deck	No shading	100% shaded
Roof Deck Material	Plywood	Oriented strand board
Roof Color	Dark roof color	Light roof color
Attic Ventilation Rate (to outdoors)	As calculated from field measurements, per protocol described in Appendix C, Test 1: ~40 ACH_{50} or 1680 cfm_{50}.	
Living Space-to-Attic Air Exchange Rate	As calculated from field measurements, per protocol described in Appendix C: ~760 cfm_{50}.	
Occupancy (humidity)	As measured	Higher occupancy (higher humidity in both living space and attic): 10% higher RH in living space; 5% higher RH in attic
Space-Conditioning Set Points	Heating set point: 18°–20°C/64°–68°F[a] (observed)[b] Cooling set point: 22°C/72°F (observed)	Heating set point: 17°–19°C/62°–66°F Cooling set point: 20°C/68°F
Duct Leakage	As measured: 29 cfm total duct leakage[d]	

[a] Per return-air temperature measurements

[b] Data from return-air temperature measurements indicate a consistent cooling set point at 22°C but a varying heating set point between 18° and 20°C.

[c] Per return-air temperature measurements

[d] Per DeltaQ test protocol

The stress case employs features that would lead to cooler, more humid conditions. We included shading and a cool roof because both would contribute to lower temperatures. We chose the “ASHRAE RP 1325 Year 1” for Daytona Beach because it was the most hygrothermally stressful weather year in close proximity to DeBary, Florida, existing in RP 1325’s database. A comparison between the observed weather and ASHRAE RP 1325 Year 1 weather for Daytona Beach can be found in Appendix D. The comparison indicates that the ASHRAE Year 1 weather is more hygrothermally stressful in the

winter, and the two datasets differ in the summer in that the observed weather is slightly warmer but also more humid, and the observed summer weather is rainier with less solar radiation, but also less windy. Considering that the modeled stress test case includes 100% shading, the impact of solar radiation in this case is minimal. Rain and driving rain, although indicative of the “wetness” of the weather, do not directly influence the simulation of the modeled roof in WUFI because no leaks are assumed based on a properly built, newly constructed roof, and the asphalt shingles have zero values for liquid transport coefficients, meaning no rain is absorbed into the roof assembly. Therefore, temperature and humidity are more indicative of hygrothermal stress in this case.

In theory, the ducts could be air sealed more effectively than what we measured, which would be a hygrothermally more stressful case (although more energy-intensive), but the assessed air leakage was already low, so the stress test situations reflect the as-is scenario.

3 Results and Findings

3.1 Field Experimentation Data Analysis

Prior to analyzing the attics in terms of moisture durability, we took field measurements to assess the airtightness of individual components and compare constructions. Monitoring of the experimental homes began between May and July of 2022 and ended in May 2023 because of project time constraints.

3.1.1 Airtightness Tests

Currently, there is not an established standard test to determine how well an unvented attic is sealed from the outdoors. The current practice within home rating programs is to test the house airtightness twice—once with the attic hatch to indoors closed and again with the attic hatch open. Table 4 compares airtightness results of the baseline attic and the attic with all measures included. Comparing air leakage with the attic hatch closed versus open provides an indication of how well air-sealed the roof deck is compared to the ceiling. If air leakage vastly increases when the attic hatch is opened, it means the roof deck is relatively leaky; however, it does not accurately determine how much the attic leaks directly to outdoors. A guarded blower test can determine this but is difficult and not practical outside research applications.

Table 4. Whole Building Airtightness With Attic Hatch Open and Closed

Unit	Air Changes per Hour at 50 Pascals (ACH_{50}) Attic Hatch Closed	ACH_{50} Attic Hatch Open (excluding attic volume) [2]	ACH50 Attic Hatch Open (including attic volume)	Hatch Open Versus Hatch Closed (% increase ACH_{50})
Baseline	4.3	12.3	11.1	158%
Diffusion port + radiant barrier + buried duct	5.4	9.7	7.9	46%

Table 4 demonstrates that the baseline (vented attic) roof deck had significantly greater outdoor air exchange compared to that of the unvented attic with diffusion port, radiant barrier, and buried ducts, as would be expected. The code requirement for whole-building airtightness in Florida is 7 ACH50. Both homes pass the whole-home airtightness requirement with the attic hatch closed. However, even if the attic were

[2] Attic volume was excluded initially from whole-unit airtightness calculations because the primary air barrier is located at the ceiling drywall. Both attic-hatch-open and attic-hatch-closed tests were performed using this same volume for the sake of comparability. A calculation was added to compare airtightness metrics for a case where the roof deck is considered the primary air barrier.

considered to be inside the air barrier (including the attic volume in the air-leakage calculation with the attic hatch open, and thus considering the roof deck to be the primary air barrier), neither attic would be considered reasonably sealed (by definition of considering the roof deck the primary air barrier instead of the ceiling). Still, the attic with diffusion ports + radiant barrier + buried duct clearly has far less air exchange than the baseline (vented attic).

This may mean that further air sealing would further emphasize the observed trends from this study. Overall, we see that the "unvented" attic with diffusion ports is indeed relatively sealed compared to typical construction, but further study may be needed to assess reasonably "sealed" roof decks.

After substantial construction completion, each home underwent whole home multipoint infiltration testing per ASTM E779. The results of these tests are provided in Table 5. The whole house infiltration value for the diffusion port + radiant barrier + buried duct attic was somewhat higher during this test (6.0 ACH50) compared to the later attic-hatch-closed test (5.4 ACH50). This could be due to inherent test uncertainty or because finishing touches on the homes increased airtightness.

After the whole home infiltration evaluations, the attics were pressurized using the blower door and tested at escalating pressures using TECLOG 4 (The Energy Conservatory 2023) until a pressure difference of at least 50 Pa was reached, and the results were converted to ACH50 using the best fit line. Results for attic infiltration rates are also found in Table 5.

Table 5. House and Attic Total Leakage Test Results of Three Townhomes With Unvented Attics

Leak Test	Diffusion Port (attic volume=2,485 ft^3)	Diffusion Port + Radiant Barrier (attic volume=2,308 ft^3)	Diffusion Port + Radiant Barrier + Buried Ducts (attic volume=2,485 ft^3)
House ACH_{50} total—attic hatch closed	5.6	6.4	6.0
Attic ACH_{50} total	40.6	44.4	54.3

The baseline home and the home with buried ducts only could not be pressurized given their level of venting, so we do not present infiltration metrics. The reported air change values are qualitatively high for the attics, and it is important to note that future air sealing strategies may be more effective than simply boarding off and foam sealing the soffit vents, as was done in this case.

3.1.2 Temperature Data

As experiments were underway, we recorded return air temperature and RH as a proxy for living space conditions and set points. It was not economical or practical to install all

sensors in all five homes, so some homes had sensors in the return air ducts, while others had sensors at the attic floor, depending on what measurements we were focused on. The return air sensors act as the best proxy for set point temperature without requiring thermostat monitoring, but the attic floor temperatures are also indicative of living space temperature trends, as seen by the alignment between these sensors in the diffusion-port + radiant barrier + buried duct home (Figure 12). Figure 13 and Figure 14 zoom in on a single representative summer and winter day, demonstrating that data were smooth and well represented by the 24-hour averages, except that zooming in helps identify thermostat setbacks. Minute-level data did not reveal additional trends.

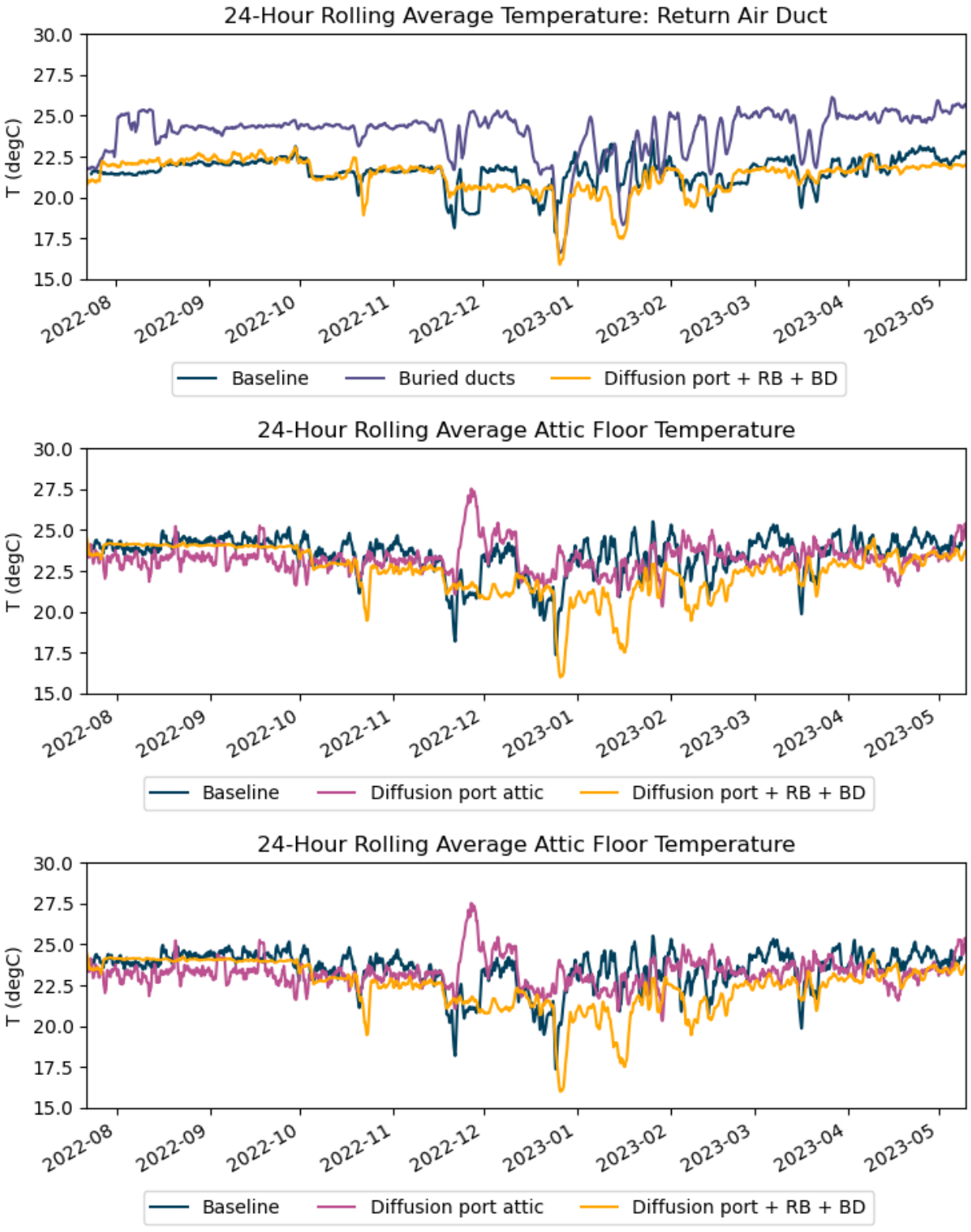

Figure 12. Home operation and impact of set points on attic conditions

RB = radiant barrier, BD = buried ducts

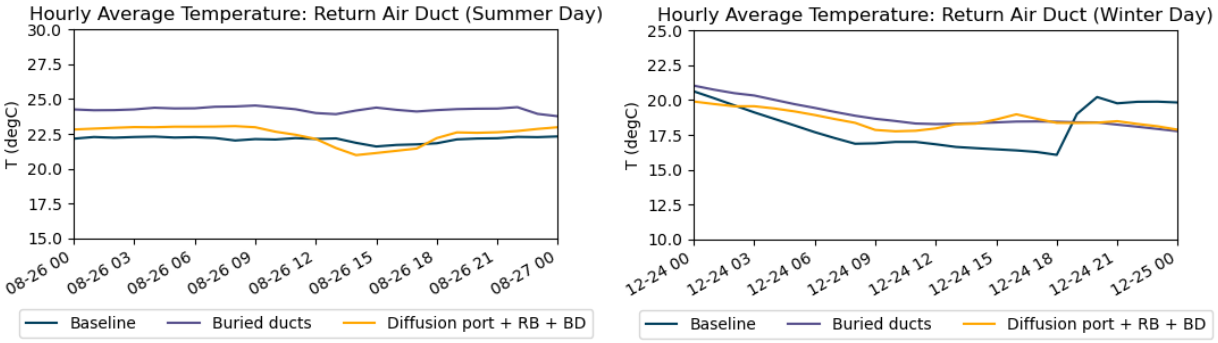

Figure 13. Hourly return air temperatures during representative summer and winter days showing smooth trends in temperature data

RB = radiant barrier, BD = buried ducts

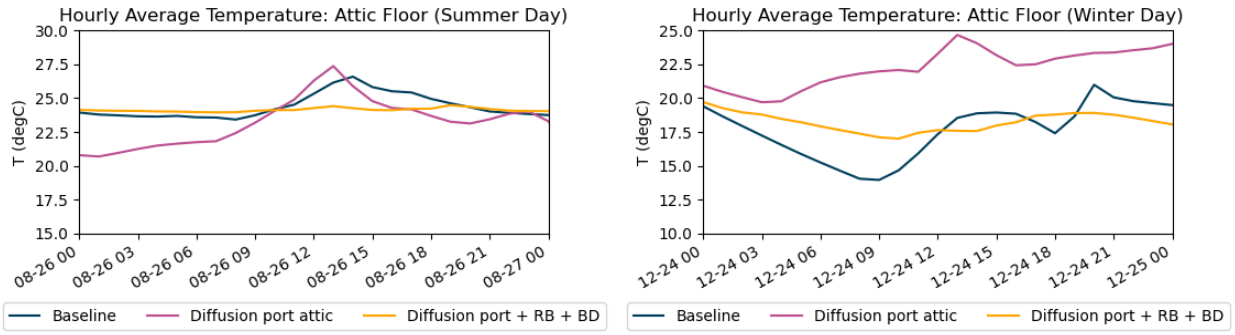

Figure 14. Hourly attic floor temperatures during representative summer and winter days showing smooth trends in temperature data

RB = radiant barrier, BD = buried ducts

The monitoring plan called for placing the attic floor temperature sensors directly on top of the ceiling drywall and then burying them under the full depth (at least 10 inches) of attic insulation. When the sensors were removed at the end of the test period, it was discovered that some insulation had been displaced or disturbed, and the attic floor sensors in the diffusion port + radiant barrier case were buried under only two inches of insulation. This sensor is not represented in the figure due to its lack of representation of attic floor temperatures. The baseline, diffusion port, and diffusion port + radiant barrier + buried duct homes have similar indoor air conditions for summer but start diverging in winter. The buried duct home's occupants seem to use a higher cooling set point, and the home is thus perhaps not as much of a worst-case condition as it could have been. This emphasizes the importance of stress test modeling mimicking more cooling. Overall, there is no evidence of daily temperature setbacks during summer, but all homes show some indication of winter setbacks during the day, particularly the baseline home. There is a spike in heating around 6:00 p.m. each evening.

3.1.3 Seasonal Data Insights

We observed temperature and RH trends throughout the period of performance for the duct-jacket surface, attic floor, roof deck, and attic air.

3.1.3.1 Duct Surface

Measurement of duct-jacket surface RH is a relatively simple method to evaluate the potential for moisture issues such as mold or condensation. Given several variables involved in contributing to mold growth, there is no specific RH value that can predict duct-jacket surface mold growth, but long-term RH averages greater than 80% should be avoided to minimize mold growth risks. Consecutive daily average duct-jacket surface RH levels greater than 90% indicate a high probability of a wet surface. Figure 15 shows hourly average duct-jacket surface RH during a hot humid period requiring cooling and also during a cold weather period requiring heating. The period from December 24–25 had outdoor temperature lows near freezing followed by a gradual warm-up. We noticed a general diurnal pattern for each attic configuration, in which the duct-jacket surface RH increases during the day and decreases overnight. Duct-jacket surface RH is not only influenced by the space conditioning runtime, but also by daily attic material adsorption and desorption of moisture. Duct-jacket surface RH was higher during the summer than during colder winter weather. The duct-jacket surface RH in winter was almost always well below 80% RH.

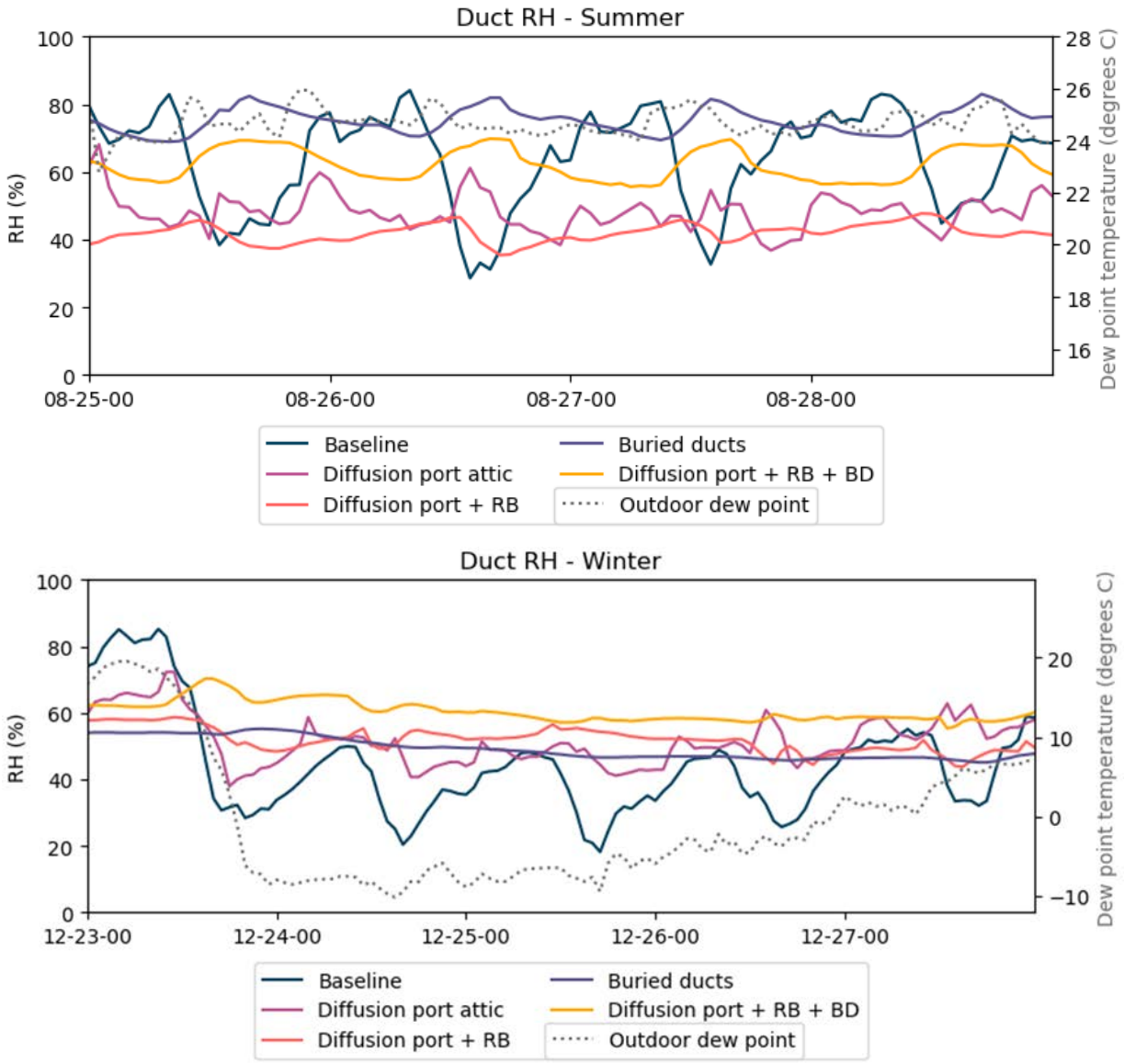

Figure 15. Duct jacket exterior RH fluctuations during representative periods within the heating and cooling seasons, by configuration

RB = radiant barrier; BD = buried ducts

Figure 15 shows that the baseline attic displayed higher peaks and the greatest diurnal cycling in duct-surface RH. Summer duct-jacket surface RH was greatest for the buried ducts in a vented attic. Buried ducts may increase RH on the duct-jacket surface in the summer, in part due to lower surface temperature when the outdoor dew point is high. During winter heating, however, the duct surface is warmed, which helps decrease the surface RH and condensation potential. The added insulation of buried ducts further buffers the duct-jacket surface from fluctuations in both temperature and RH.

In unvented attics with radiant barriers, duct-jacket surface RH showed the least variability, largely a result of reduced variability in attic temperature. In these

experimental applications, the radiant barrier helped shield lower attic materials from roof radiant heat during sunlight hours, but the air between the radiant barrier and roof deck still becomes hot. In a vented attic, this hot air will rise up towards upper attic vents and exit the attic, minimizing total heat transfer into the attic. In the unvented attic test design, however, the hot air cannot vent, thereby resulting in a hotter attic compared to a conventionally vented attic with a radiant barrier. As a result of temperature stratification, the hottest attic air temperatures are near the roof peaks. The warmer attic temperature helps decrease attic air RH, and the unvented attic reduces the moisture content from outdoors during the summer. During the winter when outdoor air is drier, the primary moisture source is usually from the indoors. The vapor diffusion port helps transport attic moisture to the outdoors.

RH and leaf wetness measurements did not indicate condensation on the outer jacket of the duct insulation of any of the experimental homes. It should be noted that the duct surface sensors were placed on the bottom of the duct jacket near the supply plenum and not elsewhere on the duct-wrap exterior surface. The bottom location allowed the opportunity to evaluate the coldest part of the exterior duct-wrap surface and possibly catch the influence of any moisture that may have run down from upper surface areas. The attic air dew point temperature usually increases with height, so it is possible that the top of duct-wrap surface RH was higher than the measurements noted on the bottom. In our visual inspections during removal of sensors and equipment, we did not find moisture on the top or bottom or on top of the drywall ceiling below the ducts.

In order to examine the relationship between burying ducts, venting, and active cooling, duct-jacket surface conditions were compared during summer when the outdoor dew point exceeded 20.6°C (69°F), indicating humid outdoor conditions that also called for significant cooling. Table 6 shows that the interior temperatures and cooling set points seem to be comparable to one another during the cooling season, but that RH at the bottom of the duct-jacket exterior surface varies significantly, as seen in Figure 15, Figure 16, and Figure 17. Burying the ducts was shown to be associated with increased duct-jacket surface RH, as predicted. Table 6 and Figure 17 also show that using diffusion ports with unvented attics may reduce duct-jacket surface RH, as demonstrated by comparing the buried-duct results with those of the diffusion port + radiant barrier + buried duct. Again, no reliable data were able to be collected for the living space conditions in the unit with diffusion port + radiant barrier, so results for that unit are not shown.

Table 6. Conditions at Exterior Duct-Jacket Surfaces During Summer Period When Outdoor Dew Point Temperature Was Greater Than 20.6°C

Configuration/Location	**Mean** [and 25th, 50th, 75th percentile] **outdoor dew point temp (°C)**	**Mean** [and 25th, 50th, 75th percentile] **outdoor temp (°C)**	**Mean** [and 25th, 50th, 75th percentile] **RH at bottom of duct jacket (%)**	**Mean** [and 25th, 50th, 75th percentile] **temp at bottom of duct jacket (°C)**	**Mean** [and 25th, 50th, 75th percentile] **living space temp (°C)**	**Mean** [and 25th, 50th, 75th percentile] **temp at attic floor (°C)**
Outdoor	**23.7** [23.0, 23.8, 24.5]	**28.1** [25.5, 27.3, 30.2]				
Baseline			**60.0** [47.3, 64.9, 73.6]	**30.3** [24.1, 26.9, 35.4]	**21.9** [21.6, 21.9, 22.2]	**24.1** [23.5, 23.9, 24.7]
Buried Ducts			**71.9** [68.4, 71.8, 75.5]	**22.9** [22.0, 22.6, 23.5]	**24.1** [23.8, 24.3, 24.6]	
Diffusion port			**46.5** [42.0, 46.2, 50.4]	**27.8** [21.3, 25.6, 32.7]		**23.3** [21.7, 23.4, 24.6]
Diffusion port + Radiant Barrier + Buried Ducts			**62.0** [57.7, 61.8, 66.9]	**20.2** [18.6, 20.8, 22.0]	**22.2** [21.6, 22.4, 22.8]	**24.0** [23.9, 24.0, 24.2]

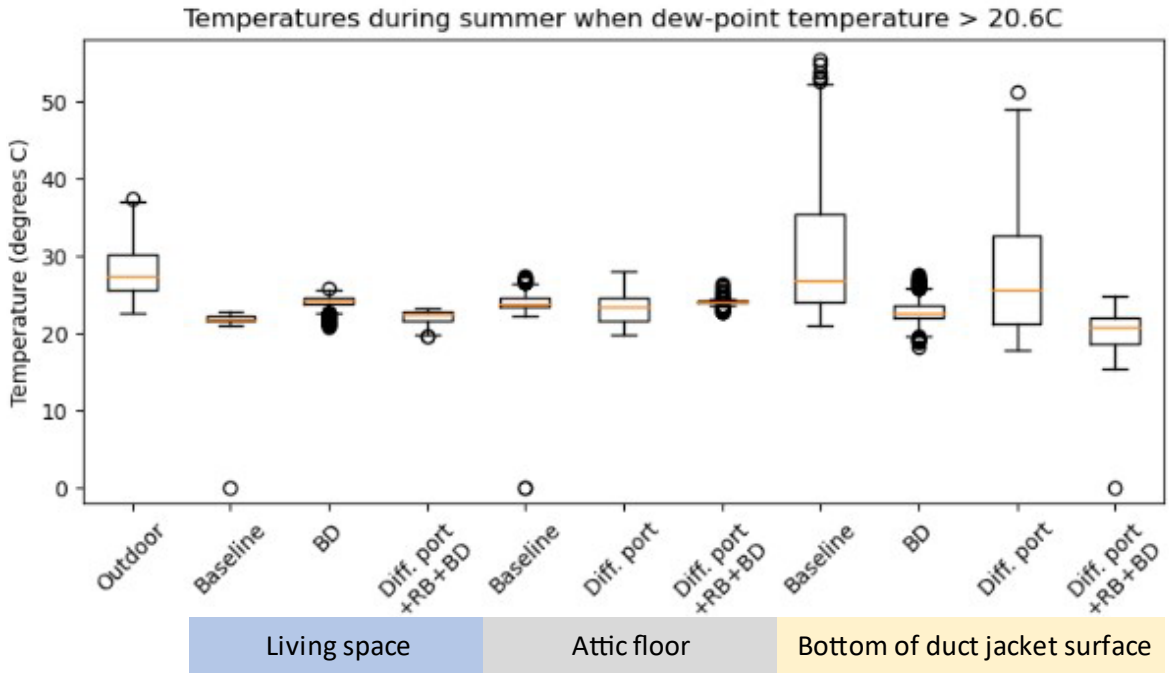

Figure 16. Box plot of hourly average temperatures across experimental homes during cooling conditions demonstrates differences primarily in duct jacket surface temperatures

Boxes represent the first to third quartile range, horizontal orange lines indicate the median, whiskers (vertical line with horizontal cap) indicate first quartile - 1.5 times the inter-quartile range and third quartile + 1.5 times the inter-quartile range, and circles indicate data points falling outside of whiskers.

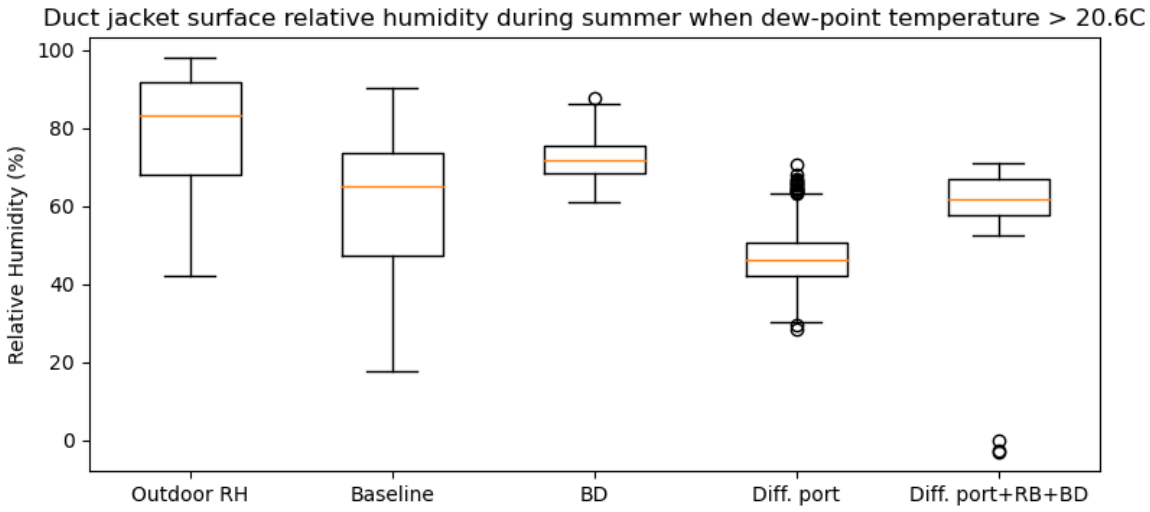

Figure 17. Box plot of hourly average duct jacket surface RH across experimental homes during cooling conditions

Attic floor conditions just beneath the ducts indicate both general attic floor durability and absence of duct condensation. Figure 18 shows that 24-hour-averaged RH remains below 80% for all attic floors where sensors were present, suggesting that likelihood of duct sweating was low, and that attic floor material durability risk was also low.

3.1.3.2 Attic Floor

Figure 18. Attic floor conditions across experimental homes

RB = radiant barrier; BD = buried ducts

How occupants operate their homes can have profound impacts on temperature and RH. Small differences in temperature and RH between each home should not be interpreted as greatly indicative of performance but, as we mentioned previously, attic floor temperature can act as a rough proxy for living space set point conditions. The swing seasons call for less space conditioning and reduce differences in temperature between attics.

Zooming into typical representative days within summer and winter (Figure 19), we can see that even during hours when ambient RH is very high the attic floor RH remains safely below 80%. Although it should be noted that home operation accounts for some variation in attic RH, the baseline home clearly derives some short-term drying benefit from venting in the winter, at least when ambient RH is mild. On the whole, however, the baseline home's RH is most susceptible to fluctuations in ambient RH.

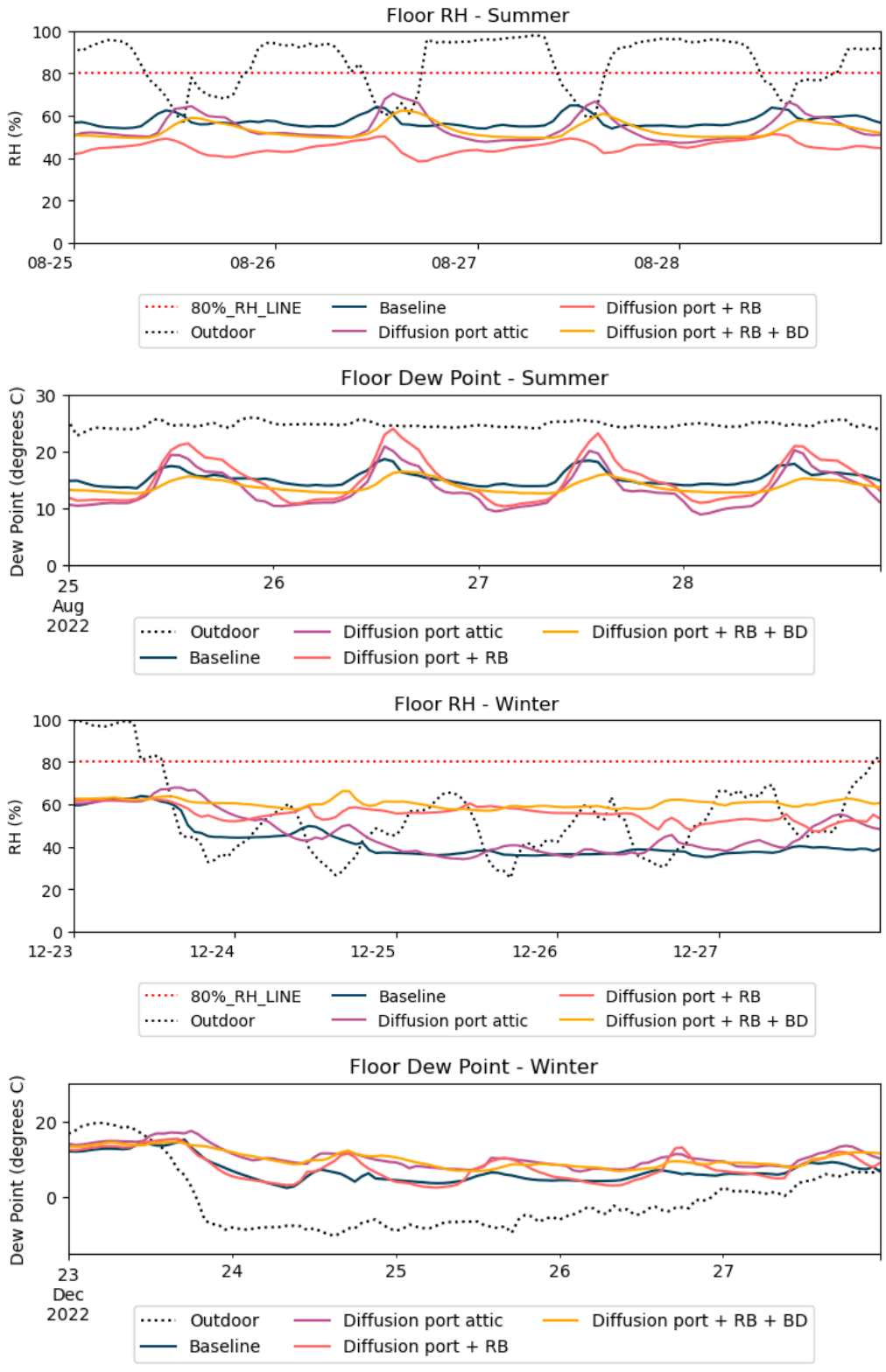

Figure 19. Attic floor humidity trends in heating, cooling seasons (hourly averages)

RB = radiant barrier; BD = buried ducts

As Figure 19 shows, when the outdoor dew point is relatively low, as it is during winter in this climate, the baseline home's interior dew point follows suit, showing that passive venting with outdoor air can help dry out the attic during winter. This is not the case during summer, when the outdoor dew point is much higher.

3.1.3.3 Attic Air at the Diffusion Port

This phenomenon also occurs on the roof deck, Figure 20 and Figure 21 show. The baseline home's RH fluctuates the most with ambient RH, which is perhaps helpful for drying when ambient RH is low, but this condition is uncommon by definition for hot, humid climates, and thus the unvented attics experience lower, and less variable trends in, RH throughout the year. Although these figures include cooling (summer) and heating (winter) periods, the outdoor temperature between December 24 and December 27 was colder than it was during the surrounding days, hence the different trends seen in the graphs. Figure 21 shows that the dew point remains much higher in the baseline attic than in the unvented attics during summer, particularly at night.

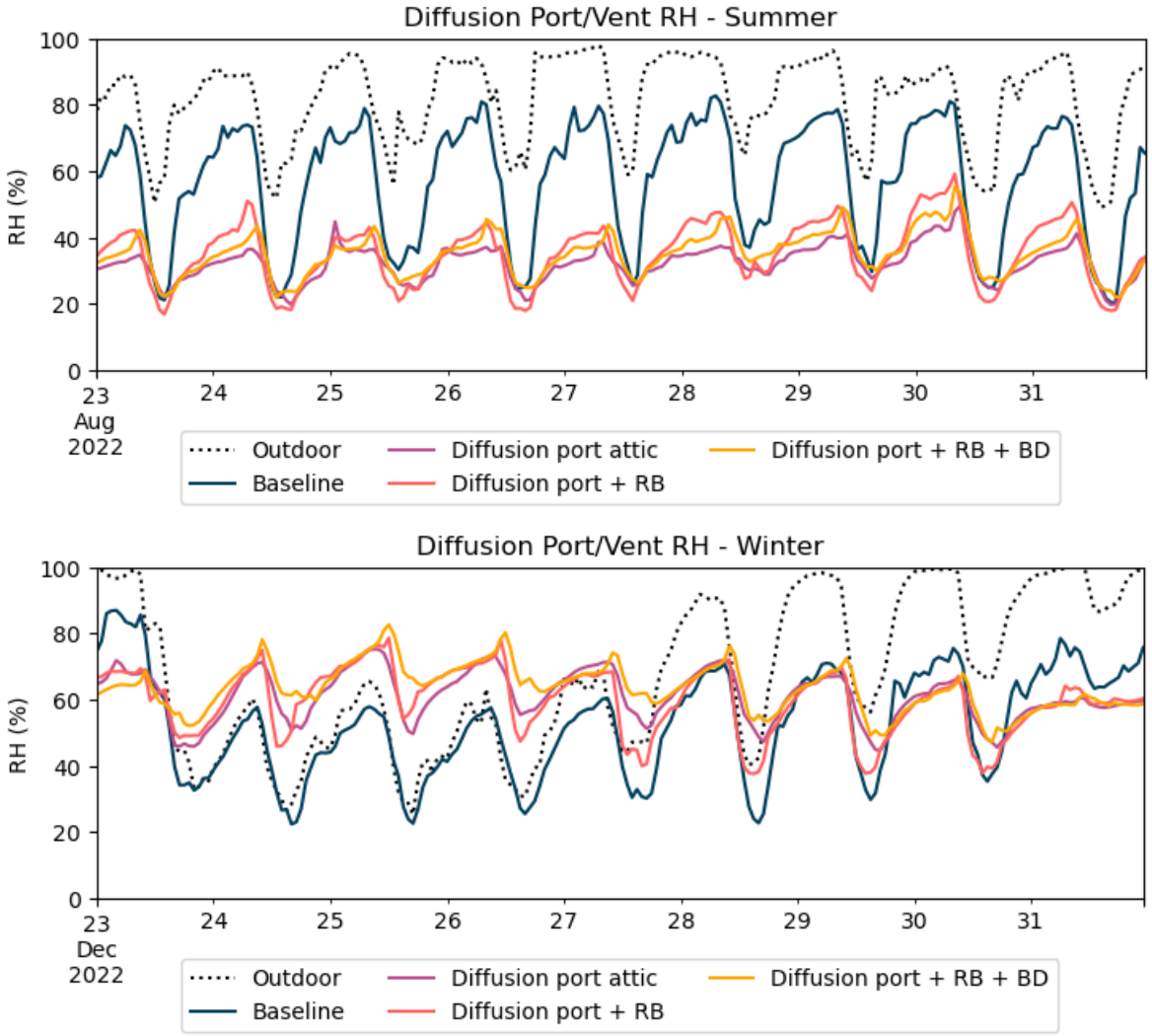

Figure 20. RH trends (hourly averages) at height of diffusion port/off-ridge vent during heating and cooling seasons (north face of roof deck)

RB = radiant barrier; BD = buried ducts

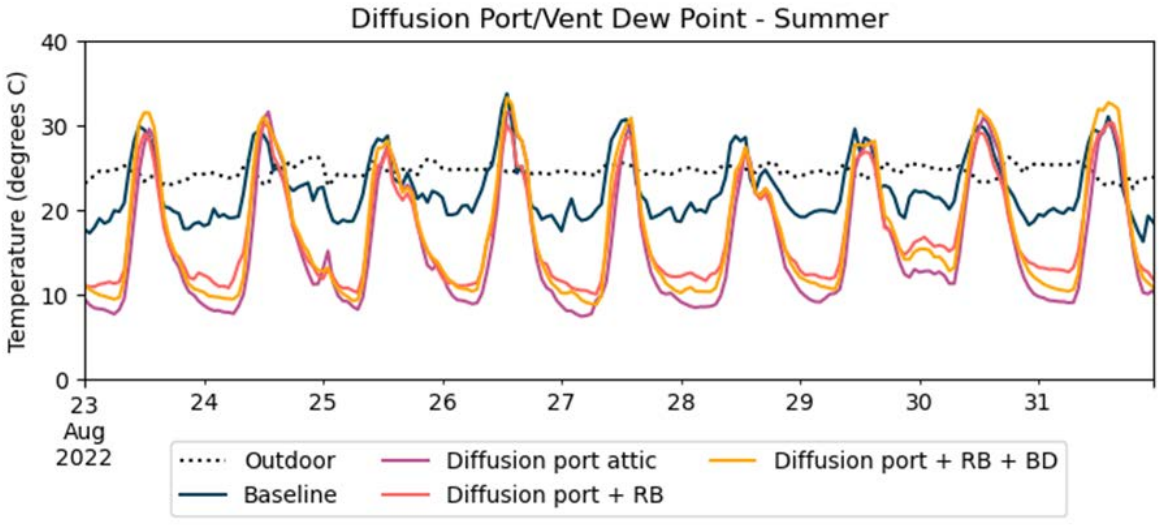

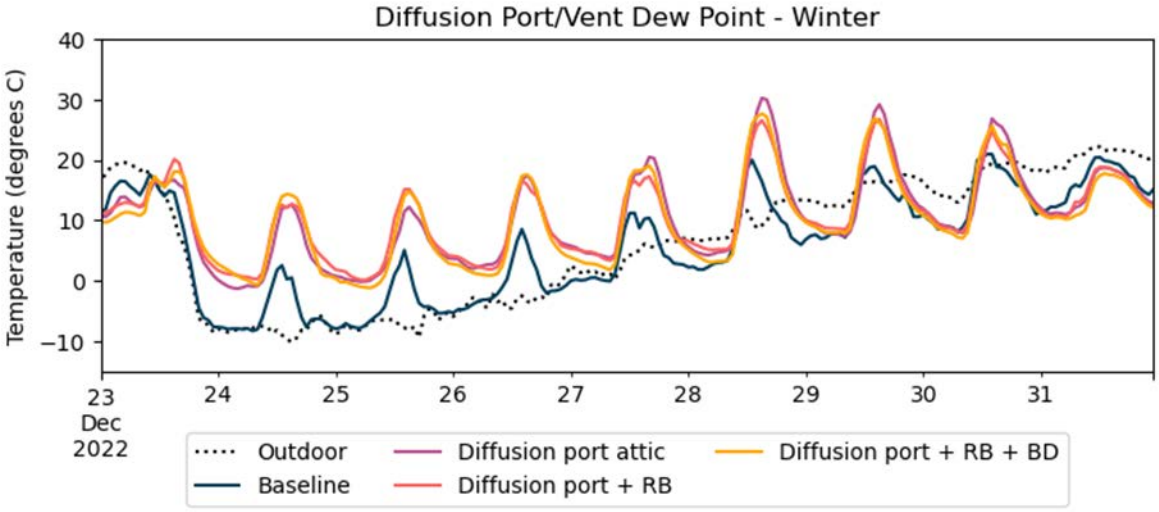

Figure 21. Dew point trends (hourly averages) of attic air at height of diffusion port/off-ridge vent during heating and cooling seasons

RB = radiant barrier; BD = buried ducts

The experimental data did not reveal any significant difference in roof deck RH as a result of radiant barriers or buried ducts. Figure 22 also shows that attic temperatures were generally higher in the unvented attics, especially during summer days, but there is no clear temperature difference among the unvented attics. We saw no clear temperature effects of radiant barriers, likely because of several confounding factors:

- The attachment of the radiant barrier in these homes was somewhat unconventional, attaching the suspended reflective sheet in an unvented attic without providing a convection pathway for outside air to enter through the soffits

and for hot air to escape via ridge vents. It may be more effective in the case of an unvented attic to install the radiant barrier using details meant for cathedral ceilings (at the roof deck surface between bays).

- The unvented + radiant barrier attic that experienced the highest peak temperatures was in a middle townhome, which reduced the surface area exposed to ambient air to allow heat to escape.
- The unvented + radiant barrier + buried duct attic had, by definition, more blown-in insulation, reducing heat transfer between the attic air and the often cooler living space below compared to the similarly positioned unvented attic (also an end unit).
- Differences in home operation and set point temperatures also contribute somewhat to the lack of direct comparability among attics.

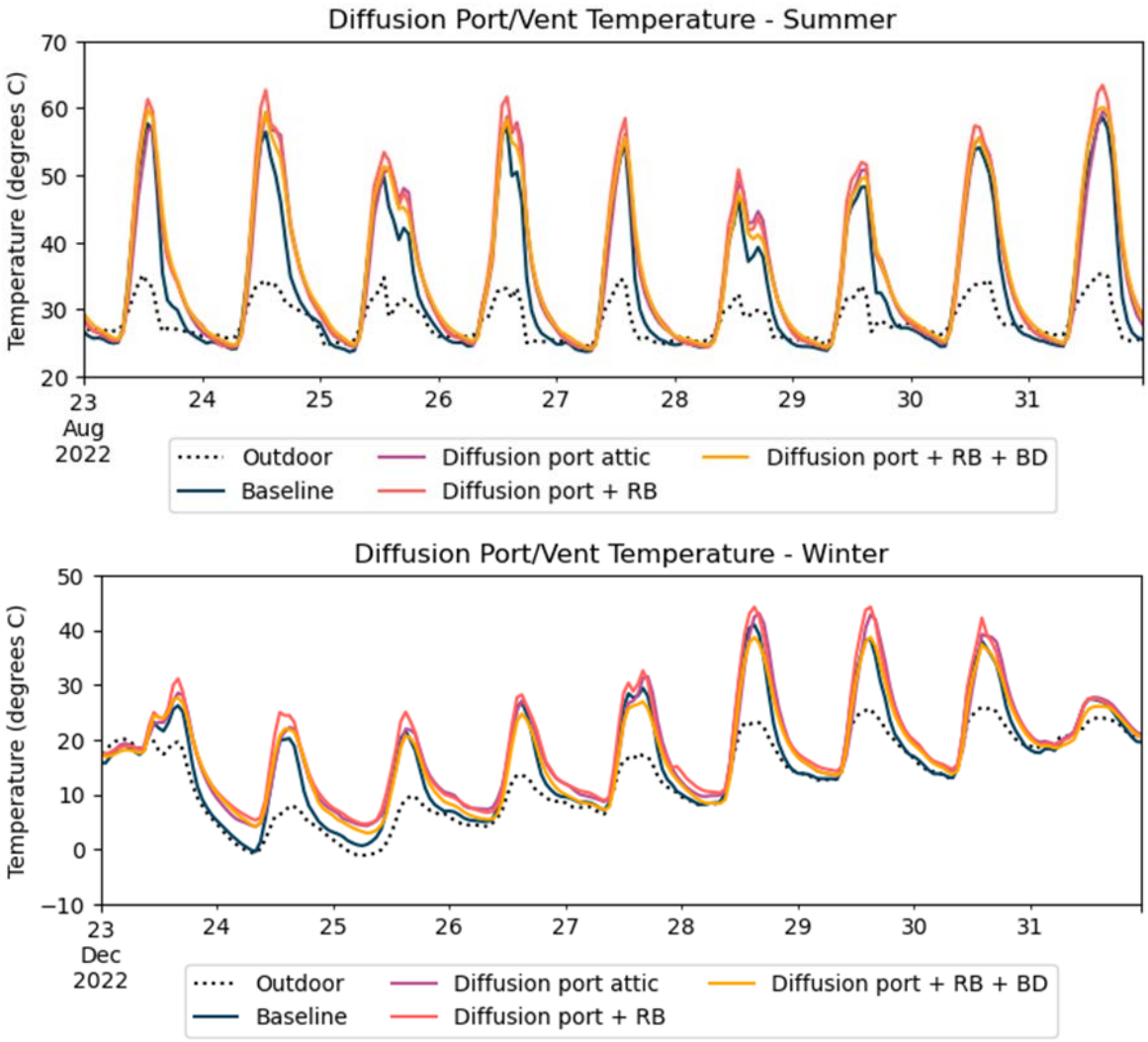

Figure 22. Temperature trends (hourly averages) of attic air at height of diffusion port/off-ridge vent during heating and cooling seasons

RB = radiant barrier; BD = buried ducts

Figure 20 and Figure 22 also reveal that the test homes' roof decks had higher RH in the winter than in the summer as a result of colder temperatures overall, interior sources of moisture versus outdoor sources, and the direction of the vapor-pressure gradient.

3.1.3.4 Attic Stratification Measurements

Attic air temperature stratification comparison between two extreme attic designs

Next, we compare the attic temperature and dew point stratification of the vented attic baseline home to the unvented attic home with vapor diffusion port, radiant barrier, and buried ducts.

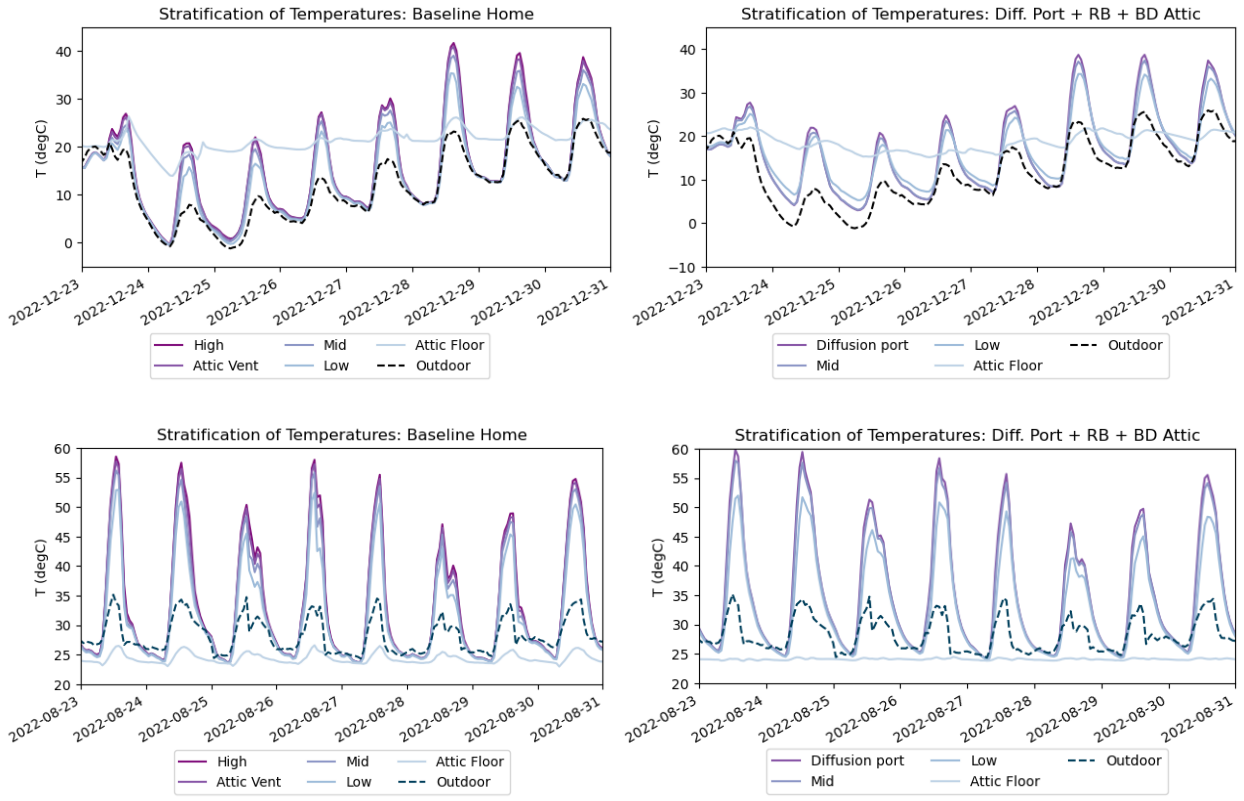

Figure 23. Temperature stratification in baseline (left) and attic with all measures (right) during winter (top) and summer (bottom). All graphs show hourly average values.

RB = radiant barrier; BD = buried ducts

Note: The temperature/relative-humidity sensor at the ridge (“High”) in the attic with diffusion ports, radiant barrier, and buried ducts failed early on in the experiments, so the nearby “Mid” (diffusion port height) sensor was the focus of the temperature and RH analysis toward the ridge in this home.

As seen in Figure 23, temperatures are stratified in both homes. In the home with diffusion ports, radiant barrier, and buried ducts, the attic floor is more insulated, and thus better buffered against temperature swings. Temperature is very similar between the two attics, which may be because (1) the unvented attic not absorbing as much radiant heat due to the radiant barrier, but (2) also not dissipating heat as much because of the lack of venting.

Attic air dew point stratification comparison between two extreme attic designs

Interior moisture accumulation was the primary durability focus of this project, but temperature comparisons among roof decks at the exterior surface can be found in Appendix A.5.

Dew point analysis can also lend some insight into each attic’s relative risk. Dew point is highest toward the ridge in the baseline attic (Figure 24); however, dew point was not noticeably stratified in the stress test home. This may be evidence of the diffusion ports working as intended, and/or a function of the suspended radiant barrier and its effects on temperature as well as the roof deck’s moisture sorption/desorption over the course

of a day. In winter, when roof deck moisture is of particular concern in this climate, dew point is lower in the baseline home, indicating that the vented attics are more readily transporting drier outdoor air into to the attic. Although the unvented attic with vapor diffusion-port roof decks may experience more moisture during winter, the attic space did not sustain any detrimental conditions based on the roof deck wood moisture content.

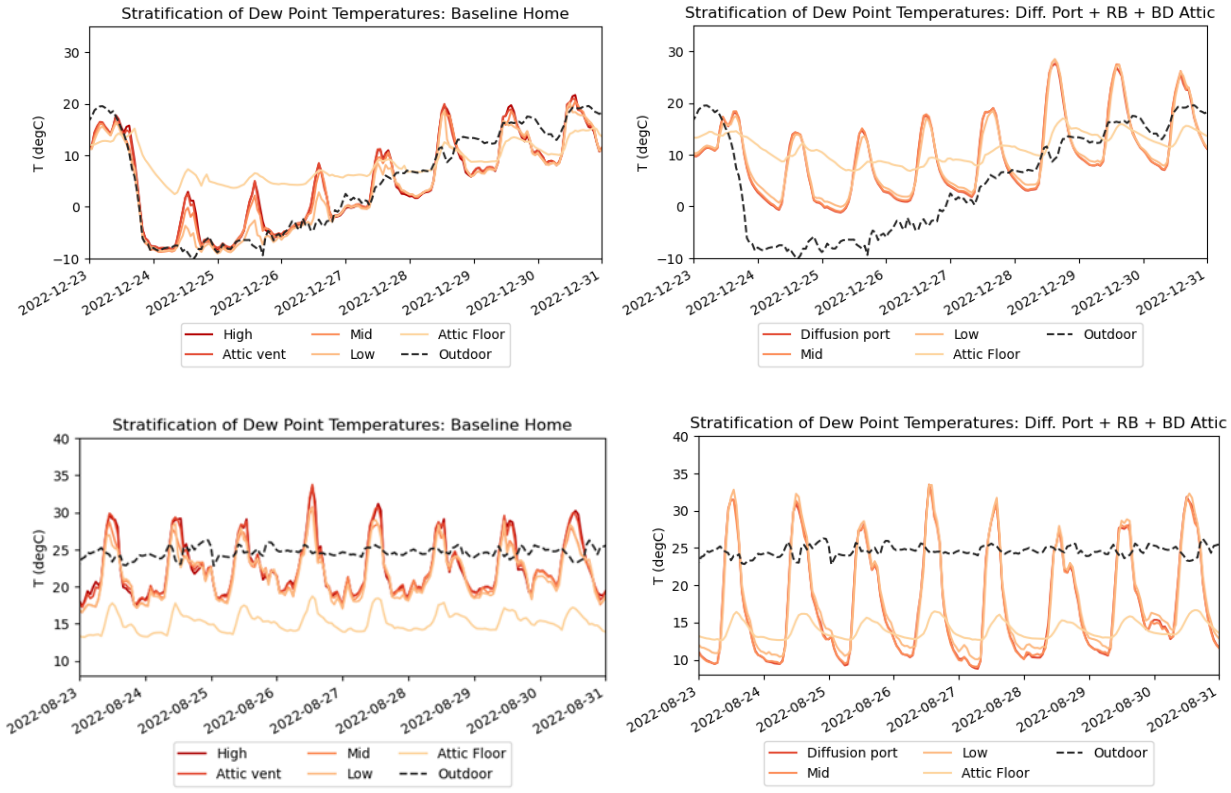

Figure 24. Dew point stratification in baseline (left) and attic with all measures (right) during winter (top) and summer (bottom); all graphs show hourly average values

RB = radiant barrier; BD = buried ducts

Past diffusion port studies of attics with insulation at the roof deck rather than the attic floor have reported dew point stratification (Ueno and Lstiburek 2015; Ueno and Lstiburek 2016). This difference influences attic air temperature extremes as well as “ping-ponging” moisture.

Attic air humidity stratification comparison between two extreme attic designs

Taking a closer look at RH, lower points within the diffusion-port attic tend to have higher RH in the winter (Figure 25), which matches a trend of temperature stratification without dew point stratification and corroborates the idea that the diffusion ports may indeed be diffusing moisture outward at the ridge.

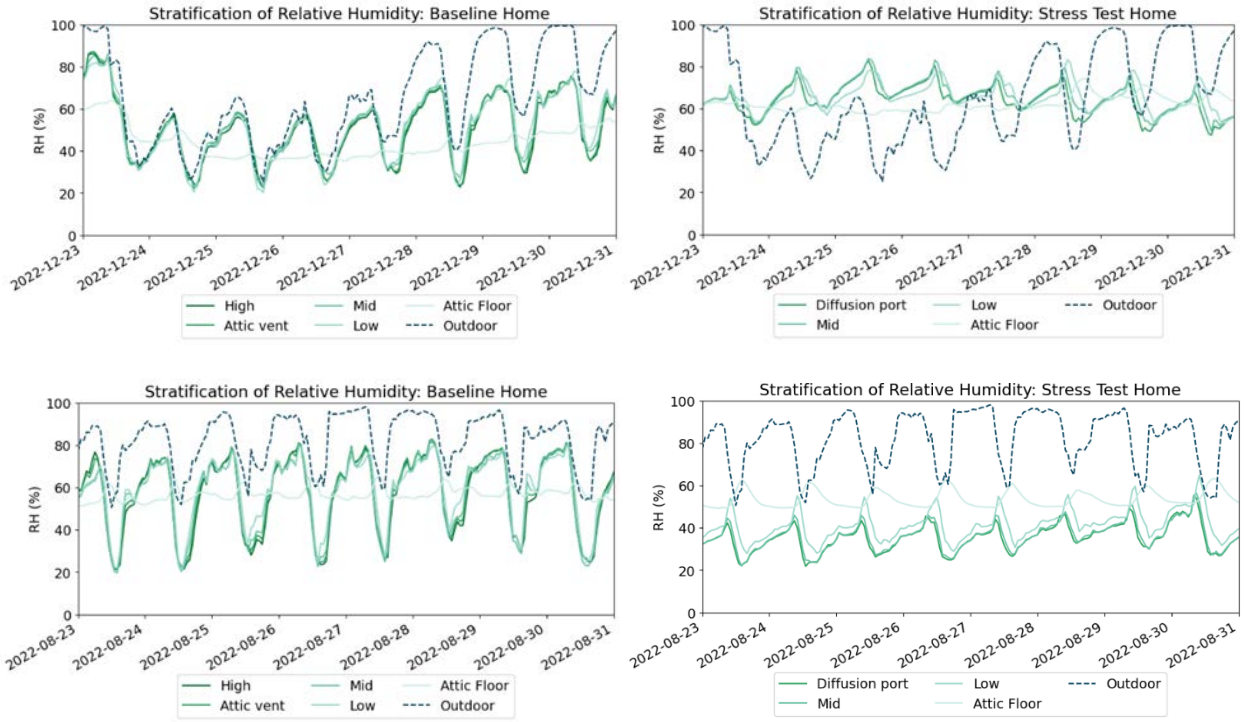

Figure 25. RH stratification in baseline (left) and attic with all measures (right) during winter (top) and summer (bottom); all graphs show hourly average value

Focusing on the humidity ratio demonstrates that moisture does not build up at the attic ridge (Figure 26). Despite the tendency for hotter, moist air to rise, the unvented attic with diffusion ports and radiant barrier does not show evidence of moisture build-up.

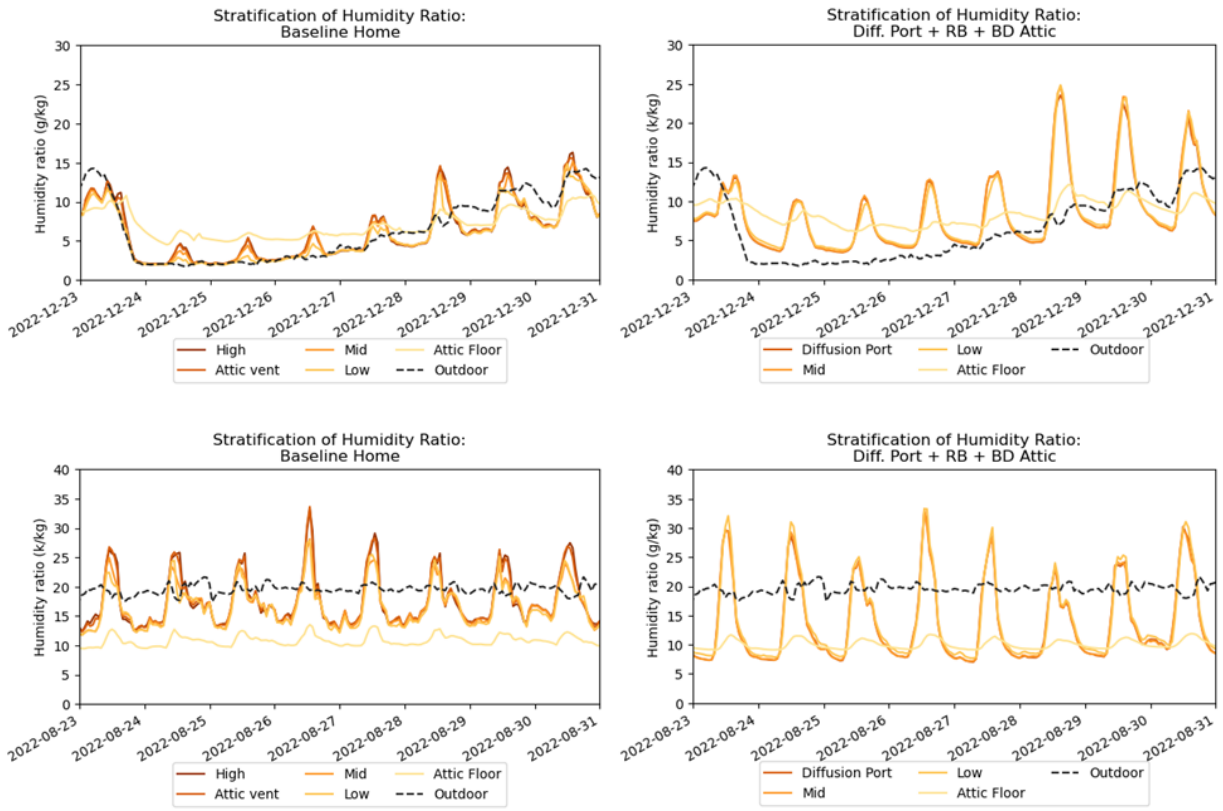

Figure 26. Humidity ratio stratification in baseline (left) and attic with all measures (right) during winter (top) and summer (bottom); all graphs show hourly average values

RB = radiant barrier; BD = buried ducts

3.1.4 Mold Risk Analysis

Evaluating mold risk per ASHRAE 160 based on observed temperatures and RH in each attic as well as the roof deck wood moisture content, it is clear that none of the attics were likely to have grown mold under the observed conditions (Figure 27). This was also confirmed by visual observation during the decommissioning of instrumentation at the end of the observation period.

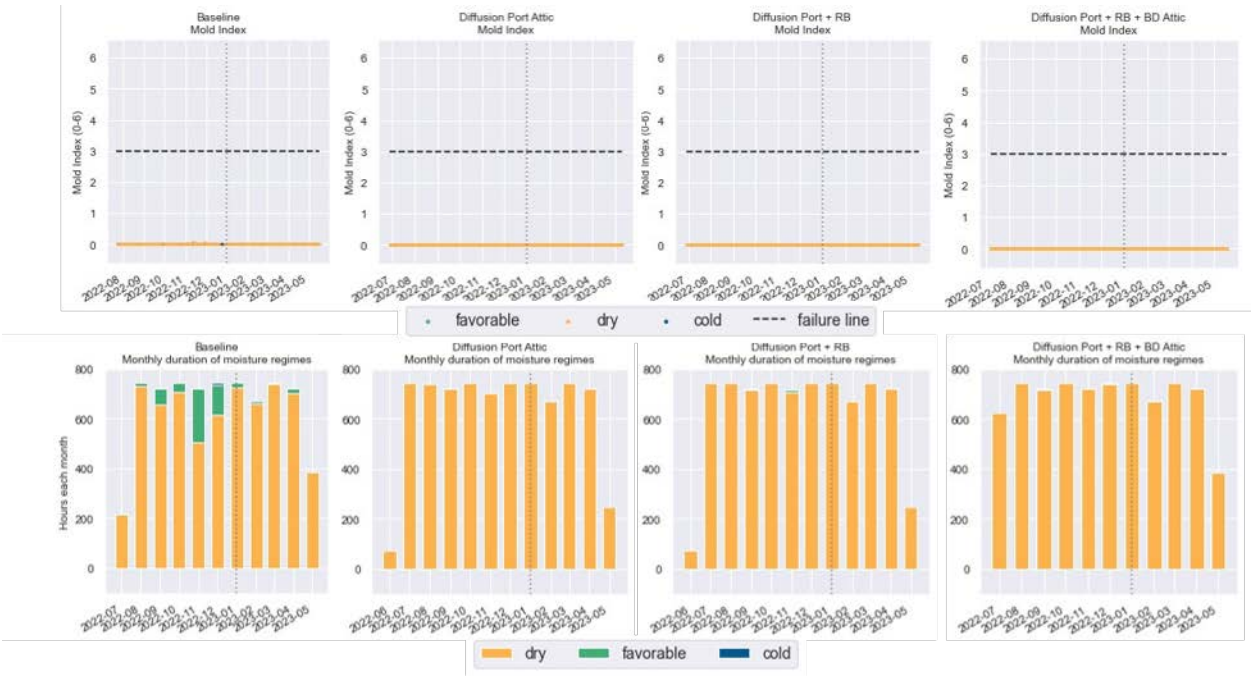

Figure 27. Mold index and monthly moisture conditions at north-facing roof ridge across experimental setups, per ASHRAE 160-2016. Moisture regimes include too dry for biological growth, favorable conditions for mold growth, and too cold for mold growth.

RB = radiant barrier; BD = buried ducts

Unvented attics prevent outdoor moisture from entering during humid weather, resulting in lower absolute humidity; however, the greatest differences in moisture risk between the baseline and unvented attics are seen in colder months. It is possible that the slightly higher temperatures achieved by not venting the roof deck yield somewhat lower mold-growth risk for diffusion-port attics. It is also conceivable that the diffusion ports effectively “pumped” out moisture that accumulated toward the roof ridge, as suggested by the lack of moisture stratification observed in the diffusion-port attics.

The attic floor analysis (Figure 28) tells a similarly uneventful story—none of the attic floor conditions were conducive to mold growth.

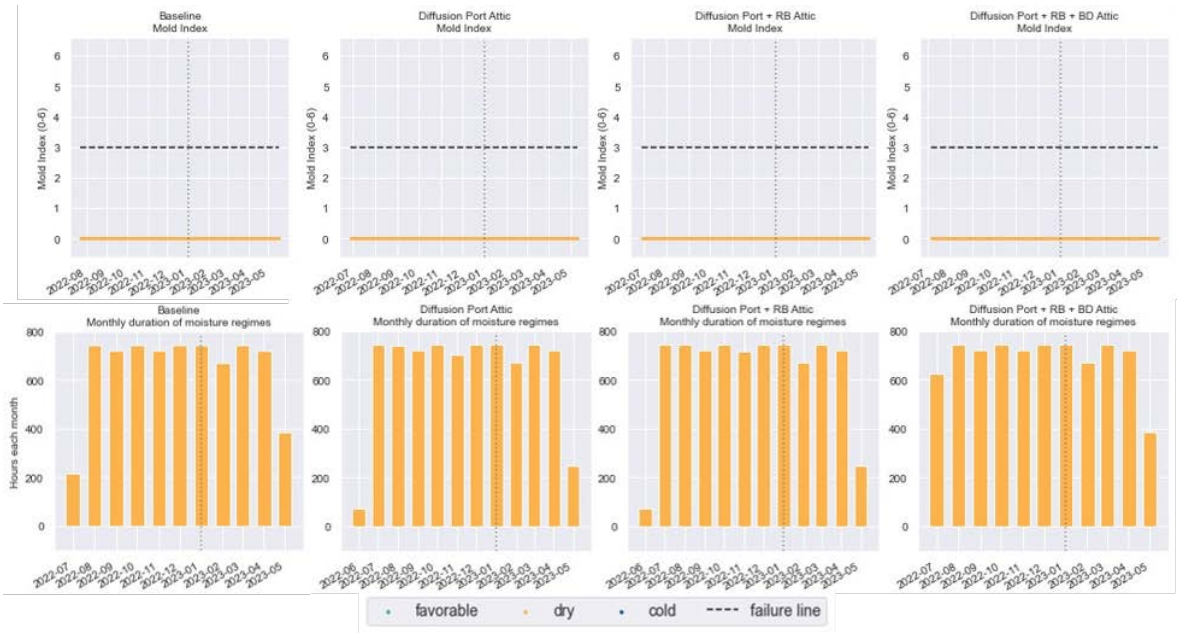

Figure 28. Humidity ratio stratification in baseline (left) and attic with all measures (right) during winter (top) and summer (bottom); all graphs show hourly average values

RB = radiant barrier; BD = buried ducts

Next, different points along the north-facing roof deck were analyzed for both the baseline and the attic with all measures included.

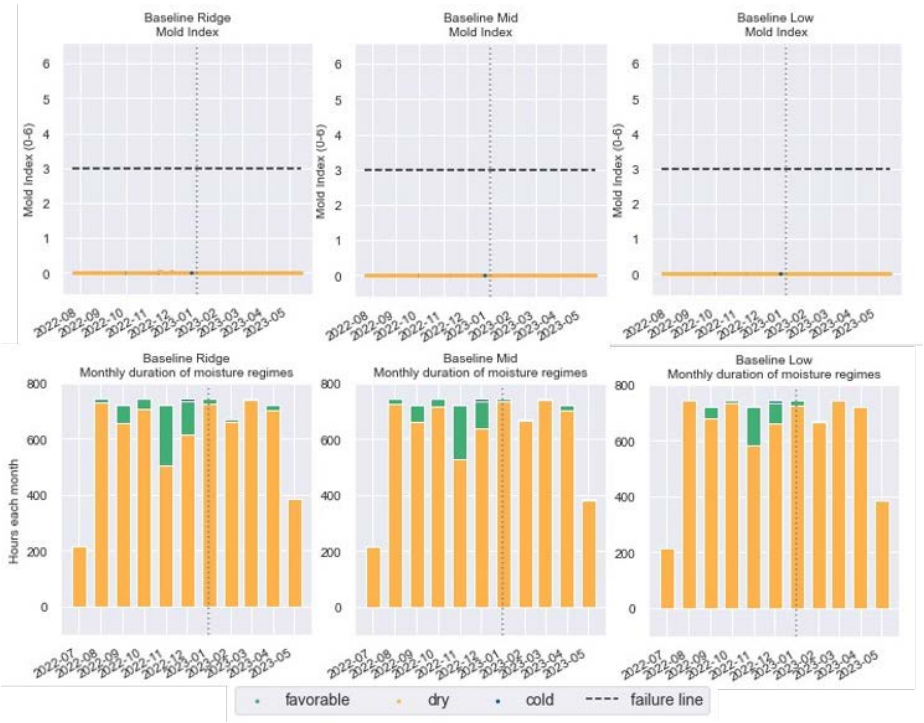

Figure 29. Mold index and monthly moisture conditions at various points along baseline north-facing roof, per ASHRAE 160-2016

As expected, the baseline attic shows slightly greater risk of moisture issues at the ridge (Figure 29). All locations in the roof deck dry out, however, and mold is not expected to grow under the observed conditions. The diffusion-port home with buried ducts and radiant barrier, however, showed higher susceptibility to mold growth at lower points along the north roof deck (Figure 30).

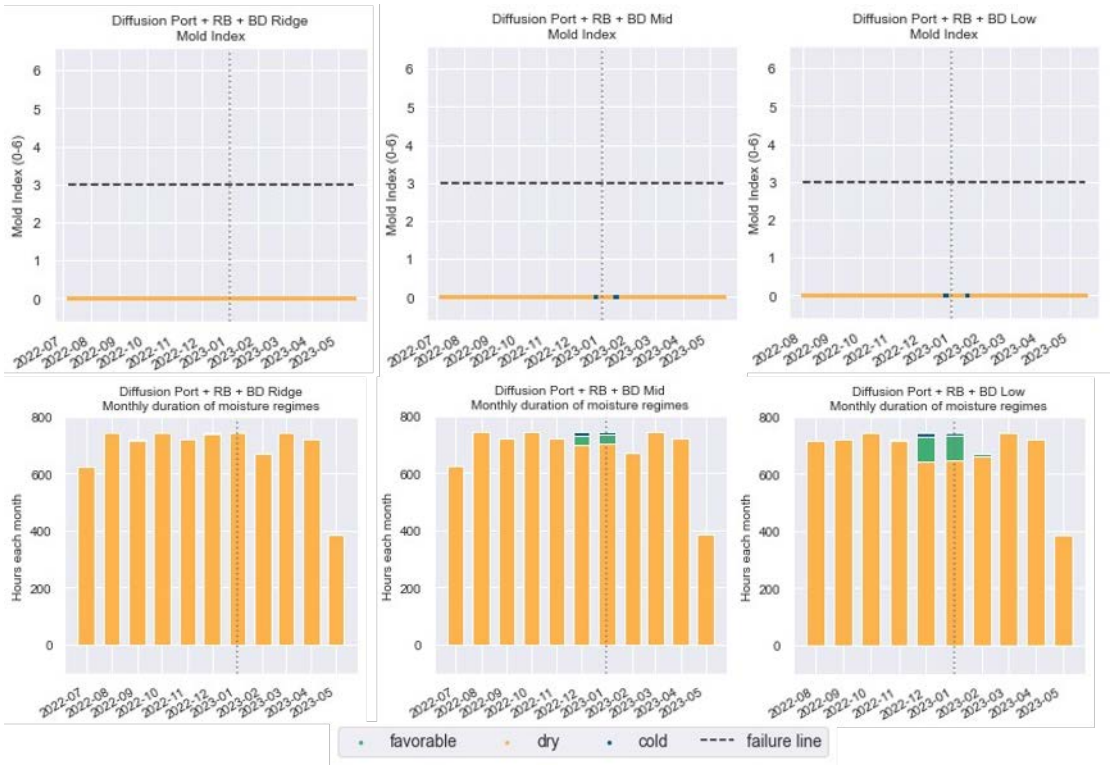

Figure 30. Mold index and monthly moisture conditions at various points along north-facing roof of the attic with diffusion ports, radiant barrier, and buried ducts, per ASHRAE 160-2016

RB = radiant barrier; BD = buried ducts

The lower parts of the roof deck are more prone to moisture issues than the higher parts in this case, possibly because of stratified temperatures (lower points in the attic are colder than higher points) but inversely stratified RH (unstratified dew point), creating conditions with a higher likelihood of moisture accumulation in lower portions of the roof deck given effective vapor diffusion ports at the ridge.

Roof deck orientation was also compared in terms of moisture risk. For this comparison, all temperature and RH sensors were located at the mid-level of the attic between the ridge and bottom of the attic. As expected based on relative exposure to solar radiation, northern exposures exhibited higher mold risk, and the southern exposure exhibited the lowest risk (Figure 31 and Figure 32).

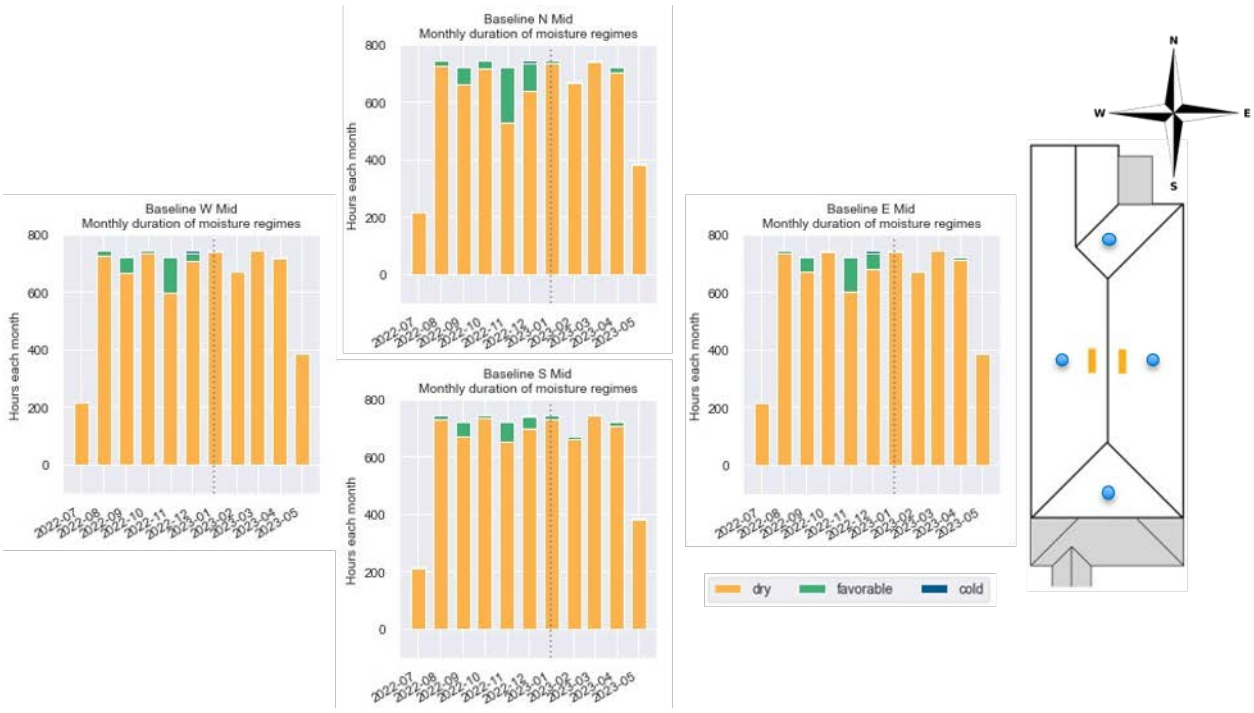

Figure 31. Monthly moisture conditions, per ASHRAE 160-2016, at each face of baseline roof

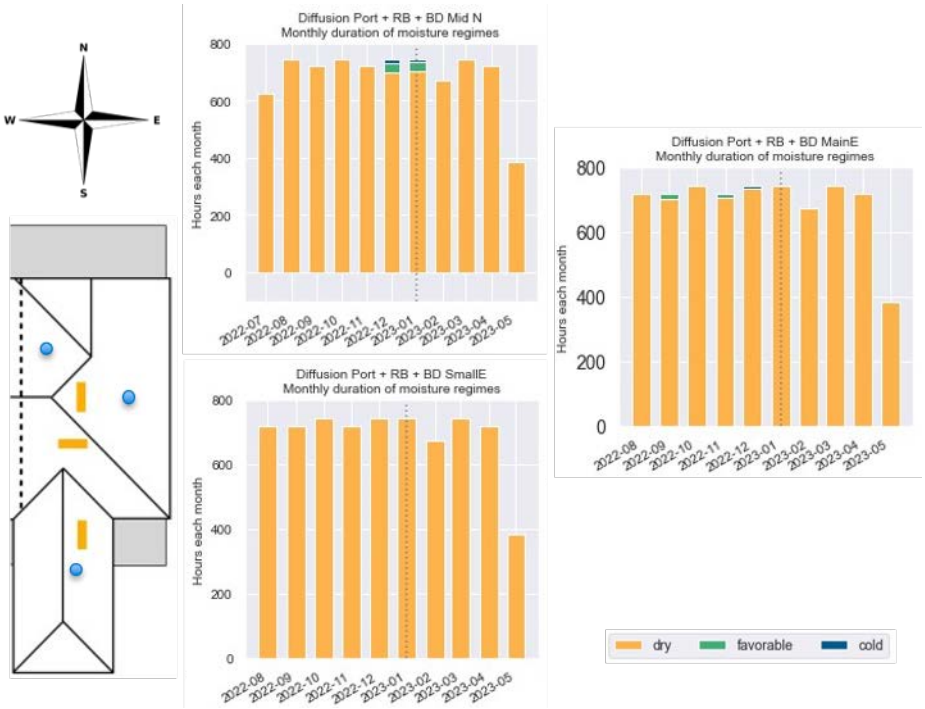

Figure 32. Monthly moisture conditions, per ASHRAE 160-2016, at each face of townhome roof with diffusion ports, radiant barrier, and buried ducts

RB = radiant barrier; BD = buried ducts

Still, all roof decks are expected to dry out over time and should not be susceptible to mold growth given the observed conditions.

3.1.5 Corrosion Risk Analysis

Corrosion risk was assessed based on observed temperature and RH of the interior surface of each home's roof deck.

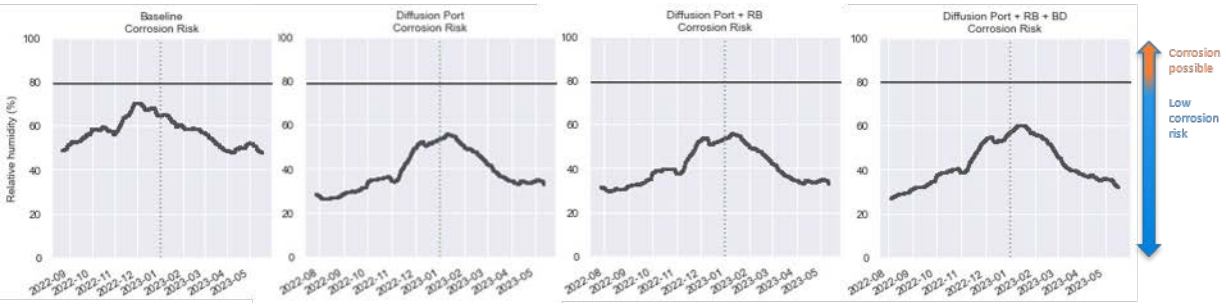

Figure 33. Corrosion risk at north-facing roof ridge across experimental setups, as determined by 30-day moving average of RH, per ASHRAE 160-2016

RB = radiant barrier; BD = buried ducts

Figure 33 indicates no risk of corrosion at roof ridge/roof deck, but average RH does increase in colder months, especially in the baseline. Because RH can be higher toward the lower elevations of unvented attics, corrosion risk was assessed at high, middle, and low points of both the baseline attic and the attic with all measures included (Figure 34).

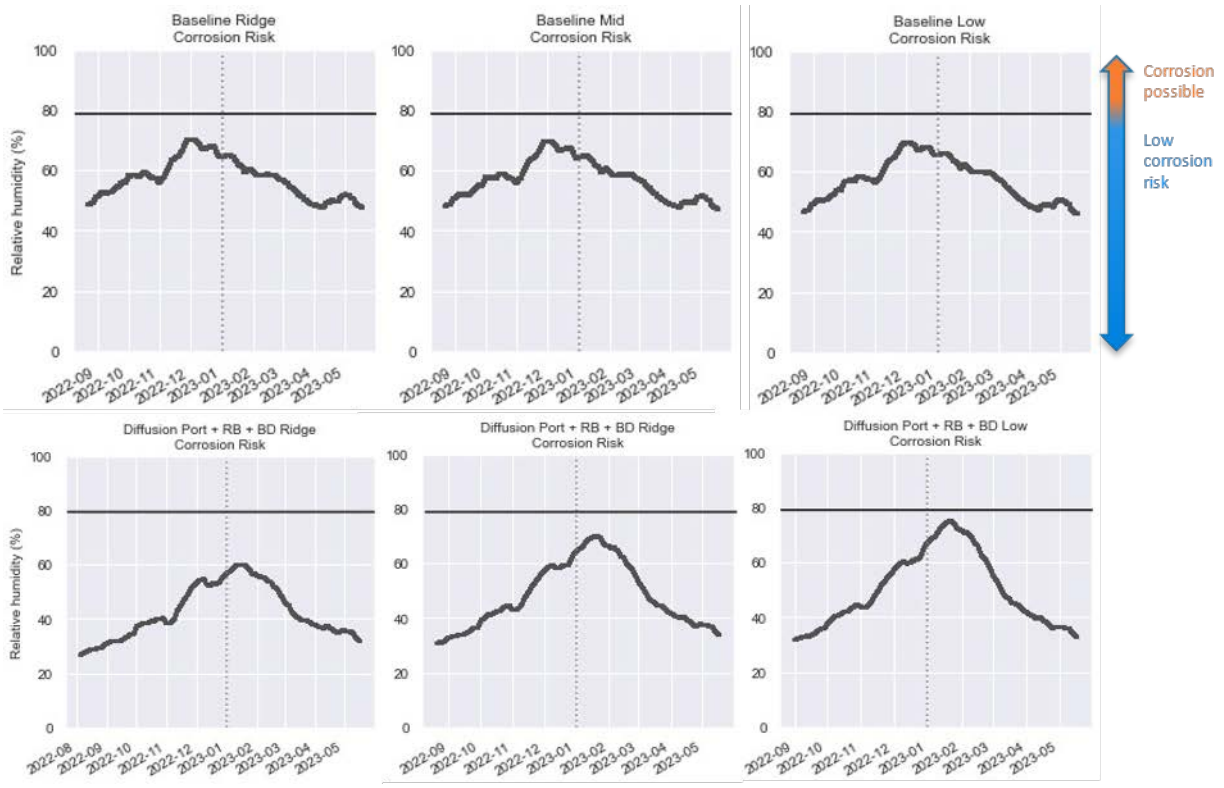

Figure 34. Corrosion risk at various points along north-facing roof of baseline and attic with diffusion port + radiant barrier + buried duct, as determined by 30-day moving average of RH, per ASHRAE 160-2016

RB = radiant barrier; BD = buried ducts

As expected, the baseline attic shows greater risk of moisture issues at the ridge, and the attic with diffusion ports, radiant barrier, and buried ducts experiences greater risk lower down in the attic. None of the attics are expected to experience corrosion under the observed conditions, but it is possible that they could with somewhat different winter conditions—a colder and/or wetter winter with higher latent gains from occupants, for example.

3.1.6 Moisture Content Analysis

Generally, it is advisable to keep wood products below 20% moisture content to avoid mold growth or biological degradation. Moisture-pin readings are not the most accurate measurements because they depend on a tuned configuration for the context and material in question (see Appendix A.1 for details), but we present moisture content readings as rough indicators and to raise concern if readings reach or remain at or above 20% for extended periods of time, with a 30% moisture content representing a greater cause for concern about rot.

Figure 10 and Figure 11 show the locations of the moisture pins within the roof decks. Figure 35 compares 24-hour rolling average moisture content at each location. Because moisture content is used here primarily to indicate the risk of rot and corrosion, and because long-term average values are used in the criteria for these failure modes, rolling average results are considered most relevant (as well as less visually noisy).

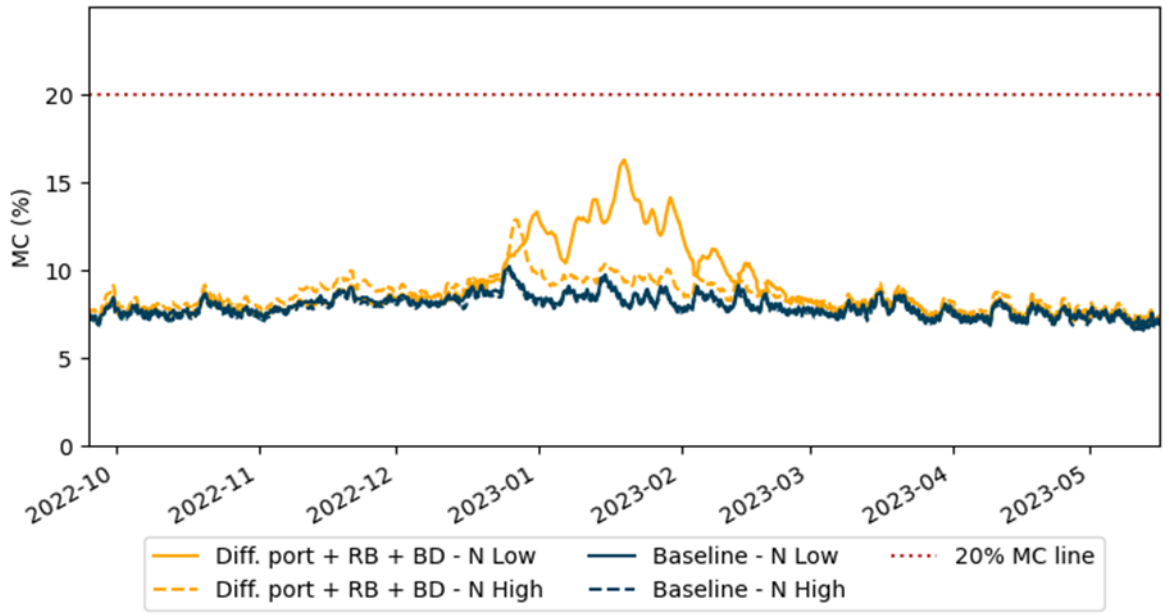

Figure 35. 24-hour rolling average of approximate moisture content of north-facing roof deck across moisture pin locations of concern in the baseline and attic with diffusion ports, radiant barrier, and buried ducts only

RB = radiant barrier; BD = buried ducts

The “Low” moisture-pin readings, for the configuration with diffusion ports + radiant barrier + buried duct in particular, are sometimes higher than the “High” readings in the winter, which is consistent with RH and mold risk being higher at lower points along the diffusion port roof deck. However, the roof deck does appear to dry out after winter. Although these measurements should not be considered exact, 24-hour average moisture content never approaches 20% and seems to follow seasonal pattern wetting/drying patterns observed in other studies of unvented attics (Withers and Martin 2022) and (Prevatt and Miller 2017).

3.1.7 Qualitative Observations

3.1.7.1 Decommissioning

Although it is not the focus of this study, limited visual data were also collected over the course of the experimental period. At the end of the data-collection period, instrumentation was removed, and the attic surfaces were observed. No evidence of moisture or biological growth was present in any of the homes, and no occupants reported any concerns throughout the study. A sample of the type of visual observations are shown in Figure 36 and in Appendix B.

Truss members are clean and dry within the diffusion port + radiant barrier attic. Datalogger enclosure shown in foreground.

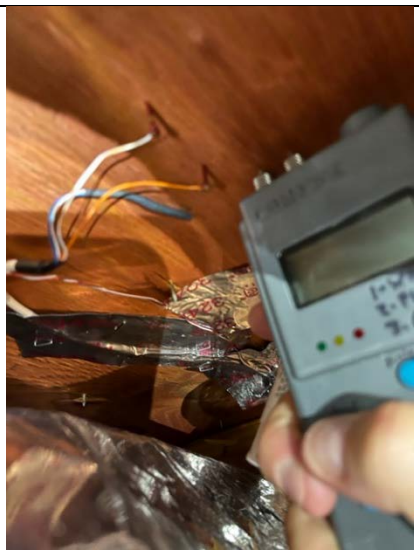

Underside of roof deck wood moisture content checked with hand-held Delmorst moisture meter next to moisture sensors.

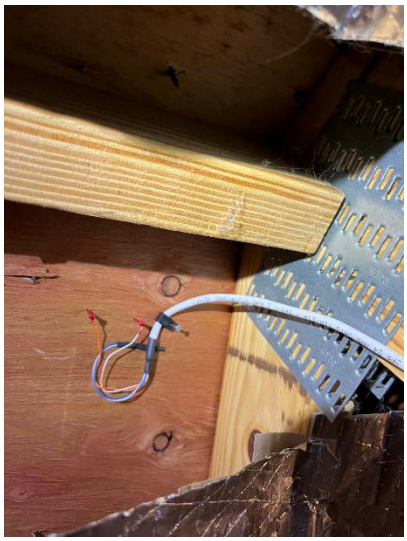

Clean and dry underside of plywood roof deck near sensors in the diffusion port + radiant barrier attic.

Checking top and bottom of buried duct-jacket surfaces for past and present signs of moisture in buried duct attics.

Figure 36. Selected photo documentation of monitoring equipment positions and instrumentation
Source: Charles Withers grants full permission to use and publish these photos.

3.1.7.2 Stressors and Resilience

An incident isolated to the second-floor hall bathroom floor occurred during the brief simulated-occupancy period for the baseline home when a humidifier was placed in the bathroom tub to generate moisture while the home was not occupied. This happened during a period of cooler weather that resulted in less of an air-conditioning load and ultimately less moisture removal. During this time, air circulation may not have been sufficient to fully distribute the bathroom moisture throughout the living space, and some water condensed on the tile floor inside the bathroom. It went on for long enough (estimated at a maximum of a couple of weeks) that we observed some minor mildew growth on some tile grout surfaces. We resolved the issue immediately and cleaned affected surfaces within the conditioned space. This could be considered a significant stressing scenario in terms of providing a brief spike in indoor humidity between roughly 11/9/2022 and 11/23/2022. Attic floor RH did increase during this time period in the baseline home, and rolling-average values remained below 80%.

The humidifier in the bathroom was scheduled to deliver the typical amount of an entire home with approximately four occupants. In real occupied homes, the internal moisture would be generated from throughout the home at different locations from different bathrooms, kitchen, laundry, and occupants. A typical amount of moisture from a few long baths or showers in the bathroom that contained the humidifier would produce much less moisture than what was generated for the whole home by the humidifier. Although tile grout mildew is not uncommon within shower enclosures, it is less common on clean tile floors, and typical bathroom moisture would not be expected to result in the floor grout mildew observed in this bathroom.

We observed no other evidence of failure in any of the homes. Wood members and roof decking within the attic appeared and felt dry to the touch when we removed the sensors. The attic floor showed no evidence of water pooling (dampness, discoloration, etc.) when we pulled the insulation back to reveal the drywall (Figure 37).

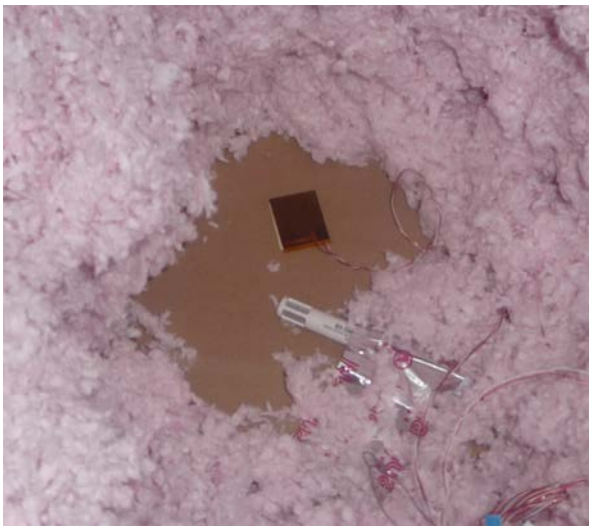

Figure 37. Attic insulation temporarily removed to reveal drywall conditions near heat-flux sensor and temperature/RH probe

Photo by the authors

Major Weather Events

Although there is no quantitative standard for recovery from major weather events, a drier/less humid attic is a good indication of resilience to hurricanes and tropical storms. Figure 38 shows the impact of Hurricane Ian on attic air and attic floor RH. None of the attics show any indication of trapping moisture. The same trends were seen in November 2022 with Tropical Storm Nicole.

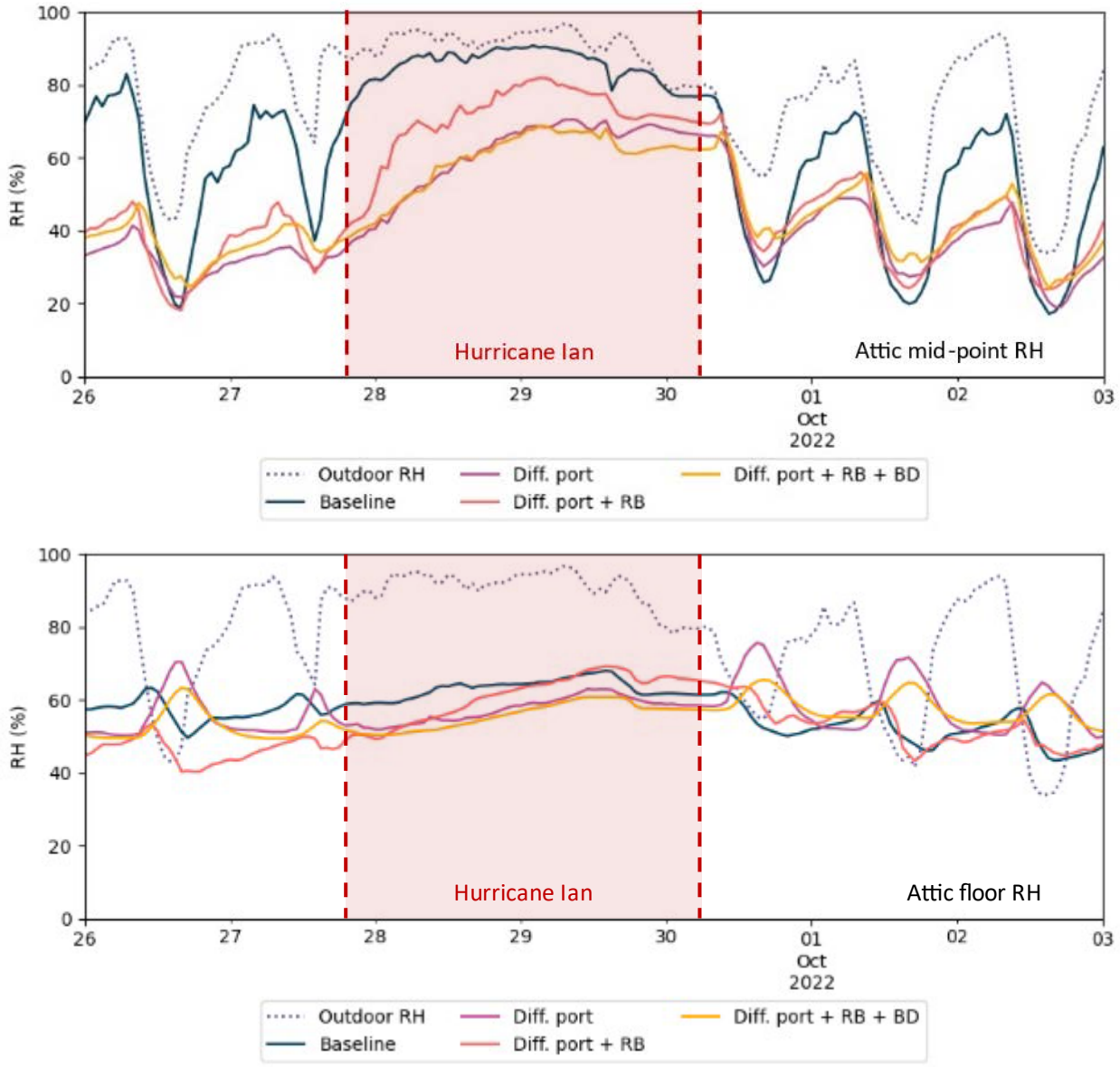

Figure 38. RH (hourly average) at mid-point (top) and attic floor (bottom) of attics before, during, and after Hurricane Ian

RB = radiant barrier; BD = buried ducts

3.2 Modeling Data Analysis

One-dimensional hygrothermal WUFI models were developed to simulate both the existing roof deck and attic floor as detailed in Section 2.3. Appendix E describes the comparison between modeled and measured data as well as adjustments to the model to better approximate field observations and data gathered.

3.2.1 Stress Testing Using Hygrothermal Model

Once these models were calibrated as much as possible using the observed outdoor and indoor/attic measurements, the “stress test” was applied to determine whether the combination of worst-case (within reason) outdoor and indoor/occupancy conditions could bring about “failure” in any of the applicable modes for the attic with all features (diffusion port + radiant barrier + buried ducts).

The parameters used for each regression, the regression type, and the 5-fold coefficients of variation of the RMSE (CV-RMSE) for training and testing the regression models to approximate living space and attic conditions are found in Table 7. We compared and chose second-order linear regressions and random-forest regressions in terms of model fit.

Table 7. Regression Model Fits for Stress Test Indoor and Attic Conditions

Dependent Variable	Measured Independent Variables Used	Regression Type	5-Fold CV-RMSE
Living Space Temperature (return-air temperature used as proxy)	Exterior dry-bulb temperature, previous hour’s exterior dry-bulb temperature, global horizontal solar radiation, wind speed, month of year	Random forest (random state=42, min_samples_leaf= 25)	2.7%
Living Space RH (return-air RH used as proxy)	Exterior RH, exterior dry-bulb temperature, previous hour’s exterior dry-bulb temperature, global horizontal solar radiation, wind speed, precipitation (mm), month of year	Random forest (random state=42, min_samples_leaf= 25)	3.5%
Attic (low) Temperature	Exterior dry-bulb temperature, global horizontal solar radiation, wind speed, living space temperature	Second-order linear regression	14.8%
Attic (low) RH	Exterior RH, exterior dry-bulb temperature, previous hour’s exterior dry-bulb temperature, global horizontal solar radiation, wind speed, precipitation (mm), month of year, living space RH	Random forest (random state = 42, min_samples_leaf = 25)	8.9%

The training data represent hot weather, cold weather, and one swing season, so it is unlikely that the regression models are over-fit to a specific season because the predicted values of the stress case fall within the range of the observed values. The stress case regressed values’ distributions are different, however. Table 8 provides the

relative feature importance values (or regression equation, in the case of the attic temperature. Feature importance values add up to a total of 1, so each importance fraction can be considered the value of importance of a feature relative to the whole.

Table 8. Relative Feature Importance List for Each Regression Model Used in the Stress Case

Dependent Variable	Independent Variable (relative feature importance/regression equation)
Living Space Temperature	Previous hour's exterior dry-bulb temperature (0.60) Month of year (0.31) Wind speed (0.03) Exterior dry-bulb temperature (0.03) Global horizontal solar radiation (0.02)
Living Space RH	Previous hour's exterior dry-bulb temperature (0.62) Month of year (0.25) Exterior RH (0.05) Wind speed (0.04) Exterior dry-bulb temperature (0.02) Global horizontal solar radiation (0.01) Precipitation (0.00)
Attic (low) Temperature	$T_{attic} = +1.15 * T_{out} - 0.63 * T_{living} + 0.56 * Sp_{wind} + 11.53$ T_{out}=Exterior dry-bulb temperature (°C) T_{living}=Living space dry-bulb temperature (°C) Sp_{wind}=Wind speed (m/s) Note: Global horizontal solar radiation had a near-zero coefficient.
Attic (low) RH	Month of year (0.61) Global horizontal solar radiation (0.16) Exterior dry-bulb temperature (0.10) Living space RH (0.07) Exterior RH (0.03) Wind speed (0.02) Previous hour's exterior dry-bulb temperature (0.00) Precipitation (0.00)

Because indoor RH is dependent on how much the space-conditioning system must heat up or cool down the outdoor and indoor air, it follows that RH depends more heavily on outdoor temperature than on outdoor RH. Although it may be counterintuitive

that the RH of the attic would depend primarily on outdoor temperature instead of outdoor RH, it is likely that attic temperature—directly influenced by outdoor temperature—has a greater influence on attic RH by suppressing it when temperatures are high and increasing it when temperatures are low.

Because we found that the attic with diffusion ports + radiant barrier + buried duct had colder and wetter conditions toward the lower section of the attic, the lower attic sensor (see Figure 9) was used in these regression analyses. Therefore, the modeled roof deck results should be considered representative of the lower portion of the attic directly above the insulation.

Figure 39 shows the roof deck results for a 10-year run using the stress test model with the diffusion port + radiant barrier + buried duct described in Table 3 and the post-processing described in Appendix E. Each winter, the mold index at the interior surface of the roof deck increases, with substantial mold growth risk within two years. There is some leveling off in the later years, but the colder, more humid conditions of the stress case render mold risk high when many mold-prone conditions are combined. It is important to remember, however, that we intend this “stress test” case to represent unlikely but possible stressful conditions—not conditions that would necessarily be expected to persist year after year. Additionally, more research is needed to determine whether risk can be mitigated under stressful conditions with design and construction strategies such as further attic floor air sealing to reduce moisture entering from the occupied space or increased attic-volume-to-surface-area ratio to allow for greater dispersion of occupant-generated moisture.

Using the same stress case conditions but higher heating thermostat set points (20°C/68°F rather than 19°C/66°F) in the model yields much lower mold risk, as shown in Figure 40. This is not to say that occupants should be encouraged to increase their set points and therefore energy expenditure—it is simply a demonstration of the sensitivity of the model and an indication that occupant behavior is incredibly important in evaluating hygrothermal success and failure for new building strategies.

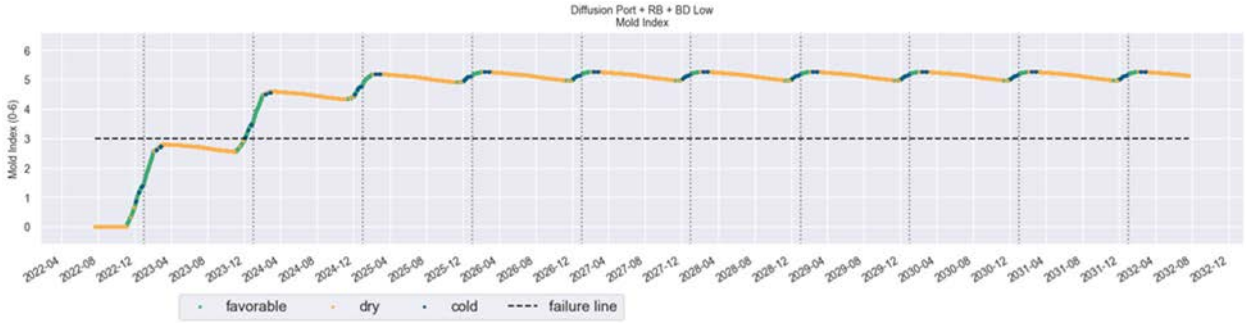

Figure 39. Modeled mold index calculation for stress test condition at north-facing roof deck interior surface

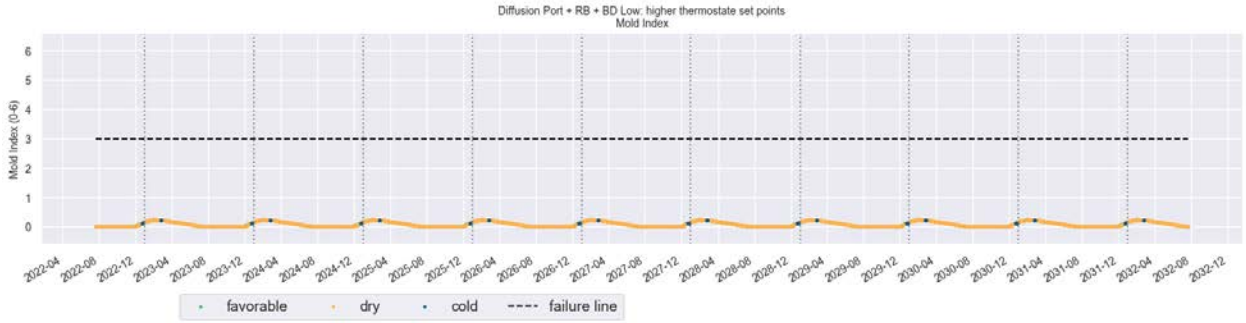

Figure 40. Modeled mold index calculation for stress test condition with altered heating set point (20°C/68°F) at north-facing roof deck interior surface

The stress test corrosion analysis (Figure 41) tells a similar story—corrosion risk according to ASHRAE 160 is present for a large portion of each year. This criterion may be a conservative estimate of corrosion risk, however, because 80% RH is the point at which exposed metal can begin to corrode. Meanwhile, the RH only sometimes reaches 100%, meaning that metal fasteners and exposed nails are not wet year-round. Still, the fact that there is wetting for any amount of time under these stressful conditions indicates that measures should be taken to avoid the combination of stress case conditions. On the other hand, increasing the heating set point from 66°F to 68°F yields a much less risky scenario for potential corrosion (Figure 42).

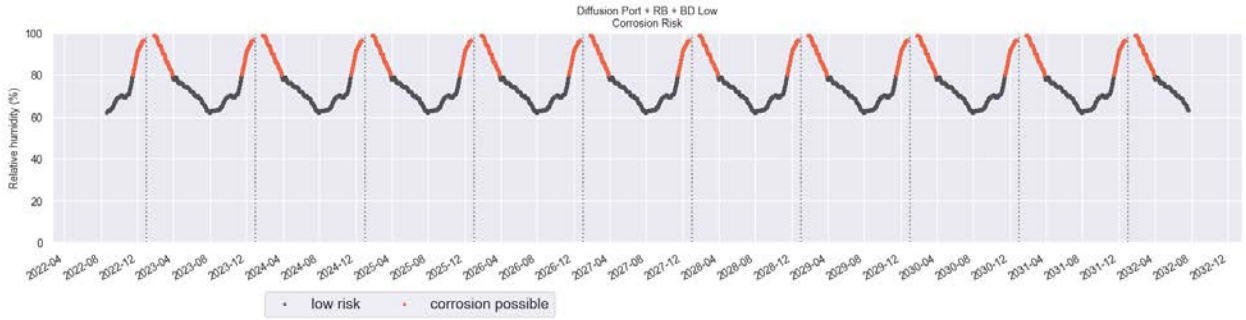

Figure 41. Modeled corrosion risk for stress test condition at north-facing roof deck

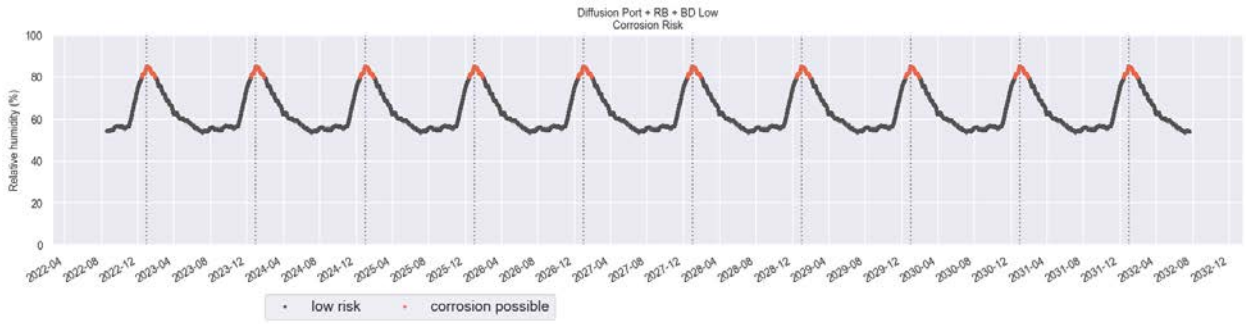

Figure 42. Modeled corrosion risk for stress test condition with altered heating set point (20°C / 68°F) at north-facing roof deck

Figure 43 shows the modeled mold index at the top surface of the attic floor under the “stress test” conditions over 10 years. Mold index rises quickly but does not reach a

value of 3. Although some may not consider this “failure,” it should not be considered safe given that even a mold index of 2 indicates microscopic mold growth. On the other hand, if the cooling set point is raised to 22.2°C (72°F) rather than 20°C (68°F), the mold index barely increases at all and never even reaches 1 (Figure 44). This emphasizes the importance of occupant behavior and duct leakage on attic floor durability. Although the stress test conditions raise a slightly concerning scenario for the attic floor, these conditions are, again, unlikely to occur all at once in a sustained fashion.

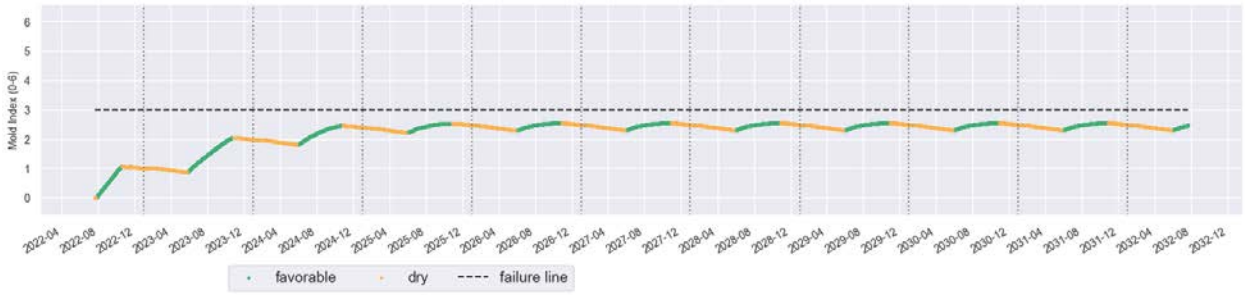

Figure 43. Modeled mold index calculation at attic floor for stress test condition

Figure 44. Modeled mold index calculation at attic floor for stress test conditions with increased cooling set point (22.2°C/72°F)

4 Discussion and Conclusions

4.1 Conclusions

Our field experiments indicate that, as these homes were constructed and under the conditions we observed, unvented attics with blown-in attic floor insulation that use diffusion ports, radiant barriers, and buried ducts did not pose moisture issues. Although RH can be high at times at duct-wrap surfaces, our data indicate that surfaces dry out enough that we measured and observed no evidence of moisture accumulation. Even the home with vented attic and buried ducts did not show evidence of moisture-related issues at the attic floor under the conditions we observed. Ongoing work by the FSEC Energy Research Center (FSEC) and Owens Corning centered on buried ducts in vented attics, however, will inform design considerations for this configuration. This is not to say that IECC-2018 and IECC-2021 model-code requirements of R-13 duct wrap are unwarranted—the RH at the duct jacket was highest for the vented attic with buried ducts, although we found no condensation under the conditions we observed. The unvented attics with diffusion ports did appear to reduce RH around the duct-wrap surface, indicating that unvented attics with diffusion ports could reduce the need for high-R duct-wrap insulation in hot-humid climates.

As we expected, the unvented attic diffusion-port homes experience more moisture risk during winter than the baseline does, but the reverse is true in the summer. The unvented attics were warmer overall than the vented attics. The higher average temperatures help to depress the RH when absolute moisture in the air is the same. The unvented attic has another advantage to lower RH during warm, humid weather, namely that unvented attics help limit the moisture in outdoor air from entering the attic. This, combined with higher temperatures, further depresses the attic air RH. Withers et al. found that simply “unventing” an existing vented attic in Florida that had R-30 insulation and low-slope (3:12) roof pitch resulted in the one-story home’s increased annual cooling energy usage by 8.2% (Withers, Fenaughty, and Sonne 2020). Although higher attic air temperatures can negatively affect energy efficiency in hot climates, the effect is likely small in the context of new construction because of the insulation on the attic floor (at least R-38 in climate zone 2), which separates the attic air from the conditioned space. When considering the additional insulation added to bury ducts (another R-11 over the parts of the attic with duct runs), this further reduces the impact of higher attic temperatures, and super-insulating the ducts reduces duct loss effects. Ongoing experiments investigate the precise energy use implications of buried ducts, and future investigations should explore their effects alongside unvented attics.

During prolonged cold weather, moisture comes primarily from indoor rather than outdoor sources. This puts the unvented attic at more risk if the interior moisture is not managed effectively. This is when the vapor diffusion port is most needed to allow the higher moisture content in these attics to pass through to the drier, cold outdoors.

Data from field experiments indicate cyclic drying across seasons. Also, as we expected, north roof decks experience the greatest risk of moisture issues, although they do not appear to be crossing any threshold of failure in the experiments

documented here (mold index, corrosion, or moisture content). Perhaps surprisingly, lower points in an unvented roof deck appear to be more susceptible to moisture failure. This may be as a result of:

- Inverted stratification trends of temperature and RH within the unvented attic during the winter
- Convective looping as the result of the suspended radiant barrier creating a downward convective current at the interior of the sheathing, affecting roof deck moisture adsorption and desorption
- Moist indoor air entering the attic during winter and condensing on the nearest cool surface, the lower roof sheathing
- The functionality of the diffusion ports.

Occupant set points have significant impact on the RH and dew point of attic surfaces. Comparing homes with different set points is not an apples-to-apples comparison, and it is helpful to accompany the field observations with sensitivity modeling and/or larger-scale field experiments. The stress case sensitivity modeling found that occupant set points can mean the difference between extreme mold and corrosion risk and very minimal risk.

Hurricane Ian and Tropical Storm Nicole also allowed for the evaluation of resilience after this type of extreme weather event. None of the attics showed evidence of bulk water intrusion, nor did they trap moisture from the storms. The unvented attics experienced lower RH at the midpoint of the attic than did the baseline attic during and directly after these extreme weather events, indicating the potential resilience advantages of unvented attics, provided they are designed to sufficiently prevent bulk water intrusion.

Hygrothermal models are most useful when used for comparing options and scenarios, and this study is no exception. Although the roof deck and attic floor models could be tuned to a certain extent, they showed biases in temperature and humidity during certain seasons. For example, before post-processing, the attic floor model developed here was slightly overpredictive of cooling season moisture issues, and the roof deck model was under-predictive of heating season moisture issues. These limitations are likely attributable to the complex physics inherent to attics, and unvented attics in particular, which can include high temperature gradients, convective air currents, unequally distributed temperature and humidity, and, in this case, the presence of a draped radiant barrier that may disproportionately influence air and moisture levels adjacent to the roof deck. We need more information on the effects of draped radiant barriers in unvented attics as well as how air and moisture move within attic spaces. For example, research shows that insulated assemblies with radiant barriers can develop convection loops that lead to diminished thermal resistance (Verschoor 1977; Belusko, Bruno, and Saman 2011). Further investigation is needed, however, to quantify the

moisture effects of convection loops on uninsulated, sloped roof decks with draped radiant barriers.

In order to understand the limits of the construction methods we evaluated, we modeled stress test conditions using hygrothermally challenging conditions unlikely to persist for multiple years on end. Some of these conditions included cool, humid weather; high latent loads from occupants; a cool roof; and stressful set points. The modeled stress test results for the roof deck are more alarming than the attic floor results in terms of the mold index. Corrosion also seems highly likely under these high-stress conditions. Next steps for modeling include further investigation of the discrepancies between modeled and observed conditions, particularly in terms of the behavior of attic air behind the radiant barrier and circulating within the attic in general. Future work could use these tuned models to perform additional sensitivity analyses on both the attic floor and the roof deck, altering additional inputs to determine what measures are most effective in mitigating mold and corrosion risk.

4.2 Applications to Building Practice

The safe use of buried R-8 ducts in attics with radiant barriers in hot, humid climates may be facilitated by an unvented attic with vapor diffusion ports under certain conditions. We will need more research, however, to determine the required level of attic air sealing, occupancy limitations, type of roof exterior, moisture sensitivity of exterior duct-wrap surfaces, influence of building geometry, and climate.

4.3 Limitations

Given that moisture failure can occur as a result of dripping, “sweating” ducts on the attic floor, the attic floor hygrothermal simulation is best seen as a rough indication of hygrothermal performance. Boundary conditions of temperature and RH were measured at the attic floor and at select locations below the ducts, but these measurements cannot fully capture all heterogeneous conditions experienced below the ductwork at the attic floor or on upper portions of the duct-wrap surface buried under insulation.

Without directly modeling ductwork in the attics, our modeled stress testing cannot precisely account for the direct effect of condensation dripping off the ductwork and onto the attic floor. Instead, this analysis focuses on increases in RH, in part as a direct effect of attic air interactions with duct-wrap surfaces. FSEC Energy Research Center and Owens Corning are simultaneously working on directly studying condensation on ductwork in various scenarios, including additional points of measurement on the ductwork.

Aside from Hurricane Ian and Tropical Storm Nicole, the weather we observed happened to be fairly warm compared to past years. As a result, additional observational study would be valuable to capture real-life moisture performance in the context of colder or wetter weather as well as to validate the stress test models.

Moisture measurement setups experienced faulty design and technical difficulties at first. Additionally, moisture content was so low within the studied materials that

measurements fell outside the bounds of accuracy for the equipment used, which is intended to cover the range of concern for moisture content in wood-based materials. This was considered to be acceptable because lower moisture content translates to low concern, but it also meant limited ability to compare measurements to modeled values.

Moisture measurements were focused on OSB and plywood roof decks, which display slightly different properties and mathematical correlations with moisture-pin measurements compared to solid wood members. Various adjustments have been validated to convert moisture-pin measurements to OSB- and plywood-specific measurements, including the Boardman (Boardman, Glass, and Lebow 2017) and Straube (Straube, Onysko, and Schumacher 2002) equations. Because the resulting values would be within 2%–4% of directly measured values, however, the raw data have been presented here, with the note that the degree of certainty is within several percentage values, both because of the materials and because of the range of observed values. The highest measured moisture-content values were below the threshold of concern, so we did not think conversions were necessary.

4.4 Future Work

Based on conversations with the project partners, we recommend further investigation looking into different building parameters. Scaled-up experimental home development with simplified instrumentation and monitoring would be able to confirm and generalize the trends we observed. Buildability and moisture risk could be evaluated using the following variations:

- Different roof heights
- Gable ends versus soffits
- Roof reflectance
- Configurations of diffusion ports
- Depth of blown-in insulation
- Varying methods of achieving and measuring attic airtightness
- Variations in attic floor airtightness
- Presence or absence of radiant barrier.

This future study could also help measure resilience to additional extreme-weather events, as well as energy tradeoffs between unvented attics and higher insulation levels.

We also recommend field experiments with a higher degree of control over set points and occupancy (perhaps unoccupied homes) as well as more refined measurements to refine and further develop the hygrothermal models as we mentioned above.

Subsequently, a sensitivity analysis and in-depth hygrothermal modeling for a wider range of climates would be valuable in understanding the broader geographic applicability of unvented attics with vapor diffusion ports. One central goal would be to define what requirements would define an adequately “unvented attic” in terms of cfm50 per square foot or ACH50. This would help establish production-friendly building practices for attic sealing. Currently, there is no explicit guidance on what metric should be used to determine if an attic is “unvented.”

Secondarily, the sensitivity analysis would do well to investigate:

- Impact of reflective roofs
- Drying potential of differing amounts of conditioned supply air to the attic
- Impact of the radiant barrier on both energy consumption and moisture risk
- Climate limitations
- Occupancy extremes.

Ideally, hygrothermal and computational fluid dynamics models would be combined and validated in a single simulation program, facilitating higher predictive value of models containing unconditioned or semi-conditioned space. In this way, technology advancement could lead to lower-cost exploration of the full suite of attic-construction technologies, including buried ducts, suspended radiant barriers, different configurations of attic venting, and varying amounts of conditioned supply air, without assuming perfectly mixed air. Building these multifunctional models at the same time as performing controlled field experiments would be an efficient way to accomplish many of these future goals.

References

ACCA (Air Conditioning Contractors of America Association, Inc.). 2016. Manual J Residential Load Calculation (8th Edition - Full) [ANSI/ACCA 2 Manual J - 2016]. Arlington, Virginia. Air Conditioning Contractors of America Association, Inc. https://www.acca.org/store#/productDetail/DB68FDFC-BB20-E511-80F5-C4346BAC9A78/.

ANSI/ASHRAE (American National Standards Institute/American Society of Heating, Refrigerating and Air-Conditioning Engineers, Inc.). 2017. *Climatic Data for Building Design Standards.* ANSI/ASHRAE Standard 169-2013. Atlanta, Georgia. American Society of Heating, Refrigerating and Air-Conditioning Engineers, Inc.

ANSI/ASHRAE. 2021. *Criteria for Moisture-Control Design Analysis in Buildings.* ANSI-ASHRAE Standard 160. ANSI/American Society of Heating, Refrigerating and Air-Conditioning Engineers.

ASTM. 2015a. *Test Method for Determination of Emittance of Materials near Temperatures Using Portable Emissometers.* ASTM Standard C1371. West Conshohocken, Pennsylvania. ASTM International.

ASTM. 2015b. *Standard Practice for Installation and Use of Interior Radiation Control Coating Systems in Building Systems.* ASTM Standard Specification C1321. West Conshohocken, Pennsylvania. ASTM International.

Bailes, A. 2012. “Water Loves Cold and Other HVAC Duct Failure Stories.” Energy Vanguard. Accessed October 30, 2023. https://www.energyvanguard.com/blog/Water-Loves-Cold-and-Other-HVAC-Duct-Failure-Stories.

Belusko, M., F. Bruno, and W. Saman. 2011. “Investigation of the thermal resistance of timber attic spaces with reflective foil and bulk insulation, heat flow up. *Applied Energy 88*(1), 127–137. https://www.sciencedirect.com/science/article/pii/S0306261910002862#fig1.

Boardman, C. R., S.V. Glass, and P.K. Lebow. 2017. “Simple and accurate temperature correction for moisture pin calibrations in oriented strand board.” *Building and Environment, 112*, 250–260.

California Energy Commission. 2015. *2016 Residential Compliance Manual.*

DOE (U.S. Department of Energy). 2011. *Guide to Cool Roofs.* Washington, DC. Energy Efficiency and Renewable Energy Information Center.

Fallahi, A., H. Durschlag, D. Elliot, J. Hartsough N. Shukla, and J. Kosny. 2013. *Internal Roof and Attic Thermal Radiation Control Retrofit Strategies for Cooling-Dominated Climates.* U.S. Department of Energy Building Technologies Office.

Griffin, D.M. 1977. “Water Potential and Wood-Decay Fungi.” *Annual Review of Phytopathology 15*, 319–329.

ICC (International Code Council). 2017. *2018 International Energy Conservation Code.*

Lstiburek, J. 2016. “Building Sciences: Ping Pong Water and the Chemical Engineer.” *ASHRAE Journal*, 62–70. https://technologyportal.ashrae.org/Journal/ArticleDetail/1755.

Lstiburek, J. 2020. “Building Sciences: Conditioned Unvented Attics and Unconditioned Unvented Attics: But with Fiberglass and Mineral Wool.” *ASHRAE Transactions 62*.

Lstiburek, J., and P. Cole. 2017. *New Code Options for Insulating, Sealing, and Controlling Moisture in Unvented Attics in Residential Buildings.* U.S. Department of Energy.

Mallay, D. 2016. *Compact Buried Ducts in a Hot-Humid Climate House.* U.S. Department of Energy.

Marden, C., and N. Conarroe. 2023. Personal communication.

Miller, W.A., S. Railkar, M.C. Shiao, and A.O. Desjarlais. 2016. “Sealed Attics Exposed to Two Years of Weathering in a Hot and Humid Climate.” Presented at Thermal Performance of the Exterior Envelopes of Whole Buildings XIII International Conference. Clearwater, Florida. ASHRAE.

Pallin, S., P.R. Boudreaux, S. Jo, M. Perez, and A. Albaugh. 2016. “Simulations of Indoor Moisture Generation in U.S. Homes.” Presented at Symposium on Advances in Hygrothermal Performance of Building Envelopes: Materials, Systems and Simulations. 261–290. Orlando, Florida. ASTM International. https://doi.org/10.1520/STP159920160111.

Prevatt, D., and W. Miller. 2017. “Phase II Analytical Assessment of Field Data for Sealed Attics in Florida Climate Zones 1 and 2-Predicting Moisture Buildup in Roof Sheathing.”

Rudd, A.F., and J. Lstiburek. 1998. “Vented and Sealed Attics in Hot Climates.” *ASHRAETransactions,* x(2).

Salonvaara, M. 2011. *RP-1325—Environmental Weather Loads for Hygrothermal Analysis and Design of Buildings.* ASHRAE.

scikit-learn. 2023. sklearn.ensemble.RandomForestRegressor. Accessed from scikit-learn: https://scikit-learn.org/stable/modules/generated/sklearn.ensemble.RandomForestRegressor.html.

Shapiro, C., A. Magee, and W. Zoeller. 2013. *Reducing Thermal Losses and Gains With Buried and Encapsulated Ducts in Hot-Humid Climates.* Consortium for Advanced

Residential Buildings. Oak Ridge, Tennessee. U.S. Department of Energy: Building America.

Straube, J., D. Onysko, and C. Schumacher. 2002. “Methodology and Design of Field Experiments for Monitoring the Hygrothermal Performance of Wood Frame Enclosures.” *Journal of Building Physics* 26(2), 123–151.

The Energy Conservatory. 2023. *TECLOG 4*. https://energyconservatory.com/downloads/teclog3/.

Ueno, K. 2016. *Unvented Roof Research: Reasearch and Reality*. Building Science Corporation. Accessed April 30, 2019. http://nesea.org/file/11407/download?token=4smhIvIF.

Ueno, K., and J. Lstiburek. 2015. *Field Testing Unvented Roofs With Asphalt Shingles in Cold and Hot-Humid Climates.* Building Science Corporation. U.S. Department of Energy/Building America. https://www.nrel.gov/docs/fy15osti/64543.pdf.

Ueno, K., and J. Lstiburek. 2016. *Field Testing of an Unvented Roof with Fibrous Insulation, Tiles, and Vapor Diffusion Venting.* Building Science Corporation. U.S. Department of Energy/Building America. https://www.nrel.gov/docs/fy16osti/64999.pdf.

Verschoor, J.D. 1977. *Effectiveness Of Building Insulation Applications.* Johns-Manville Sales Corporation. Port Hueneme, California. Naval Construction Battalion Center, Civil Engineering Laboratory. https://apps.dtic.mil/sti/citations/ADA053452.

Viitanen, H., and T. Ojanen. 2007. “Improved model to predict mold growth in building materials.” *Thermal Performance of the Exterior Envelopes of Whole Buildings X–Proceedings CD* 2–7.

Wei, J., C. Chappel, A. Pande, and M. Christie. 2014. *Residential Ducts in Conditioned Space/High Performance Attics.* California Statewide Codes and Standards Enhancement (CASE) Program.

Withers, C.R., and E. Martin. 2022. “Seasonal Moisture Impacts on Roof Deck Moisture in Unvented Attics in North Florida.” Presented at Thermal Performance of the Exterior Envelopes of Whole Buildings XIII International Conference 649–657. Clearwater, Florida. ASHRAE. https://publications.energyresearch.ucf.edu/wp-content/uploads/2023/04/FSEC-PF-1275-23.pdf.

Withers, C., K. Fenaughty, and J. Sonne. 2020. “Measured Energy and Moisture Performance Impacts from Vented and Unvented Attic With Insulation On Top of Ceiling in the Hot Humid Climate Zone.” *ACEEE 2020 Summer Study on Energy Efficiency in Buildings Conference Proceedings.* https://publications.energyresearch.ucf.edu/wp-content/uploads/2021/05/FSEC-PF-1264-21.pdf.

Zabel, R.A., and J.J. Morrell. 1992. *Wood Microbiology: Decay and Its Prevention.* San Diego, California: Academic Press.

Appendix A. Field Experiment Data Acquisition

A.1 Measurement Protocols

All measurements were sampled on 20-second intervals, with the exception of the wind speed measurement, which was sampled at 2 kHz, then averaged each 20-second interval. Separate tables of data were stored on intervals of 1 minute, 15 minutes, 60 minutes, and 24 hours. For each of these tables, the values obtained at 20-second intervals were averaged or totaled, depending on the measurement. For wind speed and direction, maximum, minimum, and standard deviation were also stored in each table.

Time Stamp Definition

Each record in each table has a time stamp. This value represents Local Standard Time (for Florida, Eastern Standard Time). The time represents the end of the data storage interval. For example, in the 15-minute data, a time stamp of 10:15 represents the statistics (average, minimum, maximum) of 20-second-sampled measurements over the period of 10:00:20 through 10:15:00.

A.2 Full Sensor Set and Specification for Field Experiments

Table 9 and Table 10 show the full descriptions and list of locations of each sensor and measurement.

Table 9. Sensor Models

Description	Manufacturer	Part Number	Accuracy
Heat Flux Sensor	Omega	HFS-5	-
Split-Core DC-Output Current Transformer	NK Technologies	AT1-005-000-SP (0-50A)	± 2 %FS
		SC100-2L (10-200A)	± 1 %FS
Leaf Wetness Sensor	METER Group	22121-1	-
T&RH sensor: Temperature	E + E Elektronik	EE08	± 0.2 °C
T&RH sensor: RH			± 2 %RH
Thermocouple	Omega	HFS-5 (Type T)	± 0.2 °C
Wood Moisture Content (MC)	Oak Ridge National Laboratory	-	-
Thermistor	Honeywell	192-103LET-A01	± 0.2 °C
Differential Pressure Sensor	Setra	26410R1WD11T1F	± 1.25 Pa
Anemometer	RM Young	03102	± 0.5 m/s
Wind Vane	RM Young	03302	-

Description	Manufacturer	Part Number	Accuracy
Pyranometer (horizontal)	Apogee	SP510	± 5.0 %
Pyrgeometer (horizontal)	Apogee	SL-510-SS	± 5.0 %
Pyrgeometer temperature			± 1.0 °C
Rain Gauge	Campbell Scientific	ClimaVue 50	± 5.0 %

Table 10. Full Sensor List

Note that RB stands for radiant barrier, and BD stands for buried ducts

Sensor type	Home	Zone	Location	Detailed location	Purpose
T/RH	Buried ducts	Outdoor environment	Roof	Shielded	Ambient T/RH measurements at site
Anemometer	Buried ducts	Outdoor environment	Roof	Unobstructed, above ridge line	Wind speed near roof
Wind vane	Buried ducts	Outdoor environment	Roof	Unobstructed, above ridge line	Wind direction near roof
Pyranometer	Buried ducts	Outdoor environment	Roof	Horizontal, upward-facing; unobstructed, above ridge line	Solar radiation at peak of roof
Pyrgeometer	Buried ducts	Outdoor environment	Roof	Horizontal, upward-facing; unobstructed, above ridge line	Net IR radiation at peak of roof and IR from sky (based on temperature measurement)
Rain gauge	Buried ducts	Outdoor environment	Roof	Unobstructed, above ridge line	Hourly rain accumulation at site
T/RH	Baseline	Attic	North roof deck	Low location (near to the attic floor)	Variation of surface temperature and RH of the north roof deck from top to bottom
T/RH	Baseline	Attic	North roof deck	Center location	Variation of surface temperature and RH of the north roof deck from top to bottom
T/RH	Baseline	Attic	North roof deck	High location above the diffusion port	Variation of surface temperature and RH of the north roof deck from top to bottom

Sensor type	Home	Zone	Location	Detailed location	Purpose
T/RH	Baseline	Attic	East roof deck	Center location	Surface temperature and RH of the center of east roof deck
T/RH	Baseline	Attic	West roof deck	Center location	Surface temperature and RH of the center of west roof deck
T/RH	Baseline	Attic	South roof deck	Center location	Surface temperature and RH of the center of south roof deck
T/RH	Baseline	Attic	Attic air	Air T/RH along the ridge line above the diffusion port	Part of temperature and RH stratification measurements along the ridge
T/RH	Baseline	Attic	Attic air	Air T/RH along the ridge line at same height as the diffusion port	Part of temperature and RH stratification measurements along the ridge
T/RH	Baseline	Attic	Attic air	Air T/RH halfway between the ridge and the insulation	Part of temperature and RH stratification measurements along the ridge
T/RH	Baseline	Attic	Attic air	Air T/RH at the top of the insulation	Part of temperature and RH stratification measurements along the ridge
T/RH	Baseline	Attic	Attic floor	In the master bedroom along the attic floor gypsum board	T/RH for the attic/insulation interface
T/RH	Baseline	Conditioned space	Air handling unit (AHU) return vent	2nd Floor AHU return vent	Air conditions in the conditioned space
T/RH	Baseline	Attic	Supply duct start	Inside the longest duct run that supplies the back half of the home Near the AHU	Duct supply conditions
T/RH	Baseline	Attic	Supply duct end	Inside the longest duct run that supplies the back half of the home.	Duct supply conditions

Sensor type	Home	Zone	Location	Detailed location	Purpose
				Near the plenum at the back of the home.	
Heat Flux	Baseline	Attic	North roof deck	Center location	Heat flux at the OSB/Attic Air interface
Heat Flux	Baseline	Attic	South roof deck	Center location	Heat flux at the OSB/Attic Air interface
Heat Flux	Baseline	Attic	Attic floor	In the master bedroom along the attic floor gypsum board	Heat flux for the attic/insulation interface
Moisture pin	Baseline	Attic	North roof deck	Lower location (near to the attic floor)	Moisture content variation top to bottom of north roof deck
Moisture pin	Baseline	Attic	North roof deck	Center location	Moisture content variation top to bottom of north roof deck. Center moisture content of OSB
Moisture pin	Baseline	Attic	North roof deck	Upper location (near to the ridge above the diffusion port)	Moisture content variation top to bottom of north roof deck
Moisture pin	Baseline	Attic	South roof deck	Center location	Center moisture content of OSB
Moisture pin	Baseline	Attic	East roof deck	Center location	Center moisture content of OSB
Moisture pin	Baseline	Attic	West roof deck	Center location	Center moisture content of OSB
Leaf wetness sensor	Baseline	Attic	Bottom side of supply duct near AHU	Bottom side of the duct near the AHU	Presence of condensation at ductwork
Induction clamp	Baseline	Conditioned Space	HVAC power panel	In the 2nd floor HVAC power panel	Monitor the runtimes of the HVAC system

Sensor type	Home	Zone	Location	Detailed location	Purpose
Pressure differential	Baseline	Attic and conditioned space	Attic Floor	One end connected to tube inside open space of attic; other end connected to tube open to living space	Pressure differential between the attic and conditioned space
Thermistor	Baseline	Outdoor environment	North roof deck	Under a shingle in the center of roof deck. Approximately near the interior centrally located sensors	Outside boundary condition temperature
Thermistor	Baseline	Outdoor environment	South roof deck	Under a shingle in the center of roof deck. Approximately near the interior centrally located sensors	Outside boundary condition temperature
T/RH	Baseline	Attic	Bottom side of supply duct near AHU	Bottom side of the duct near the AHU	Presence of condensation at ductwork
T/RH	Buried ducts	Conditioned space	AHU return vent	2nd Floor AHU return vent	Air conditions in the conditioned space
T/RH	Buried ducts	Attic	Supply duct start	Inside the longest duct run that supplies the back half of the home Near the AHU	Duct supply conditions
T/RH	Buried ducts	Attic	Supply duct end	Inside the longest duct run that supplies the back half of the home. Near the plenum at the back part of the home.	Duct supply conditions
T/RH	Buried ducts	Attic	Shaft liner	Center of the shaftliner, halfway up in height, halfway depth of attic	Help understand the heat flow and RH difference across the party wall; quantify the impact of the adjacent unit

Sensor type	Home	Zone	Location	Detailed location	Purpose
Leaf wetness sensor	Buried ducts	Attic	Bottom side of supply duct near AHU	Bottom side of the duct near the AHU	Presence of condensation at ductwork
Induction clamp	Buried ducts	Conditioned Space	HVAC power panel	In the 2nd floor HVAC power panel	Monitor the runtimes of the HVAC system
T/RH	Buried ducts	Attic	Bottom side of supply duct near AHU	Bottom side of the duct near the AHU	Presence of condensation at ductwork
T/RH	Diffusion port	Attic	Supply duct middle	Inside a duct run that supplies the back half of the home, about midway between air handler and grille	Monitor duct interior conditions and determine when space conditioning is operating
T/RH	Diffusion port	Attic	Bottom side of supply duct near AHU	Bottom side of the insulated duct near the AHU	Presence of condensation at ductwork
T/RH	Diffusion port	Attic	Attic Floor	In the master bedroom along the attic floor gypsum board	T/RH for the attic/insulation interface
T/RH	Diffusion port	Attic	Attic air	Air T/RH along the ridge line at same height as the diffusion port	Monitor attic air conditions above the diffusion port to identify conditions conducive to failure and compare to conditions above diffusion port
T/RH	Diffusion port	Attic	Attic air	Air T/RH along the ridge line above the diffusion port	Monitor attic air conditions at the diffusion port to identify conditions conducive to failure and compare to conditions at diffusion port
Moisture pin	Diffusion port	Attic	North roof deck	Lower location (near to the attic floor)	Moisture content variation top to

Sensor type	Home	Zone	Location	Detailed location	Purpose
					bottom of north roof deck
Moisture pin	Diffusion port	Attic	North roof deck	Upper location (near to the ridge above the diffusion port)	Moisture content variation top to bottom of north roof deck
T/RH	Diffusion port + RB	Attic	Supply duct middle	Inside a duct run that supplies the back half of the home, about midway between air handler and grille	Monitor duct interior conditions and determine when space conditioning is operating
T/RH	Diffusion port + RB	Attic	Bottom side of supply duct near AHU	Bottom side of the insulated duct near the AHU	Presence of condensation at ductwork
T/RH	Diffusion port + RB	Attic	Attic Floor	In the master bedroom along the attic floor gypsum board	T/RH for the attic/insulation interface
T/RH	Diffusion port + RB	Attic	Attic air	Air T/RH along the ridge line at same height as the diffusion port	Monitor attic air conditions above the diffusion port to identify conditions conducive to failure and compare to conditions above diffusion port
T/RH	Diffusion port + RB	Attic	Attic air	Air T/RH along the ridge line above the diffusion port	Monitor attic air conditions at the diffusion port to identify conditions conducive to failure and compare to conditions at diffusion port
Moisture pin	Diffusion port + RB	Attic	North roof deck	Lower location (near to the attic floor)	Moisture content variation top to bottom of north roof deck

Sensor type	Home	Zone	Location	Detailed location	Purpose
Moisture pin	Diffusion port + RB	Attic	North roof deck	Upper location (near to the ridge above the diffusion port)	Moisture content variation top to bottom of north roof deck
T/RH	Diffusion port + RB + BD	Attic	North roof deck	Low location (near to the attic floor)	Variation of surface temperature and RH of the north roof deck from top to bottom
T/RH	Diffusion port + RB + BD	Attic	North roof deck	Center location	Variation of surface temperature and RH of the north roof deck from top to bottom
T/RH	Diffusion port + RB + BD	Attic	North roof deck	High location above the diffusion port	Variation of surface temperature and RH of the north roof deck from top to bottom
T/RH	Diffusion port + RB + BD	Attic	East roof deck, main attic	Attached to center of the diffusion port	Used for estimating a difference in conditions across the vent
T/RH	Diffusion port + RB + BD	Attic	Attic air	Air T/RH along the ridge line above the diffusion port	Part of temperature and RH stratification measurements along the ridge
T/RH	Diffusion port + RB + BD	Attic	Attic air	Air T/RH along the ridge line at same height as the diffusion port	Part of temperature and RH stratification measurements along the ridge
T/RH	Diffusion port + RB + BD	Attic	Attic air	Air T/RH halfway between the ridge and the insulation	Part of temperature and RH stratification measurements along the ridge
T/RH	Diffusion port + RB + BD	Attic	Attic air	Air T/RH at the top of the insulation	Part of temperature and RH stratification measurements along the ridge
T/RH	Diffusion port + RB + BD	Attic	Attic floor	In the master bedroom along the attic floor gypsum board	T/RH for the attic/insulation interface

Sensor type	Home	Zone	Location	Detailed location	Purpose
Heat Flux	Diffusion port + RB + BD	Attic	Attic floor	In the master bedroom along the attic floor gypsum board	Heat flux for the attic/insulation interface
Heat Flux	Diffusion port + RB + BD	Attic	North roof deck	Center location	Heat flux at the OSB/Attic Air interface
Pressure differential	Diffusion port + RB + BD	Attic and conditioned space	Attic Floor	One end connected to tube inside open space of attic; other end connected to tube open to living space	Pressure differential between the attic and conditioned space
Moisture pin	Diffusion port + RB + BD	Attic	North roof deck	Lower location (near to the attic floor)	Moisture content variation top to bottom of north roof deck
Moisture pin	Diffusion port + RB + BD	Attic	North roof deck	Center location	Moisture content variation top to bottom of north roof deck. Center moisture content of OSB
Moisture pin	Diffusion port + RB + BD	Attic	North roof deck	Upper location (near to the ridge above the diffusion port)	Moisture content variation top to bottom of north roof deck
T/RH	Diffusion port + RB + BD	Outdoor environment	North roof deck	Under the vent cover on the center diffusion port	Used for estimating a difference in conditions across the vent
Thermistor	Diffusion port + RB + BD	Outdoor environment	North roof deck	Under a shingle in the center. Approximately near the interior centrally located sensors	Outside boundary condition temperature
T/RH	Diffusion port + RB + BD	Attic	Shaft liner	Center of the shaftliner, halfway up in height, halfway depth of attic	Help understand the heat flow and RH difference across the party wall; quantify the impact of the adjacent unit

Sensor type	Home	Zone	Location	Detailed location	Purpose
T/RH	Diffusion port + RB + BD	Conditioned space	AHU return vent	2nd Floor AHU return vent	Air conditions in the conditioned space
T/RH	Diffusion port + RB + BD	Attic	Supply duct start	Inside the longest duct run that supplies the back half of the home. Near the AHU.	Duct supply conditions
Leaf wetness sensor	Diffusion port + RB + BD	Attic	Bottom side of supply duct near AHU	Bottom side of the duct near the AHU	Presence of condensation at ductwork
Induction clamp	Diffusion port + RB + BD	Conditioned Space	HVAC power panel	In the 2nd floor HVAC power panel	Monitor the runtimes of the HVAC system
T/RH	Diffusion port + RB + BD	Attic	Supply duct end	Inside the longest duct run that supplies the back half of the home. Near the plenum at the back part of the home.	Duct supply conditions
Heat Flux	Diffusion port + RB + BD	Attic	East roof deck, main attic	Center location	Heat flux at the OSB/Attic Air interface place in the center both in height and depth
Moisture pin	Diffusion port + RB + BD	Attic	East roof deck, main attic	Center location	Center (both height and depth) moisture content of OSB
T/RH	Diffusion port + RB + BD	Attic	East roof deck, main attic	Center location	Center (both height and depth) measurement of T/RH of OSB attic air interface
Thermistor	Diffusion port + RB + BD	Attic	East roof deck, main attic	Under a shingle in the center. Approximately near the interior centrally located sensors	Outside boundary condition temperature

Sensor type	Home	Zone	Location	Detailed location	Purpose
T/RH	Diffusion port + RB + BD	Attic	South roof deck	Center location	Center (both height and depth) measurement of T/RH of OSB attic air interface
T/RH	Diffusion port + RB + BD	Attic	East roof deck, smaller attic	High location near and above the diffusion port	T/RH for the OSB and attic air interface of the smaller attic
Moisture pin	Diffusion port + RB + BD	Attic	East roof deck, smaller attic	High location near and above the diffusion port	Moisture content for the OSB and attic air interface of the smaller attic
T/RH	Diffusion port + RB + BD	Attic	Bottom side of supply duct near AHU	Bottom side of the duct near the AHU	Presence of condensation at ductwork

A.3 Moisture Pin Circuit

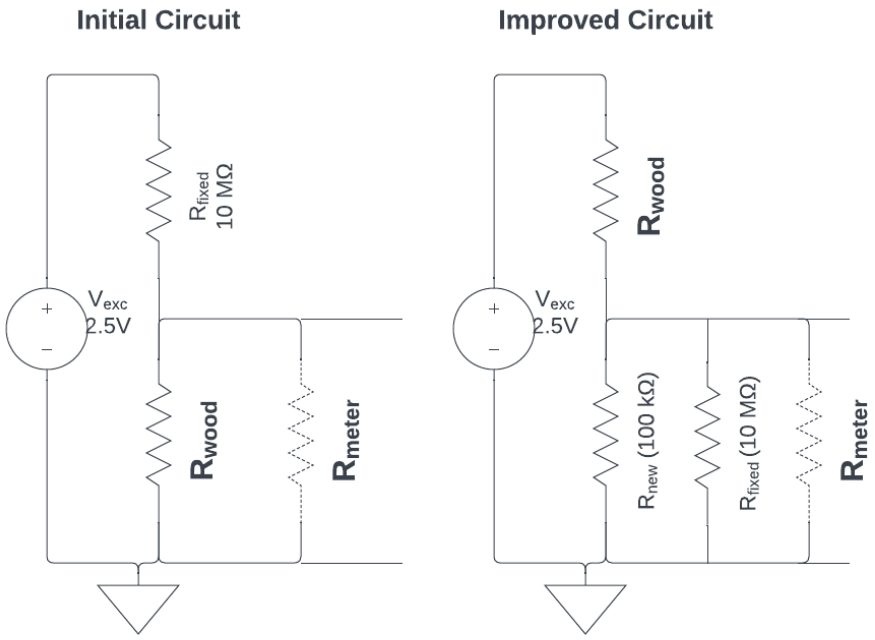

Figure 45. Circuit for measuring moisture pin resistance

Moisture pins were deployed in the roof decks as described in Section 2.2.3, but the initial circuit design was not usable for low-moisture roof decking, prompting a post-

installation redesign. The problem with the initial circuit was that the input impedance of the meter/logger (Rmeter) was in parallel with the wood resistance (Rwood). Because Rwood is quite large (>10 megaohms when the wood is dry, the parallel combination of meter and wood resistance was appreciably lower than wood resistance, causing the calculated moisture content to be in error. In the corrected circuit, the input impedance of the meter/logger (Rmeter) is in parallel with an added 100 kiloohms resistor, resulting in an effective resistance of 99 kiloohms. Because Rmeter is much larger than 99 kiloohms, it now only slightly lowers the effective resistance of the lower leg of the voltage divider and results in a much more accurate measurement of the wood resistance and calculated moisture content. Figure 46 shows moisture content measured by the moisture pins using the improved circuit versus that reported by a typical inexpensive handheld electrical resistance moisture meter (General MM9 meter).

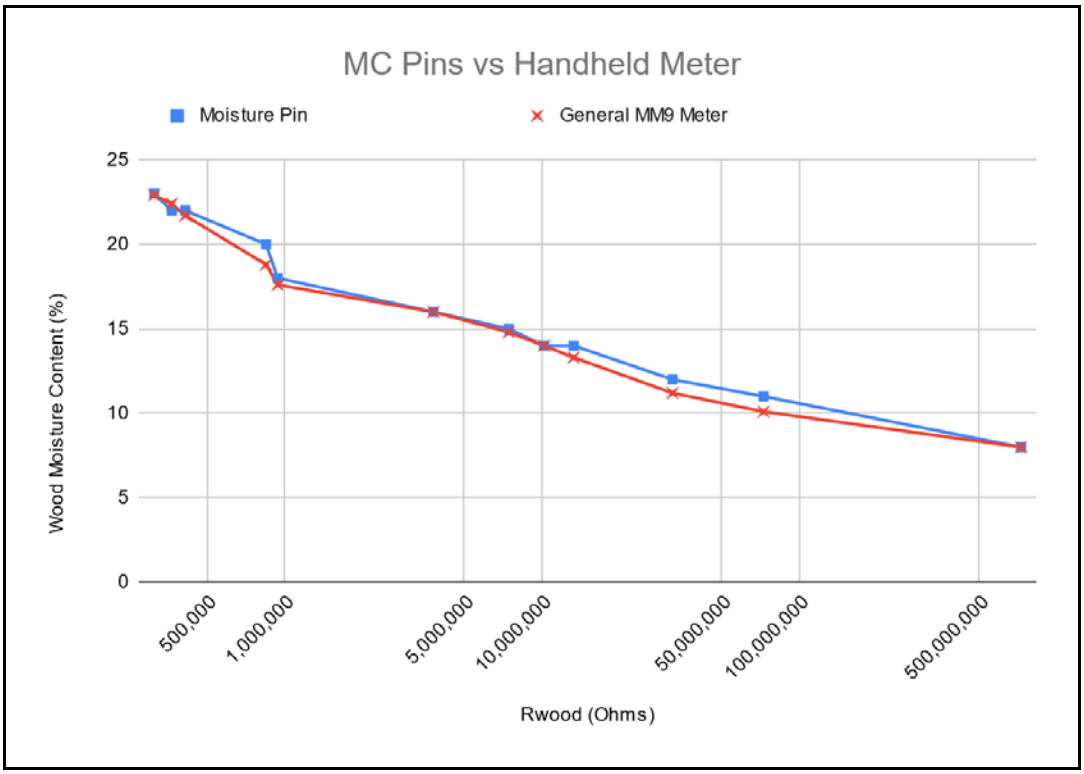

Figure 46. Moisture content reported by moisture pins versus handheld meter

A.4 Occupancy Simulation

Internal generated sensible and latent loads impact the runtime of central cooling and heating systems and influence resulting interior moisture levels. The project considered the need for simulating occupancy by generating heat and moisture in unoccupied homes. It was considered safer to not operate unsupervised heating sources in the building, and the primary focus of the testing was to evaluate potential for detrimental moisture impacts from specific building practices. Therefore, internal latent load was a higher priority than sensible loads. Internal moisture could safely be generated by using a commercial-grade humidifier located within a shower/tub in a bathroom and using a small floor fan to help circulate moisture into the main house zone.

Bathroom used for latent generation

Humidifier and water treatment filters located within shower stall

Figure 47. Photos show bathroom and humidifier location used at the baseline home

Photos by the authors

The amount and schedule of internal generated moisture was based upon guidance from Pallin et al. (2016). Given the size of the four-bed, four-bath baseline home, a daily total of 10.9 kg (24.0 lb) of water vapor was generated with a variable profile throughout the day.

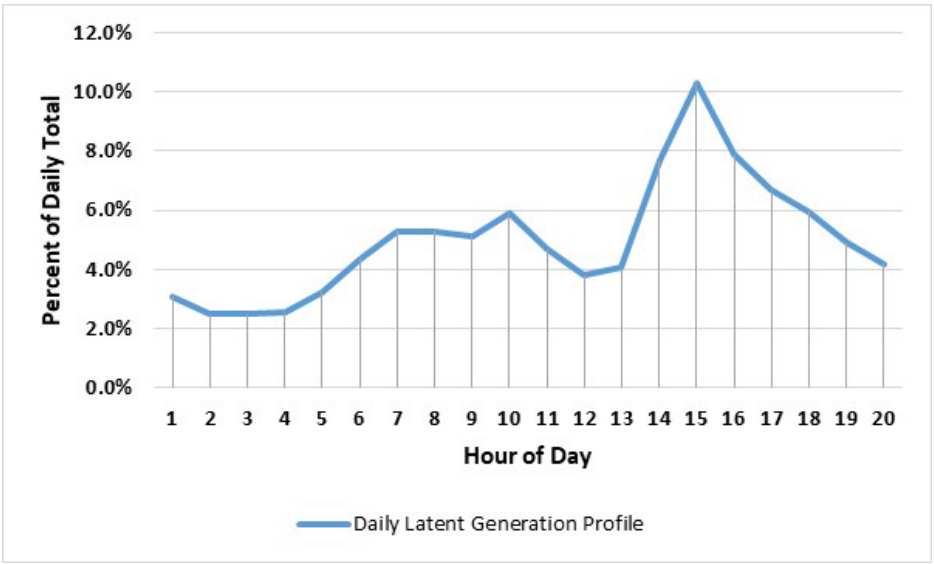

Figure 48. Daily internal latent generation schedule

The original plan was to install automated humidification in at least three homes, but humidification was only installed in one home because the other units were either already occupied or would be shortly after monitoring had begun. We operated a humidifier in the baseline home from September 22 through November 23, 2022, with one interruption. The humidifier was turned off in preparation for Hurricane Ian on September 27 and was not restarted until October 13.

The test homes started out unoccupied, but by the time monitoring had begun, most were beginning to be occupied.

Approximate occupancy dates for each home are provided in Table 11.

Table 11. Dates of Occupancy

Configuration	Occupancy Date
Baseline	December 2022
Buried ducts	July 2022
Diffusion port	June 2022
Diffusion port + RB	June 2022
Diffusion port + RB + BD	October 2022

A.5 Roof Deck Temperature Comparison

Although the accumulation of moisture was the primary focus of durability, the roofing industry may be interested in the differences in temperature between the vented and unvented attics' exterior roof decks. The baseline and attic with all measures were instrumented with thermistors measuring exterior roof deck temperature, per Figure 10 and Figure 11. The unvented attic with radiant barrier and buried duct did not have a south-facing thermistor because its only south-oriented roof was part of a smaller section of attic that was only somewhat connected to the main attic; therefore, only the two homes' north roof decks can be directly compared in Figure 49. South baseline and east unvented + radiant barrier + buried duct roof deck temperatures are also provided for reference, as they receive more solar radiation than does the north roof deck.

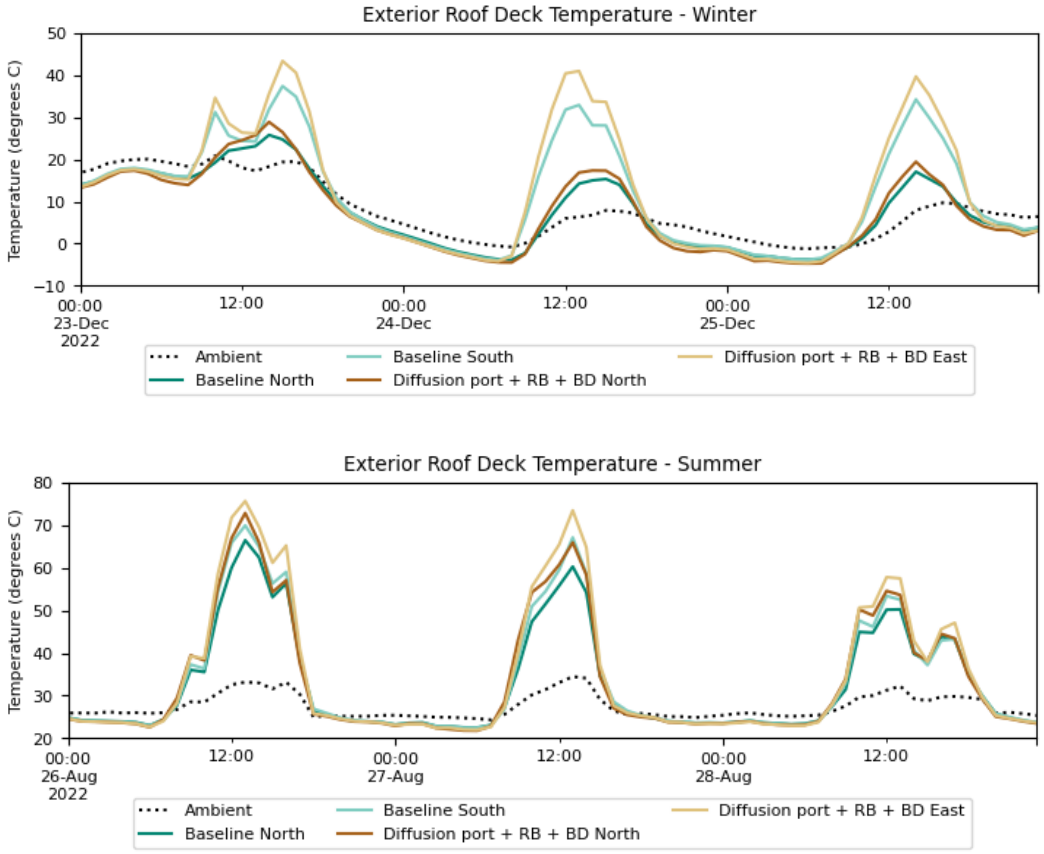

Figure 49. Exterior roof deck surface temperature (hourly average) during cold and hot representative periods

Appendix B. Attic Instrumentation Details

All photos in this section were taken by the report authors.

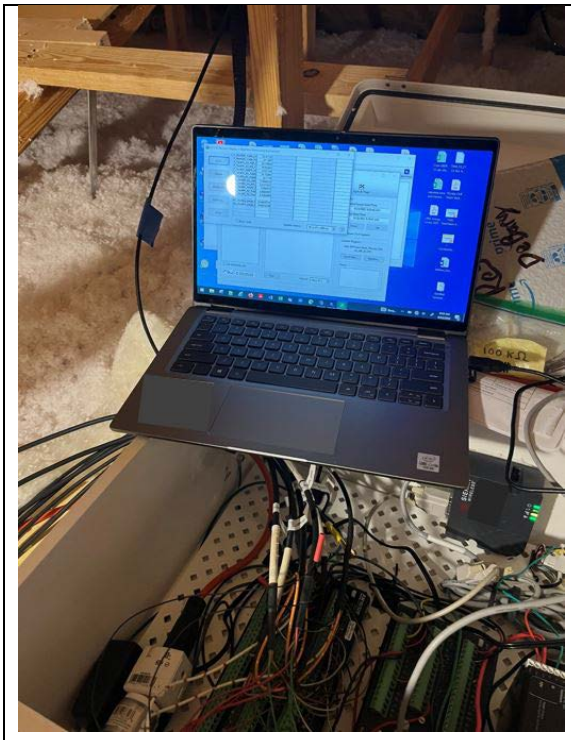

Figure 50. Datalogging box near attic hatch

Figure 51. Datalogging box near attic hatch

Figure 52. Meteorological station showing windspeed, wind direction, temperature and RH sensors, rain gauge, and pyranometer

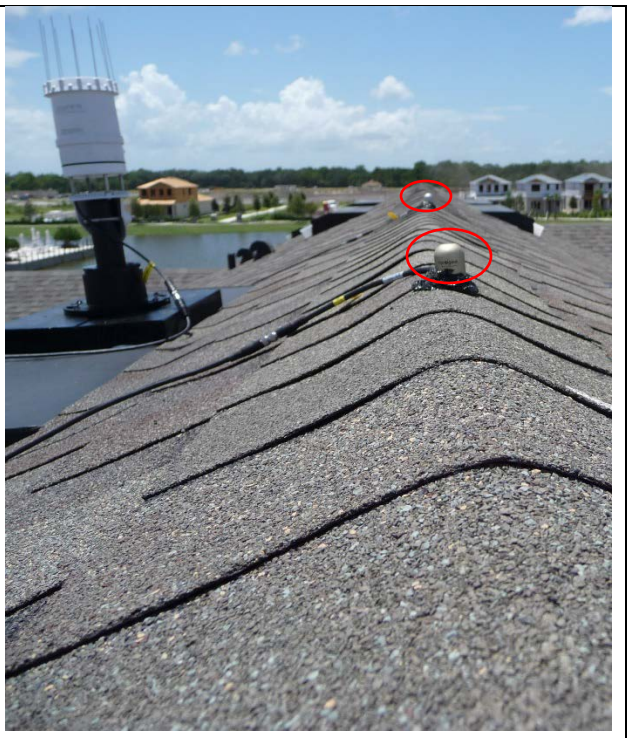

Figure 53. Rain gauge, pyrgeometer, and pyranometer located on rooftop

Figure 54. Exterior roof deck temperature measurement under shingle

Figure 55. Attic air temperature and RH strata with radiation shielding inside baseline attic

Figure 56. Roof heat flux, wood moisture content, and T&RH sensors between roof deck and radiant barrier

Figure 57. Radiant barrier access seams resealed with foil tape after roof deck sensors installed

Figure 58. Duct-wrap surface wetness sensor and T&RH sensor located on bottom of supply trunk duct near plenum in diffusion port + radiant barrier + buried duct attic

Figure 59. Duct-wrap surface wetness sensor and T&RH sensor located on bottom of supply trunk duct near plenum in baseline attic

Figure 60. Indoor air temperature and RH measured within return next to intake grille

Figure 61. Supply air temperature and RH measured at a downstream location of a branch duct

Figure 62. Differential pressure measurement from attic with reference to house indoor

Figure 63. Differential pressure indoor reference through small tube near light in 2nd floor hallway

Figure 64. Southeast view of north section of diffusion port + radiant barrier + buried duct attic after all sensors installed and final insulation blown over ducts

Figure 65. View toward party wall of diffusion port + radiant barrier + buried duct attic after all sensors installed and final insulation blown over ducts

Appendix C. Calculation to Determine Attic Component Airtightness

This procedure employs the use of Energy Conservatory's TECLOG software to simultaneously record pressure readings of the attic and living space compared to outdoors.

Attics can be pressurized (we refrain from depressurizing the attic to avoid drawing blown insulation into the fan) across one range (e.g., 5 Pa to 65 Pa), while the living space can be both pressurized and depressurized across a different range. (i.e., the ranges need not match, but they should be as comprehensive as possible.)

The objective of these tests is to arrive at an equation that can be used to estimate the airflow rate from the attic to the living space, as well as airflow rate between the attic and the outdoors, given measured values of the pressure difference or ΔP (PA – PL).

This procedure could be used in a whole-building model to provide hourly air exchange schedules, but it was not used directly in the 1D models discussed here. Only the ACH50 numbers derived using this protocol were ultimately used as reference for airtightness of the roof deck and attic floor.

Assumptions:

1. An airflow rate across a porous boundary can be characterized using the following equation form:

   $F = C(P_1-P_2)^n$
   where:
   F = airflow rate (m^3/min)
   P_1 = total pressure on side 1 of the boundary (Pa)
   P_2 = total pressure on side 2 of the boundary (Pa)
   C = empirical constant (m^3/Pa^n)
   n = empirical constant (unitless)

2. The constants C and n for a particular boundary are the same regardless of the direction of airflow across the boundary.

To obtain the values of constants C and n a number of points must be measured over a wide range of flow rates; a best fit algorithm is used to find the best fit values of C and n given the pairs of F and ΔP measurements.

Test #1: multipoint test to measure attic leakage to outdoors and living space:

$$\mathbf{F_{fan} = F_1 = C_1(P_A-P_O)^{n1}} \qquad \textbf{Eq. C-1}$$

Measurements required (Note: MAKE SURE TO TEST AT LOW ΔP RANGES: 5–20 Pa):

1. F_{fan}
2. $\Delta P_1 = P_A - P_O$
3. $\Delta P_3 = P_A - P_L = 0$

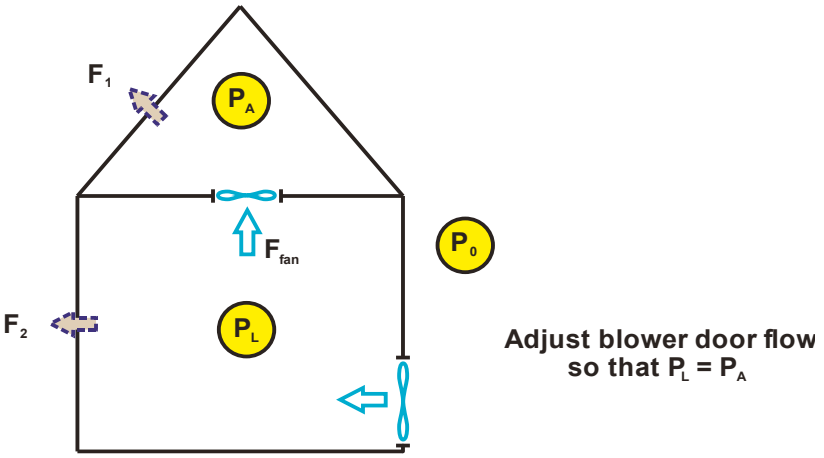

Figure 66. Flows and pressures during attic floor airtightness Test #1

Test #2: multipoint test to measure total house leakage:

$$F_{fan} = F_1 + F_2 = C_1(P_O - P_A)^{n1} + C_2(P_O - P_L)^{n2} \quad \text{Eq. C-2}$$

$$F_{fan} = F_3 + F_2 = C_3(P_A - P_L)^{n3} + C_2(P_O - P_L)^{n2} \quad \text{Eq. C-3}$$

Measurements required:

1. F_{fan}
2. $\Delta P_1 = P_o - P_A$
3. $\Delta P_2 = P_O - P_L$
4. $\Delta P_3 = P_A - P_L$

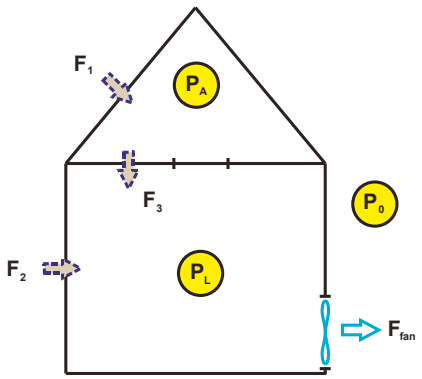

Figure 67. Flows and pressures during attic floor airtightness Test #2

The multipoint data from Test #1 can be used to derive the two constants C_1 and n_1 using a linear regression or multivariate minimization routine. With C_1 and n_1 known, the multipoint data from Test #2 can be used to simultaneously determine the four unknown constants C_2, n_2, C_3, and n_3 using Equations C-2 and C-3 and a multivariate minimization routine. The premise is that there is a unique set of constants that will satisfy both equations for all measurements. The RMSE error between measured fan flow rate and predicted flow rate can be used as the function to minimize. In the example given below, the RMS error in the prediction of the fan flow rate F_{fan} was calculated according to Equation C-4:

$$RMSE = \sqrt{\frac{\sum_{n=1}^{N}(E_n^2)}{N}} \qquad \textbf{Eq. C-4}$$

where:
N = number of calculated values of F_{fan} (N = 19 in this example)
E_n = Error in calculated F_{fan}, row n ($E = F_{fan,calc'd} - F_{fan,meas}$)

In more comprehensible language, the RMS error is the square root of the mean of the squares of the errors.

Table 12. Example of Measured and Predicted Values From Both Blower Door Tests

	Measured Values				**Predicted Values**					
Test #	F_{fan}	ΔP	ΔP	ΔP	F_1	F_2	F_3	F_{fan}	F_{fan}	Error
		out-attic	out-in	attic-in	$C_1(P_O-P_A)^{n1}$	$C_2(P_O-P_L)^{n2}$	$C_3(P_A-P_L)^{n3}$	calculation		
	(cfm)	(Pa)	(Pa)	(Pa)	(cfm)	(cfm)	(cfm)		(cfm)	(cfm)
2	696	3.2	25.3	23.6	195.8	493.4	200.6	(F_1 + F_2)	689.2	-6.9
2	781	4.5	31.5	28.1	251.4	552.7	233.2	(F_1 + F_2)	804.1	23.1
2	855	4.7	35.8	32.3	257.8	590.6	262.4	(F_1 + F_2)	848.5	-6.1

	Measured Values				Predicted Values					
2	907	5.0	39.7	35.5	270.5	623.7	284.1	($F_1 + F_2$)	894.2	-13.1
2	979	6.0	44.9	39.7	305.7	664.2	312.6	($F_1 + F_2$)	969.9	-8.9
2	1040	7.2	50.1	43.5	348.3	703.3	337.8	($F_1 + F_2$)	1051.5	11.3
2	696	3.2	25.3	23.6	195.8	493.4	200.6	($F_3 + F_2$)	694.0	-2.1
2	781	4.5	31.5	28.1	251.4	552.7	233.2	($F_3 + F_2$)	785.9	4.9
2	855	4.7	35.8	32.3	257.8	590.6	262.4	($F_3 + F_2$)	853.1	-1.5
2	907	5.0	39.7	35.5	270.5	623.7	284.1	($F_3 + F_2$)	907.8	0.5
2	979	6.0	44.9	39.7	305.7	664.2	312.6	($F_3 + F_2$)	976.8	-1.9
2	1040	7.2	50.1	43.5	348.3	703.3	337.8	($F_3 + F_2$)	1041.1	0.9

RMS Error = 9.00 cfm

Table 13. Best Fit Values of C and n for Each Flow Path

C_1	87.65	$F_1 = 87.65\Delta P^{0.6972}$	(Test #1)
n_1	0.6972		
C_2	92.61	$F_2 = 92.61\Delta P^{0.5180}$	(Test #2)
n_2	0.5180		
C_3	13.70	$F_3 = 13.70\Delta P^{0.8494}$	
n_3	0.8494		

The values of C1 and n1 were derived from the data from Test #1 using a linear regression routine. The values of C2, n2, C3, and n3 were adjusted using a multivariate minimization routine to minimize the value of RMS error. Figure 48 shows each flow graphed as a function of pressure drop across its respective boundary.

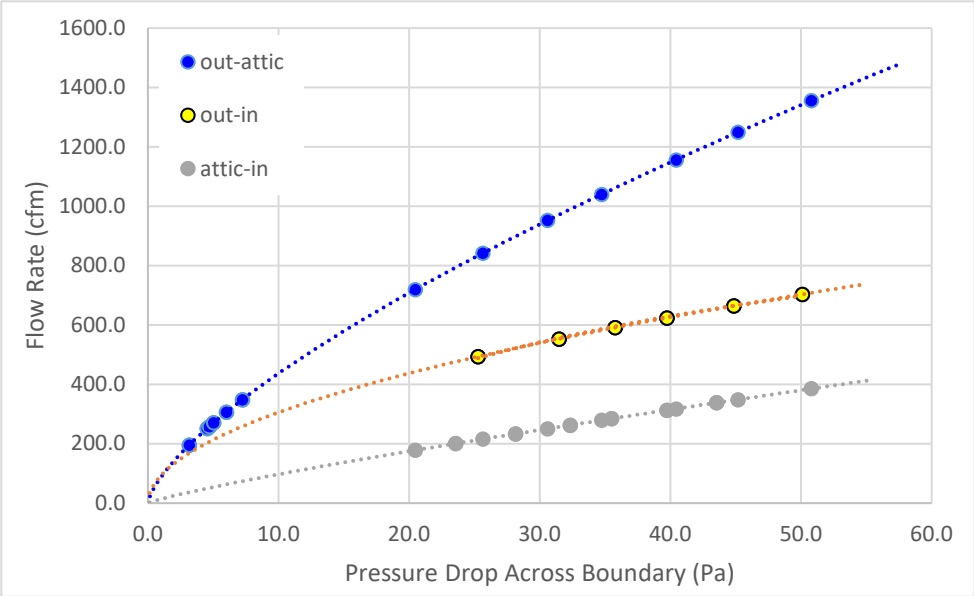

Figure 68. Predicted flow rate across each flow's respective boundary

"Out-attic" = flow between outdoors and attic space; "out-in" = flow between outdoors and conditioned space; "attic-in" = flow between attic and conditioned space.

It should be noted that there is a level of uncertainty in the shapes of the curves for the outside/attic boundary and the attic/inside boundary that could have been reduced by making additional blower door measurements at pressure drops lower than 20 Pa. Having good confidence in the flow versus ΔP curve at low values of ΔP is important because under natural conditions with low wind speeds most of the pressure differences can be in the 0–10 Pa range. In general, the uncertainty in the curve shape will be reduced with a larger range of pressure drops and larger number of points. Obtaining steady-state measurements at low pressure drops can be difficult during a windy period because local outside/inside pressure differences induced by wind are constantly changing. For this reason, it is best to wait for a calm period to make a set of blower door measurements.

Appendix D. Observed and ASHRAE Year 1 Weather Comparison

We chose the ASHRAE RP 1325 Year 1 weather for Daytona Beach (Salonvaara 2011) as the “stress case” weather for hygrothermal modeling. Its seasonal and total dry-bulb temperature, RH, and dew point are compared to the observed (measured) weather in DeBary, Florida, for the hours during which data were collected in DeBary in Figure 69, Figure 70, and Figure 71.

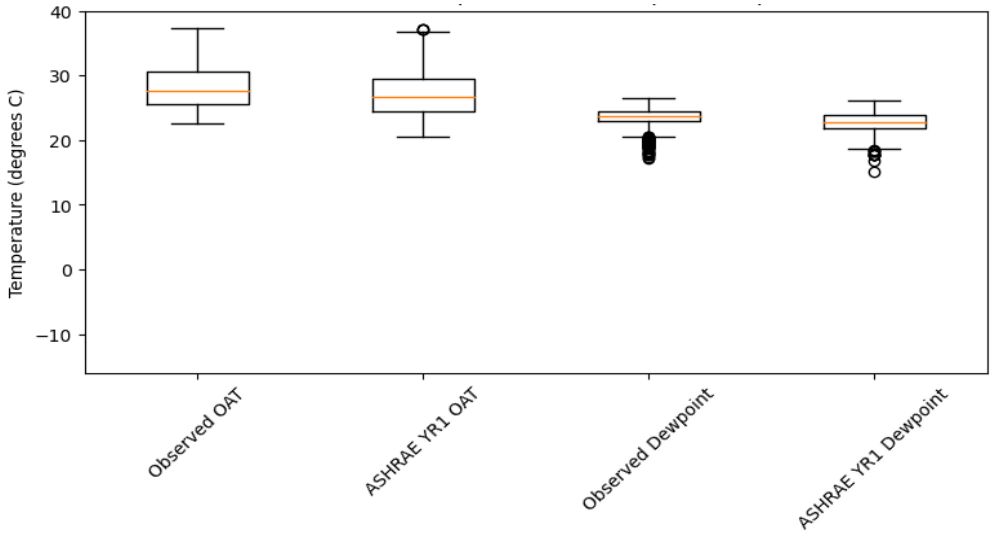

Figure 69. Dry-bulb temperature and dew point temperature comparison between the observed weather in DeBary, Florida, and the ASHRAE RP 1325 Year 1 weather for Daytona Beach, Florida, during summer

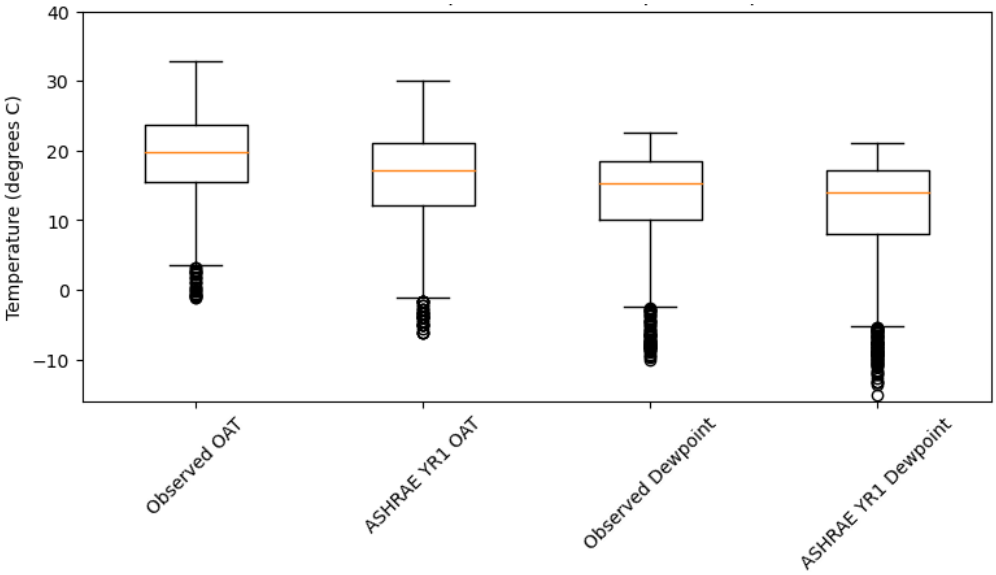

Figure 70. Dry-bulb temperature and dew point temperature comparison between the observed weather in DeBary, Florida, and the ASHRAE RP 1325 Year 1 weather for Daytona Beach, Florida, during winter

The ASHRAE Year 1 weather is all-around colder than the observed weather, but RH is higher for the ASHRAE Year 1 weather only in winter (Figure 71). Dew point is generally lower for the ASHRAE Year 1 weather, but its temperatures are also lower.

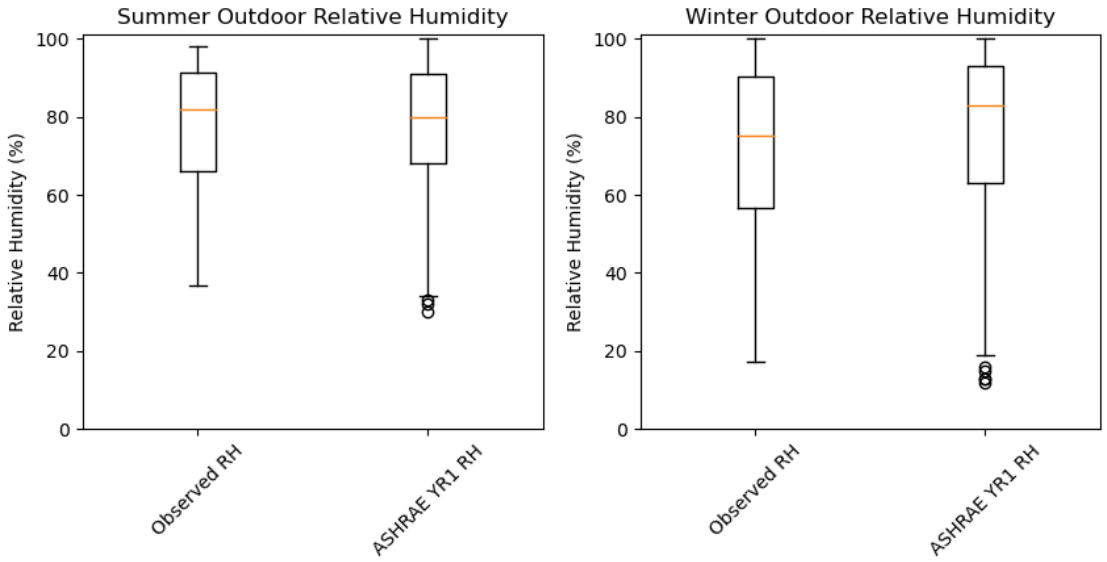

Figure 71. RH comparison between the observed weather in DeBary, Florida, and the ASHRAE RP 1325 Year 1 weather for Daytona Beach, Florida, during summer (left) and winter (right)

Table 14 shows the minimum, maximum, mean, and median values for observed and ASHRAE Year 1 dry-bulb temperature, RH, and dew point temperature.

Table 14. Minimum, Maximum, Mean, and Median Dry-Bulb Temperature, RH, and Dew Point Temperature During Observed Period (July 5–May 17) for the Observed Weather and ASHRAE RP 1325 ASHRAE Year 1 Weather

	Dry-Bulb Temperature (°C)				**RH (%)**				**Dew Point Temperature (°C)**			
	Min	Max	Mean	Median	Min	Max	Mean	Median	Min	Max	Mean	Median
Observed Weather DeBary	-1.2	37.3	23.2	23.8	17.2	100	75.7	79.8	-10.2	27.9	18.1	19.3
ASHRAE RP 1325 Daytona Beach Year 1	-6.1	37.2	20.5	21.7	12.0	100	76.7	80.0	-15.1	26.1	15.8	17.2

Two additional indicators of hygrothermal stress are driving rain and solar radiation. Wind-driven rain—a result of rain, windspeed, and wind direction—is accounted for in WUFI, and solar radiation is a factor in assembly drying, as well as material and air

temperatures. Table 15 and Figure 72 compare rainfall between the observed and ASHRAE Year 1 weather. Figure 73 compares hourly wind speed between the two climates. Figure 74 compares global horizontal solar radiation between the two during the hour between 12 p.m. and 1 p.m. local Standard Time in summer and winter, as a representation of daily “typical” solar radiation during each season.

Table 15. Rainfall Comparison Between Observed Weather and ASHRAE RP 1325 Year 1 Weather

	Total Rainfall Between 7/5 and 5/17 of the Following Year (Ltr/m^2)	**Summer Rainfall Between 7/21 and 9/22 (Ltr/m^2)**	**Winter Rainfall Between 12/21 and 3/19 of the Following Year (Ltr/m^2)**
Observed Weather DeBary	938.5	676.0	41.2
ASHRAE RP 1325 Daytona Beach Year 1	917.3	161.5	251.0

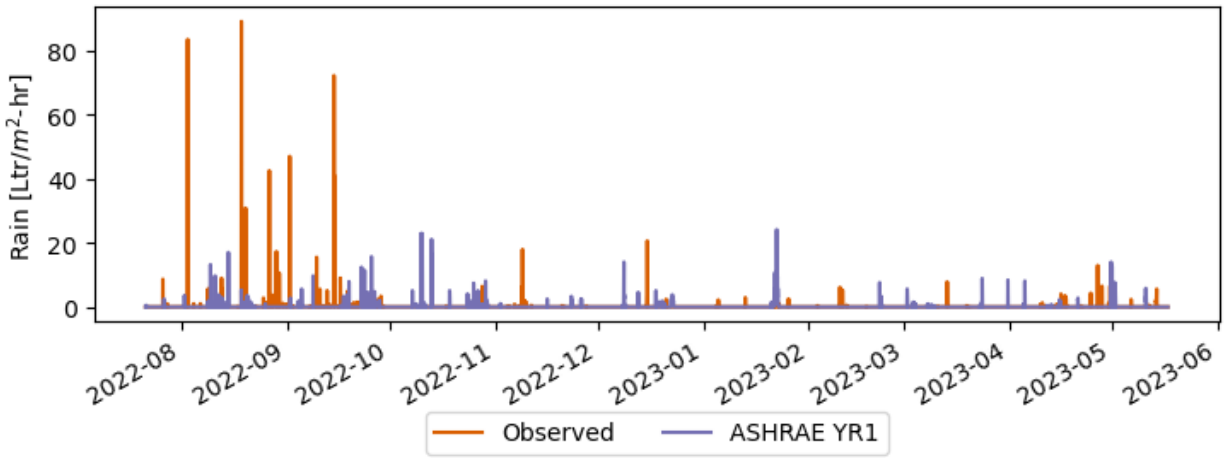

Figure 72. Comparison of hourly rainfall between the observed weather and ASHRAE Year 1 weather during the observed time period

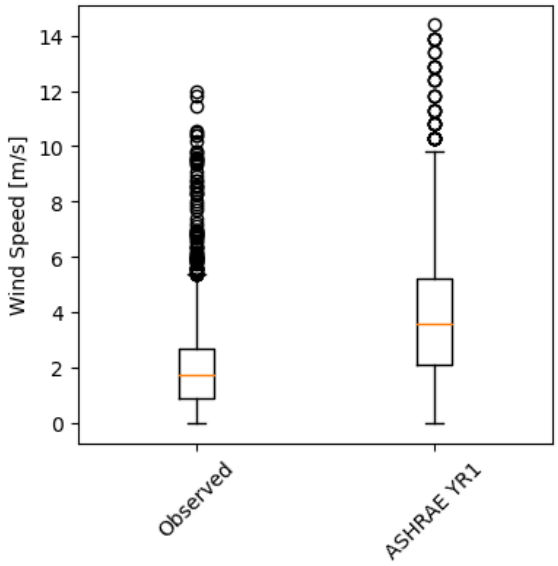

Figure 73. Hourly wind speed comparison between the observed weather and the ASHRAE Year 1 weather during the observed period

Based on a first glance at Table 15, it appears that the observed weather was wetter than the ASHRAE RP 1325 Year 1 weather, but this is really only true (and markedly so) for the summer months. During the winter and swing seasons, the ASHRAE Year 1 weather experiences significantly more rainfall (Figure 72). Figure 73 also shows that wind speed was significantly lower in the observed weather,[3] possibly because DeBary is more protected from coastal wind than Daytona Beach. Taken together, this means that, although rainfall was higher for the observed weather, driving rain may not have been.

[3] This was the case year-round—not just during a specific season.

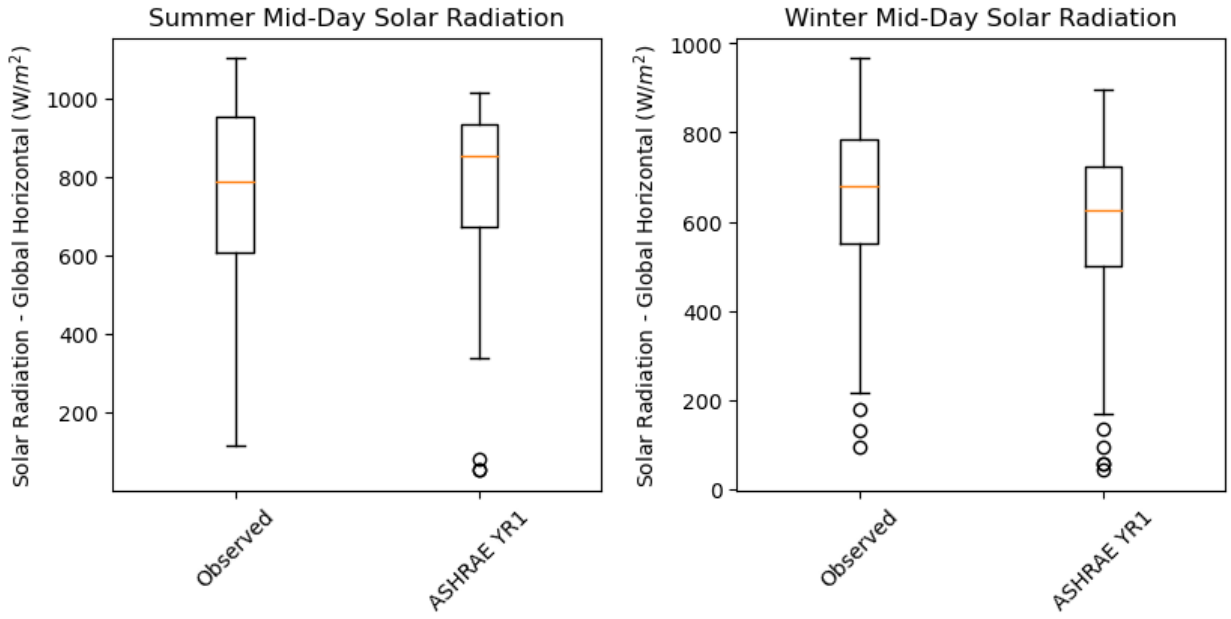

Figure 74. Global horizontal solar radiation comparison between the observed weather in DeBary, Florida, and the ASHRAE RP 1325 Year 1 weather for Daytona Beach, Florida, during summer (left) and winter (right)

The ASHRAE Year 1 representative solar radiation is also somewhat higher, on average, than that of the observed weather during the summer. The opposite is true in the winter. All in all, the “stress case” weather is clearly more stressful during the winter season, but the observed period happened to have a rainy summer season. Neither Hurricane Ian nor Tropical Storm Nicole fell within the summer or winter seasons, so their impact is seen in the swing seasons.

Appendix E. Hygrothermal Model Comparison and Adjustments

Comparison Between Model and Field Measurements

As mentioned in Section 2.3, the primary point of comparison for the measured values and the model were surface conditions at the points of concern in both the baseline attic and the attic with diffusion ports, buried ducts, and radiant barrier. The roof deck's temperature and RH were measured near the ridge, at mid-height, and at a low point (see Figure 10 and Figure 11). Because the roof deck was found to experience more moisture at the lower measurement location (discussed in Section 3.1.6), the models and comparisons are based on the Attic "Low" measurements. For the attic surface boundary conditions in both the roof deck and attic floor models, the measured attic conditions at the "low" point were used (Figure 9). For the roof deck, the measured weather files were used for exterior conditions. For the attic floor, the measured interior conditions were used. Table 2 describes the attic floor and roof deck assemblies by layer.

Comparisons and Discussion of Modeled and Measured Results

In Figure 75 and Figure 77, measured and modeled surface temperature, RH, and absolute humidity are compared at the top of the ceiling drywall ("attic floor") and at the interior of the north-facing roof deck. The comparison begins at the time the home was occupied in October. Figure 76 and Figure 78 zoom in on representative hot and cold periods to better compare modeled and observed behavior. The MBE and CV-RMSE for both assemblies are provided in Table 14.

The attic floor modeled temperatures and humidity levels correlate well with the measured values in winter, but modeled temperatures are generally lower than the measured values during summer (Figure 76), which also leads to higher predicted RH than observed in summer (Figure 76). The authors do not have a concrete explanation for why attic floor temperatures are underestimated in the model, considering that winter attic floor temperatures do not indicate overestimated insulation levels, and roof deck temperatures do not indicate higher transmitted solar radiation than what is modeled. It is possible that three-dimensional air circulation, air stratification, and other complex fluid dynamics beyond the scope of our model play a role in attic floor surface conditions. The one-dimensional attic floor model, in turn, serves as a "conservative" estimate of temperature and RH when it comes to calculating failure modes.

Although failure conditions depend on moisture content, temperature, and RH, absolute humidity is helpful in determining how well the model matches the measurements by clarifying whether differences seen in RH are due to differences in temperature. Some of the higher modeled summer RH levels cannot be accounted for by this temperature bias, and Figure 76 also shows that absolute humidity levels are slightly overpredicted

for the attic floor during summer. It is possible that there is a moisture gradient within the blown-in attic insulation not accounted for in the hygrothermal modeling software that creates this discrepancy between a) the modeled boundary conditions (based on measured values) of attic-air and living space temperature and humidity levels and b) the modeled surface temperatures and humidity levels. This explanation would align with observations of dew point being higher closer to the top of buried ducts than toward the bottom in concurrent studies performed by FSEC and Owens Corning.

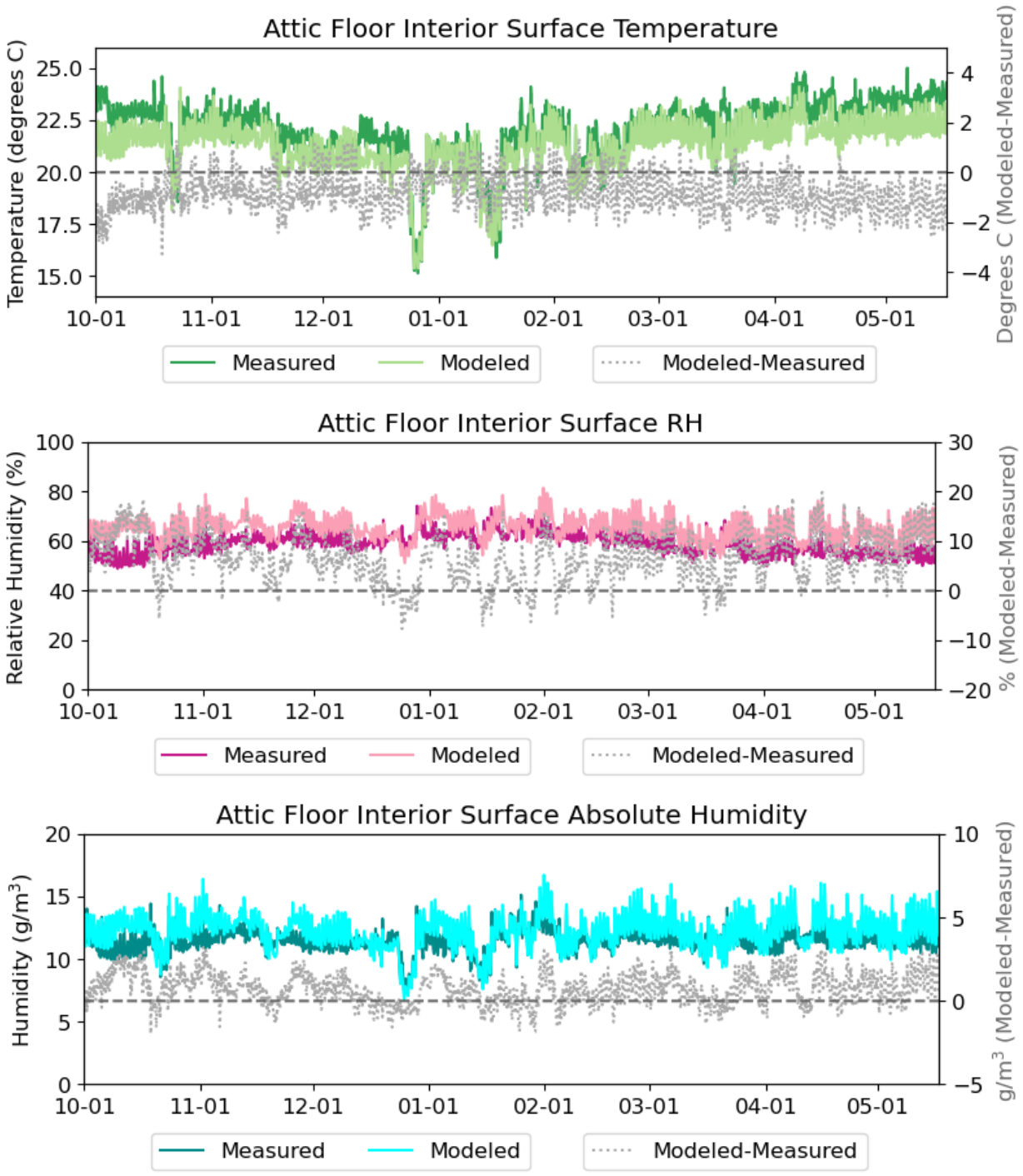

Figure 75. Measured and modeled hourly surface temperature, RH, and absolute humidity of top of ceiling drywall for home with diffusion ports, buried ducts, and radiant barrier during occupied period

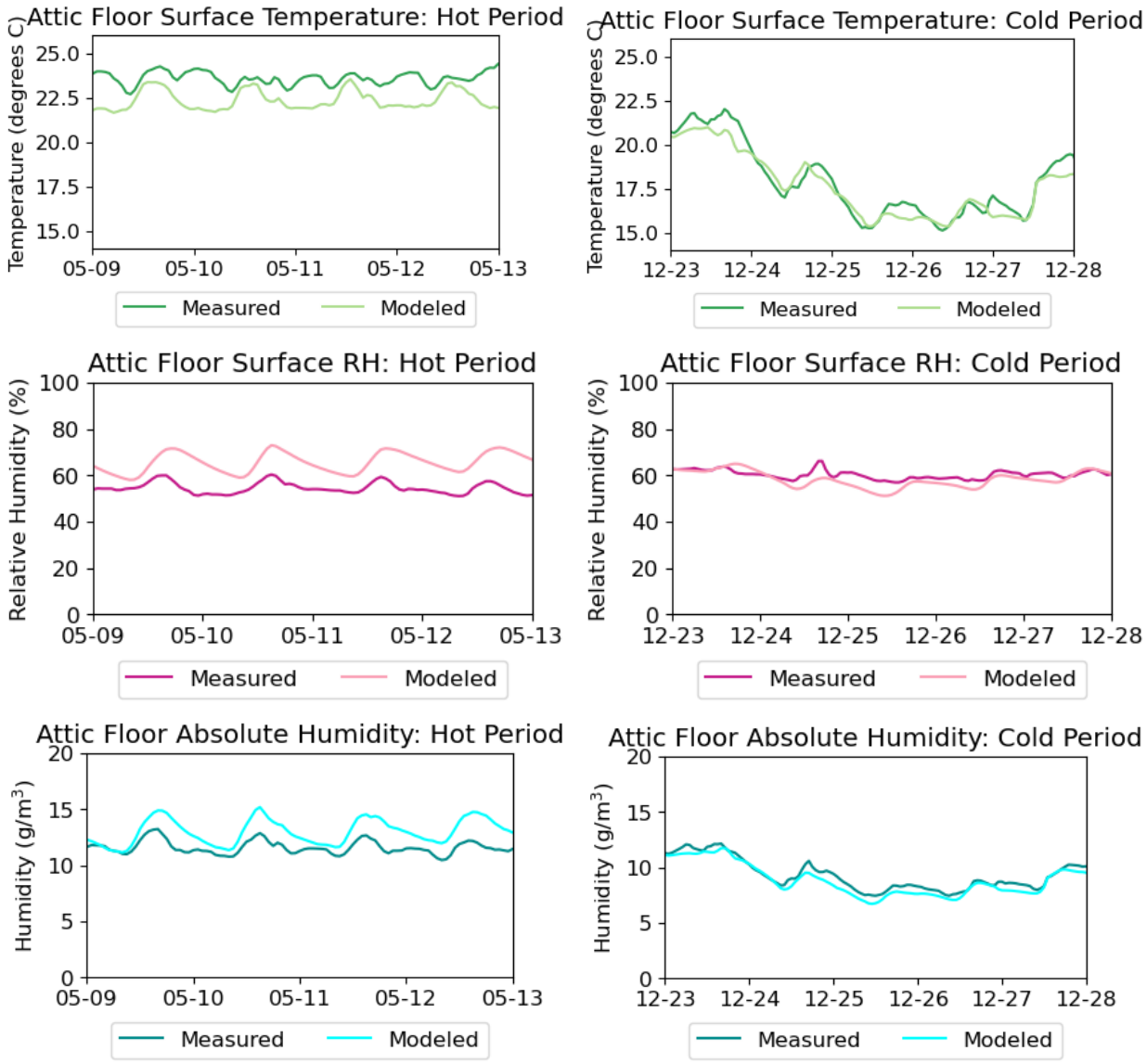

Figure 76. Measured and modeled hourly surface temperature, RH, and absolute humidity of top of ceiling drywall for home with diffusion ports, buried ducts, and radiant barrier during representative hot and cold periods

The roof deck, on the other hand, exhibits little difference between measured and modeled values during the summer (Figure 77); in contrast, the roof deck's measured and modeled values diverge for both temperature and RH during the winter (Figure 77). Roof deck interior surface temperature is overpredicted in the model, RH appears underpredicted, and RH peaks and valleys appear nearly opposite between measured and modeled values. Again, the absence of these discrepancies during summer indicates that insulation levels are not likely the culprit in the differences observed during one season but not the other, and that other factors are at play.

Looking more closely at absolute humidity, the modeled and observed values compare well during both hot and cold seasons. This shows that RH can be significantly skewed

by apparently small variations in temperature, and that the discrepancy between the model and measured values is primarily surrounding temperature. One explanation for lower measured roof deck temperature than modeled temperature could be the complex convection pathways and uneven air mixing that exist in a hot attic. It is possible that, during winter, the attic air does not experience as much heat-induced convection as it does during the summer, and that cold air pockets remain at the edges and corners of the attic, even when measured air temperature is warmer at the bottom of the attic toward the center. As this research did not involve a fluid-dynamics model or extensive regularly spaced temperature measurements, the exact explanation for the difference between measured and modeled temperature at the roof deck during winter is unknown.

In contrast to the attic floor model, the roof deck hygrothermal model can be said to be under-predictive of moisture issues, especially during the winter when concern over moisture is highest for this assembly.

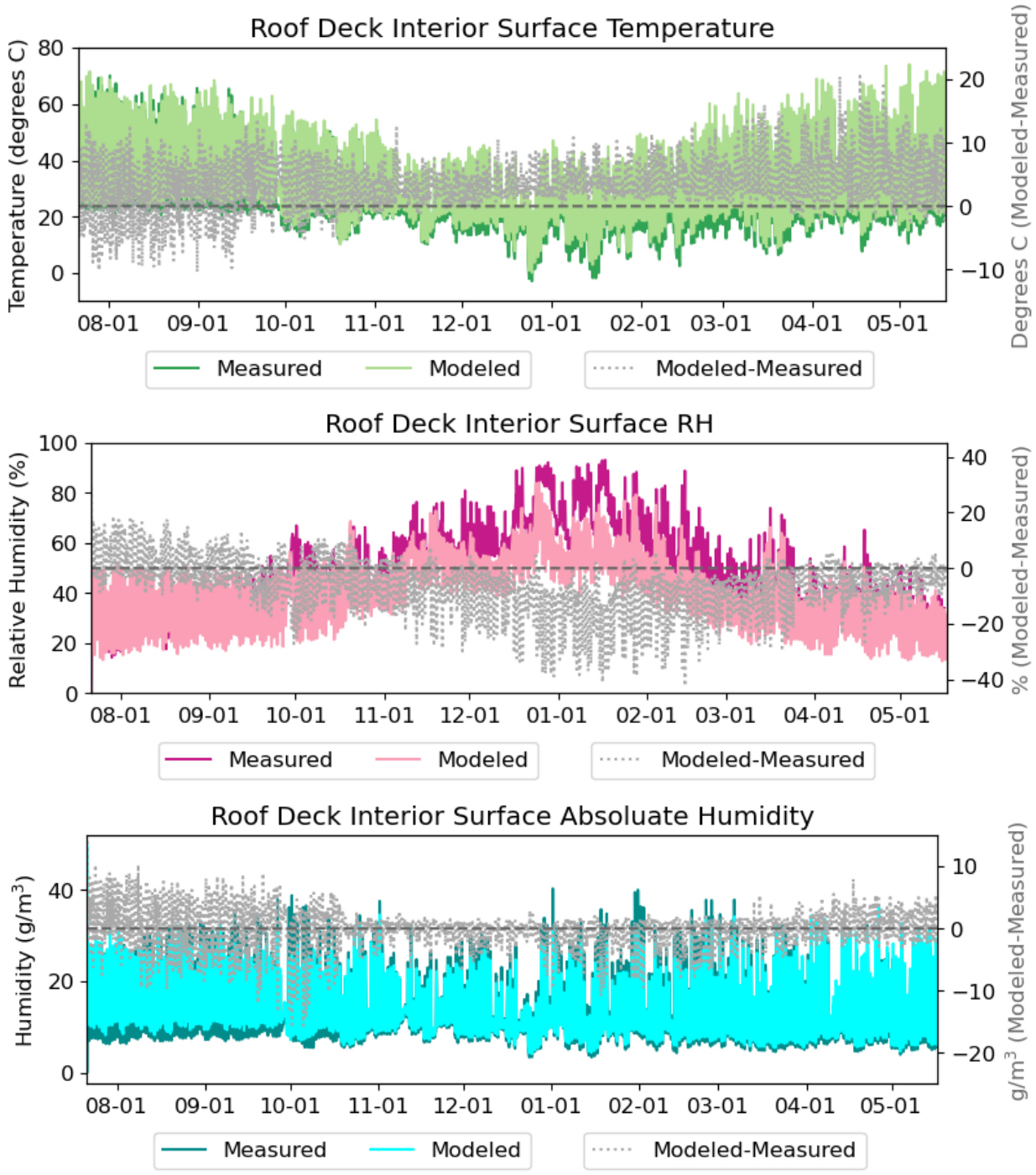

Figure 77. Measured and modeled hourly surface temperature, RH, and absolute humidity of interior roof deck (low point) for home with diffusion ports, buried ducts, and radiant barrier during occupied period

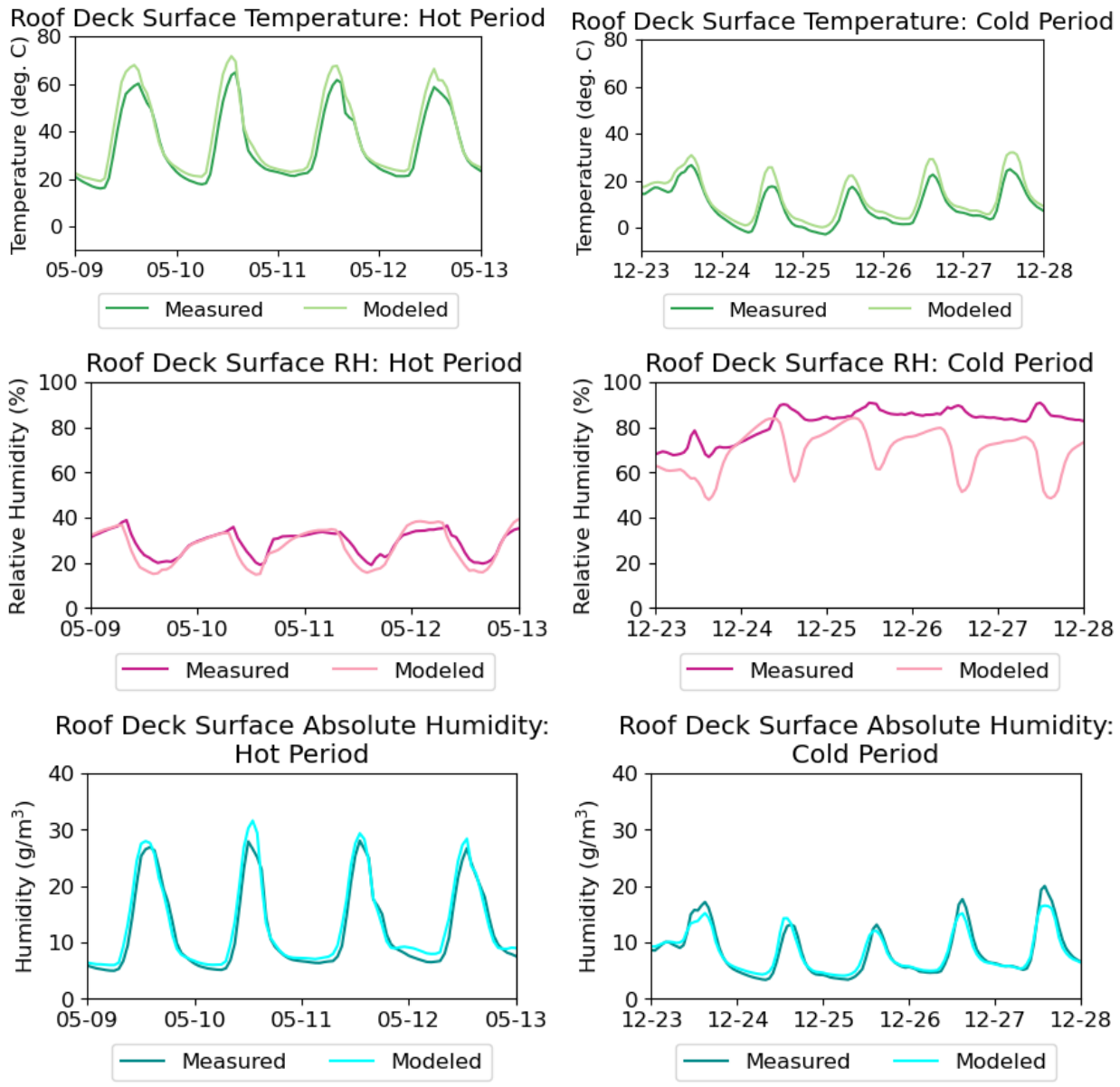

Figure 78. Measured and modeled hourly surface temperature, RH, and absolute humidity of interior roof deck for home with diffusion ports, buried ducts, and radiant barrier during representative hot and cold periods

Table 16 shows upward bias for attic floor RH and roof deck temperature, and substantial downward bias for roof deck RH. These phenomena are discussed above. Although CV-RMSE can be high for most of the listed measurements, it should be noted that these error calculations represent errors for hourly values, not for long-term trends, which are more indicative of moisture failure. Still, hourly differences are important to characterize the model in this case because the combination of each hour's temperature and RH factors into calculating the mold index.

Table 16. Quantified Errors Between Hourly Temperature, RH, and Absolute Humidity Data Points of the Measured and Modeled Attic Floor and Roof Deck

Location	Measurement/Modeled Value	Mean Bias Error	CV-RMSE
Attic Floor (drywall top surface)	Temperature (°C)	-0.83	5.0%
	RH (%)	6.50	13.8%
	Absolute humidity (g/m^3)	1.02	12.8%
Roof Deck (interior surface at low measurement point)	Temperature (°C)	3.21	18.0%
	RH (%)	-4.90	10.1%
	Absolute humidity (g/m^3)	0.23	20.5%

Adjustments to the Modeling Results

Because the attic floor model overpredicted moisture-related issues and the roof deck model underpredicted moisture-related issues, post-processing was performed on modeled surface temperature and RH values prior to analyzing predicted failure outcomes for the stress case. Based on the MBE found for each month of occupancy, adjustments were made according to MBE, as shown in example Equation 1.

Equation 1

$$T_{adj,n} = T_{mod,n} - MBE_{mo,n}$$

Where:
$T_{adj,n}$ is the adjusted surface temperature at hour n.
$T_{mod,n}$ is the modeled surface temperature at hour n.
$MBE_{mo,n}$ is the MBE for the month that includes hour n.

The same process was used for adjusting RH. This was done for both the attic floor interior surface temperature and the roof deck interior surface temperature. Table 17 shows an example of monthly MBE for the attic floor drywall surface temperature.

Table 17. Example Monthly Mean Bias Error Values Used to Calculate Post-Processed Modeled Predictions

Month	Monthly Mean Bias Error (°C)—Roof deck Interior Surface Temperature
7/2022	1.68
8/2022	1.09
9/2022	3.07
10/2022	2.18

Month	Monthly Mean Bias Error (°C)—Roof deck Interior Surface Temperature
11/2022	2.47
12/2022	3.05
1/2023	3.73
2/2023	4.21
3/2023	4.45
4/2023	4.64
5/2023	4.42
6/2023	4.42[a]

[a]Although an imperfect solution, the mean bias error value used for months during which no data were available was the previously calculated (previous month's) mean bias error.

Adjusted surface temperature and RH comparisons for the observed period are found in Figure 79, Figure 80, Figure 81, and Figure 82.

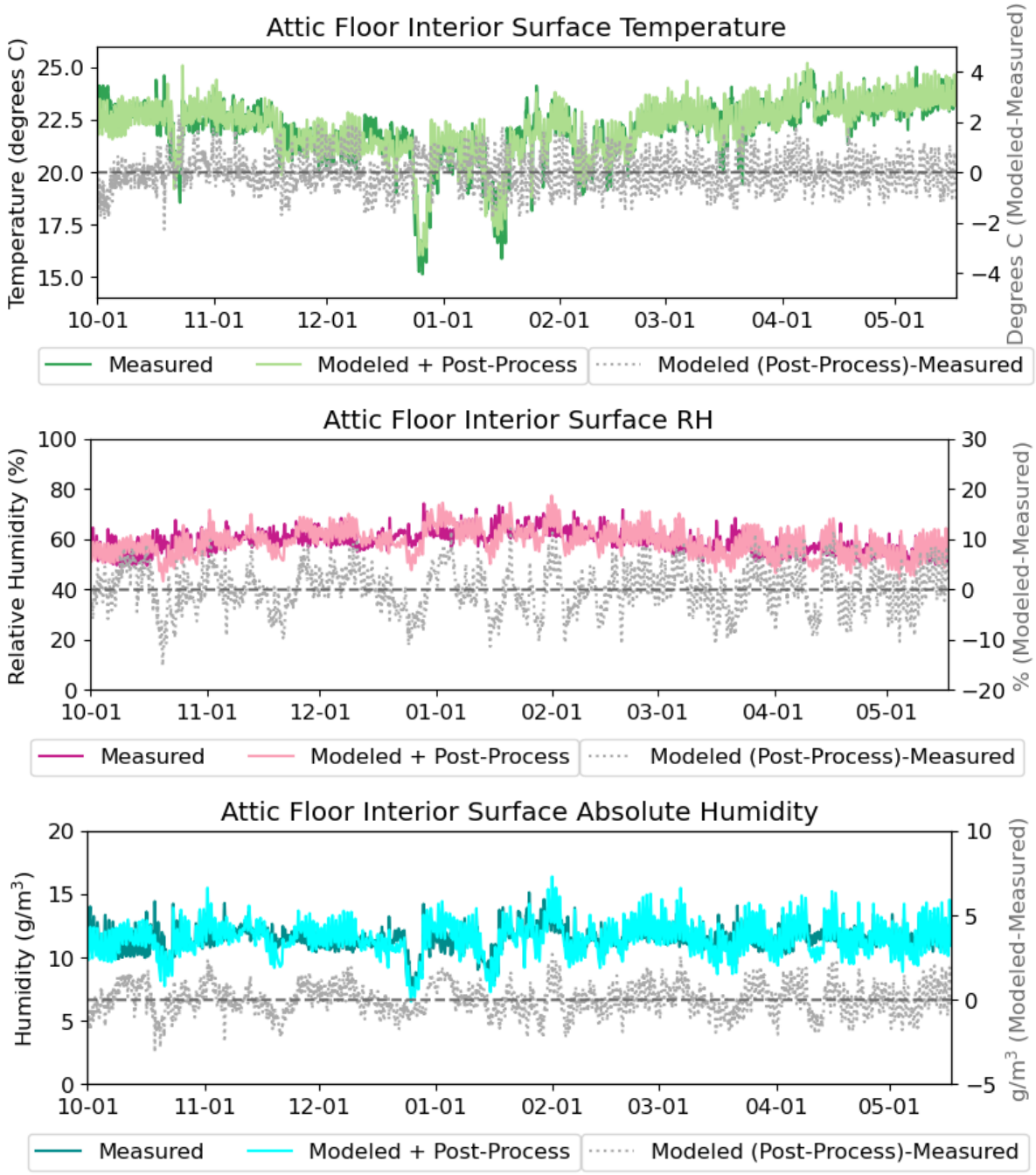

Figure 79. Measured and modeled, post-processed hourly surface temperature, RH, and absolute humidity of top of ceiling drywall for home with diffusion ports, buried ducts, and radiant barrier during occupied period

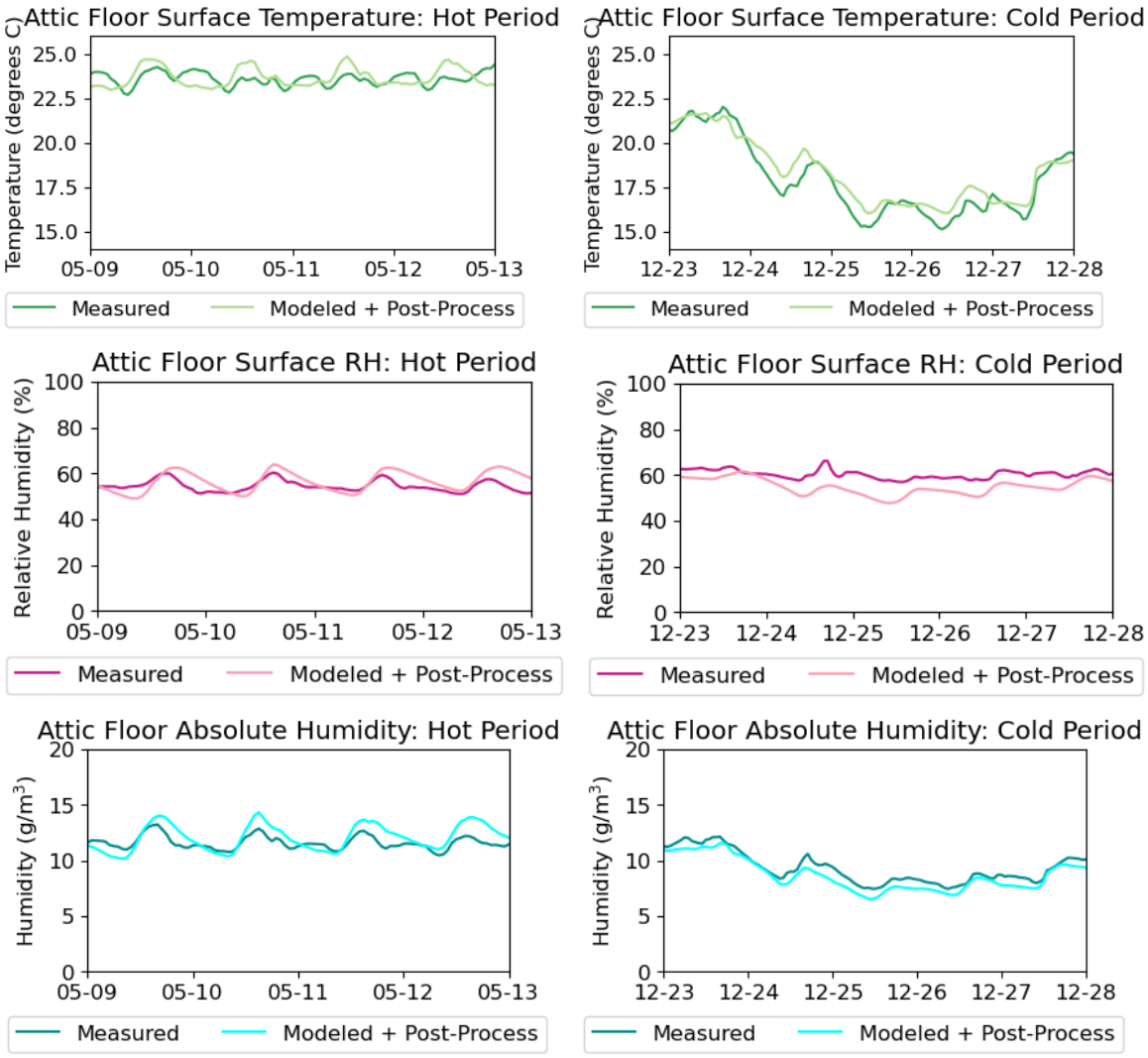

Figure 80. Measured and modeled, post-processed hourly surface temperature, RH, and absolute humidity of top of ceiling drywall for home with diffusion ports, buried ducts, and radiant barrier during representative hot and cold periods

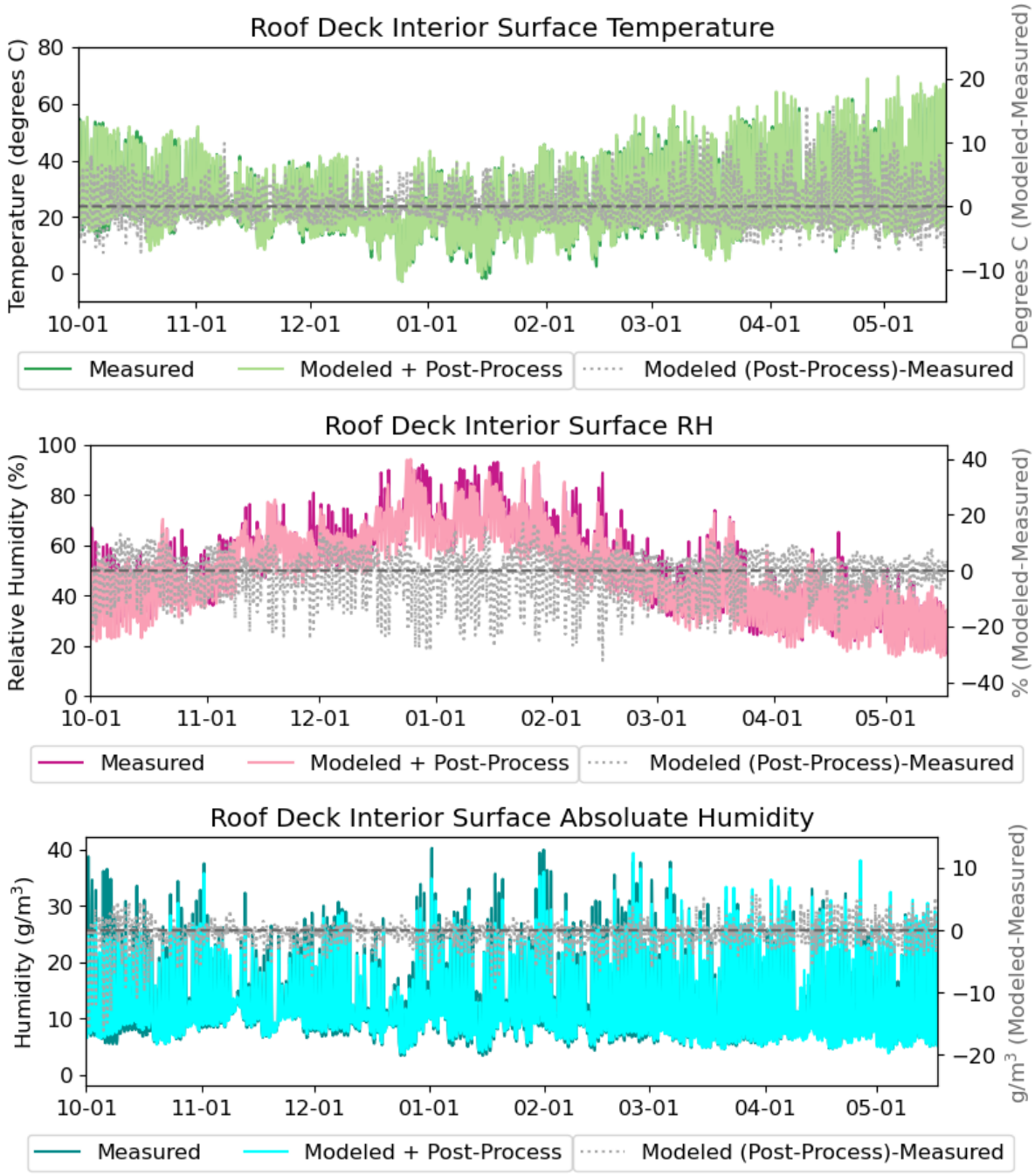

Figure 81. Measured and modeled, post-processed hourly surface temperature, RH, and absolute humidity of interior roof deck (low point) for home with diffusion ports, buried ducts, and radiant barrier during occupied period

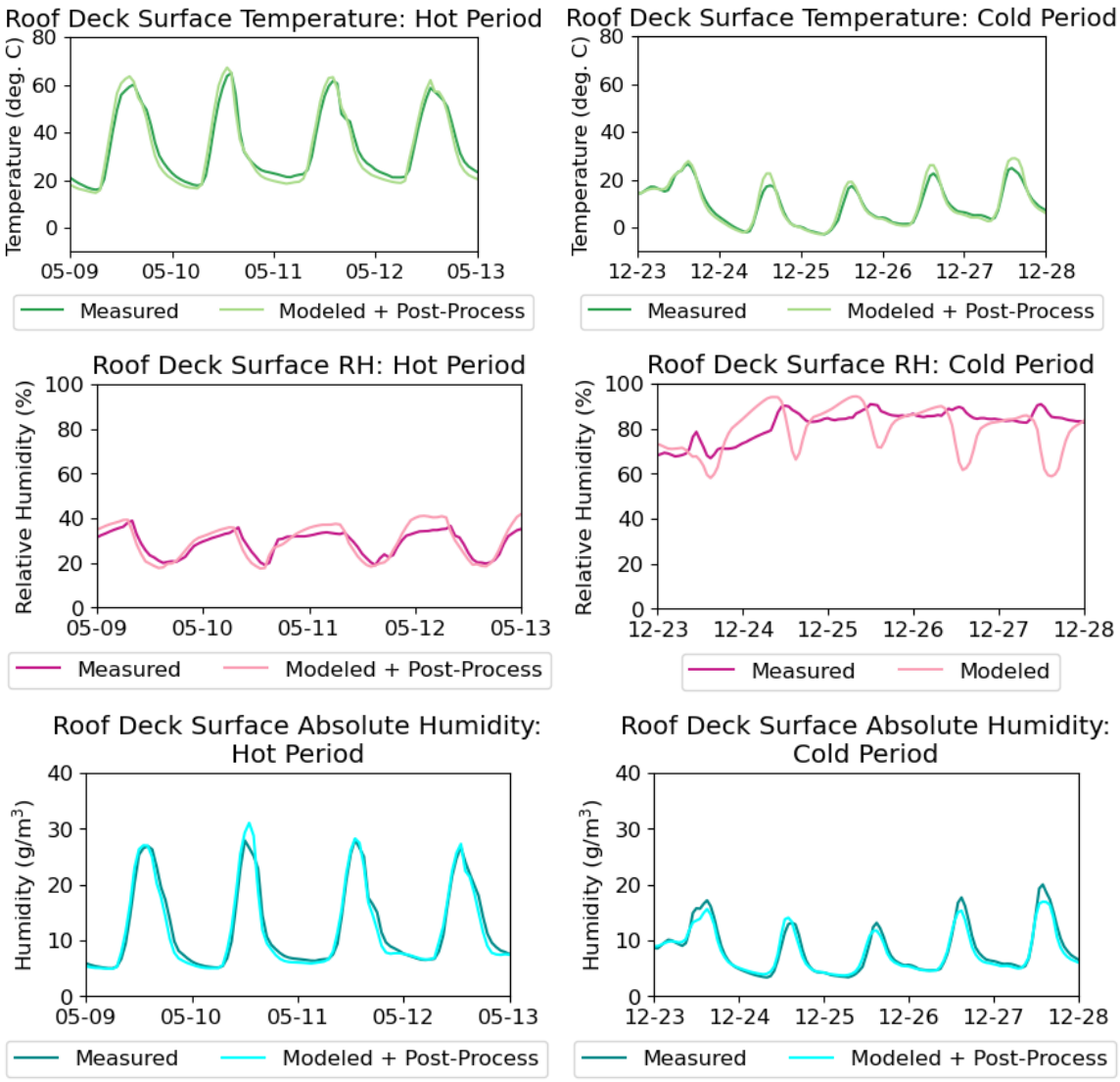

Figure 82. Measured and modeled, post-processed hourly surface temperature, RH, and absolute humidity of interior roof deck for home with diffusion ports, buried ducts, and radiant barrier during representative hot and cold periods

As seen in Figure 82, the cold-period RH at the roof deck still does not properly match up with the observed surface RH. Because of the dips in predicted RH compared to measurements, there is still a tendency for slight underprediction of mold growth at the low point of the north-facing roof deck, as seen in Figure 83. Although not within the scope of this modeling effort, future work should address more accurate ways of hygrothermal modeling of attics with combined air movement, circulation, and radiant barrier effects. Because predictive moisture performance is not perfect in this case, it is important that the stress testing incorporates lower attic temperatures than modeled for the observed case. Indeed, the stress case parameters included a shaded, reflective roof deck subject to lower occupant set points and cooler weather, as described in Table 3.

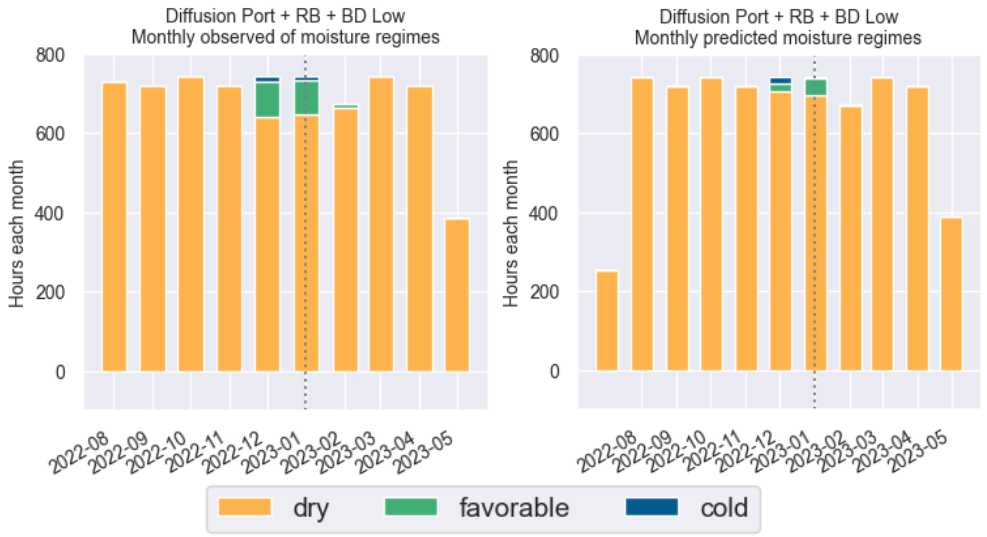

Figure 83. (left) Measured and (right) predicted, post-processed mold index at lower north roof deck interior surface for attic with diffusion port, buried ducts (BD), and radiant barrier (RB)

For more information, visit: energy.gov/eere

DOE/GO-102024-6186 • September 2024